Photodegradation of Natural Organic Matter in Plume Versus Non-plume Waters in Lake Superior

A THESIS
SUBMITTED TO THE FACULTY OF THE UNIVERSITY OF MINNESOTA
BY

Devin Rae Edge

A PARTIAL FULFILLMENT OF THE REQUIREMENTS
FOR THE DEGREE OF
MASTER OF SCIENCE

Dr. Elizabeth C. Minor

August 2021

Acknowledgements

This thesis could not have been completed without the help of many people in and outside of the UMD system, and I am extremely grateful for all their help and support. Firstly, I would like to thank Dr. Elizabeth Austin-Minor, my advisor, for her expertise, guidance, and support. My committee members, Dr. Maurer-Jones, Dr. Kathryn Schreiner, and Dr. Robert Sterner have also all been great sources of advice throughout my graduate career. In the laboratory, I have been extremely grateful for Sarah Grosshuesch and Sandra Brovold's technical expertise and assistance. I would also like to thank the captain and crew of the R/V Blue Heron for all their help in the field collecting samples and working around my irradiation setups. Thanks to my fellow graduate students and friends in and outside of the Minor Group for all your help dropping everything to collect samples and for providing enjoyable company during my time here: Ellen Cooney, Peter Conowall, John Fox, Alvin Burrows, Daniel Sandborn, Uttam Gomes, Maddie Peterson, Audrey Huff, John Zalusky, Miranda Galey, Lisa DeGuire, and the rest of our cohort. I will always treasure our friendship and the great times we had in classes and playing Dungeons and Dragons despite our busy schedules. I would also like to thank my family and Brice Hansen for their constant support and unshakeable belief in me.

This work was made possible by funding from a Chancellor's Small Grant from the University of Minnesota Duluth (The photochemistry of storm plume constituents in Lake Superior awarded to Dr. Elizabeth Minor, Large Lakes Observatory and Department of Chemistry and Biochemistry, 2019-2020), as well as a Graduate School Summer Fellowship for the summer of 2019, and a 2020 WRS Summer Stipend.

Abstract

Natural organic matter (NOM) undergoes direct and indirect photodegradation under ultraviolet (UV) light exposure, is an important source of energy for the aquatic food web and affects how much light can penetrate a water column. Photodegradation of NOM can lead to photobleaching of colored dissolved organic matter (CDOM), the release of low-molecular weight (LMW) organic species and the release of bioavailable nitrogen and phosphorus species . Photomineralization of NOM can produce carbon dioxide and carbon monoxide, removing organic carbon from the system. Recent storm events of greater intensities and frequencies have caused increased amounts of runoff, including dissolved and particulate natural organic matter, in the Laurentian Great Lakes region. This increased runoff may change the extent and types photochemistry happening in surface waters of these large lakes. The differences between the photodegradation of natural organic matter from plume-impacted water versus open lake water in Lake Superior were studied by performing irradiations under natural sunlight at 47°N latitude in August and September 2020. Terrestrially impacted samples (both before and after a storm), as well as open water samples were exposed to three days of natural sunlight. Autoclaved whole-water and filtered-water samples from before, during, and after the irradiations, along with matching dark controls, were analyzed for total and dissolved organic carbon, total and dissolved nitrogen, total and dissolved phosphorus, soluble reactive phosphorus, ammonia, and UV-Visible spectroscopy proxies (spectral slope ratios, CDOM absorbance, and $SUVA_{254}$). Irradiated filtered water samples from the terrestrially impacted and storm-impacted sites exhibited larger percent and overall changes in spectral slope ratios and greater losses of colored dissolved organic matter

(CDOM) absorbance relative to open water samples. This differed from the whole water samples, where the storm-impacted site experienced the smallest percent change in UV-Vis measurements, most likely because the particulates in this sample limited its light exposure. Except for this site, filtered water irradiations generally experienced lower percent changes and overall changes in UV-Vis measurements compared to whole water samples. An increase in DOC concentration was found in the dark sample for the whole water irradiation of the terrestrially-impacted site taken before a storm occurred, indicating potential desorption occurring when POM is included. Finally, there was also an increase in ammonium concentration in the same aforementioned whole water sample upon light exposure. The photodegradation of organic matter in Lake Superior was mainly affected by site location and whole vs. filtered treatment, and resulted in some ammonium release in whole, terrestrially-impacted samples.

Table of Contents

List of Tables

List of Figures

List of Acronyms

AQY – Apparent quantum yield

CDOM – Chromophoric dissolved organic matter

DOC – Dissolved organic carbon

DOM – Dissolved organic matter

LMW – Low molecular weight

LOD – Limit of detection

OC – Organic Carbon

OM – Organic matter

POC – Particulate organic carbon

POM – Particulate organic matter

PPRI – Photochemically produced reactive intermediates

ROS – Reactive oxygen species

SRP – Soluble reactive phosphorus

TDN – Total dissolved nitrogen

TDP – Total dissolved phosphorus

TN – Total nitrogen

TP – Total phosphorus

UV – Ultraviolet

UV-Vis – Ultraviolet-visible spectroscopy

WP – Wisconsin Point

Chapter 1. Introduction

As the effects of climate change become more pronounced, understanding the carbon cycle becomes increasingly important for identifying sources and sinks of carbon dioxide to the atmosphere. Carbon dioxide acts as a greenhouse gas, trapping heat inside the atmosphere and causing the earth's temperature to increase. To manage CO_2 emissions and mitigate climate change, carbon fluxes across various ecosystems must be studied and understood. Inland waters, including lakes, streams, rivers, and wetlands, play a significant role, contributing more to global carbon sinks to the atmosphere compared to surrounding terrestrial areas (Tranvik et al., 2009). Most lakes are also net heterotrophic, acting as a carbon dioxide efflux to the atmosphere (Hanson et al., 2003). A system is heterotrophic when the ratio of photosynthesis rate to respiration rate is less than one (Urban et al., 2005). This excess of heterotrophy is supported by terrestrially-derived organic carbon and creates an excess of amount CO_2, which can then be degassed to the atmosphere (Del Giorgio et al., 1999). The system in this study, Lake Superior, gains the majority of its organic matter via phytoplankton production (J. Cotner et al., 2004). When comparing sources and sinks of organic matter (OM) to the lake, the combined rate of primary production and allochthonous inputs are only 50-70% of the total respiration rate(J. Cotner et al., 2004). This imbalance suggests that primary production may be underestimated. It also means that Lake Superior is net heterotrophic, which has been verified by multiple studies (Cole et al., 2007; J. Cotner et al., 2004; Zigah et al., 2011). However, the lake is not emitting CO_2 at all times of the year (Atilla et al., 2011). Although Lake Superior's organic carbon budget has been studied the most

out of all the Great Lakes, more research is necessary to balance its carbon budget on an annual basis (Sterner, 2021).

Dissolved organic carbon (DOC) plays a major role in the carbon cycle in aquatic environments, linking atmospheric CO_2 and its eventual burial as organic carbon (OC) (Goldstone, 2002; Hedges, 1992; Hedges et al., 1997). In aquatic systems, gaseous CO_2 from the atmosphere is exchanged at the surface, becoming dissolved inorganic carbon (DIC), which are the aqueous inorganic forms of carbon including CO_2, HCO_3^-, and CO_3^{2-} (Meybeck, 1982). DIC is taken up by phytoplankton via photosynthesis, consuming that CO_2 from the atmosphere. These phytoplankton eventually become sources of OC upon death, which is then exchanged through the food chain or precipitated deeper into the water column. This OC can be present as DOC or particulate organic carbon (POC) depending on its size, but DOC typically makes up the majority of this pool (Wetzel, 2001). If this OC is used to fuel autotrophic or heterotrophic respiration, the resulting CO_2 may then be available for atmospheric exchange (Alin and Johnson, 2007).

Along with photosynthesis and respiration, DOM is also linked to DIC through photochemical reactions that can happen when DOM is exposed to UV light. Photochemical decomposition of DOM has been shown to produce DIC, which can then be available for exchange with the atmosphere as CO_2 (Aarnos et al., 2012). While the majority of decomposition of DOM was thought to happen via bacterial respiration in the water column and sediments, previous literature has proven that in some shallow arctic waters, bacterial respiration is surpassed by far by photodegradation of DOM (Cory et al., 2015). In some cases, this photodegradation can account for up to 94% of DOM processing in water columns (Cory et al., 2014). Photochemical degradation is also an

important process in oceans and large lakes farther south. The UniDOM model, which is primarily formid-latitudes (UK), split terrigenous DOM into two pools, T_1 and T_2, where T_1 referred to the strongly-UV-absorbing DOM, and T_2 the non- or weakly-absorbing DOM. T_1:T_2 ratios varied depending on location, with T_1 fractions varying from 13 to 65% for four UK catchments. The model predicted that of the fraction of DOM that includes compounds susceptible to photooxidation and flocculation (T_1), 52.6% of its turnover can be attributed to photooxidation (Anderson et al., 2019). Another study in 2016 in the Amazon River plume demonstrated that photochemical processes were more effective than microbial processes at degrading chromophoric DOM (CDOM) and humic-like fluorescent DOM (Cao et al., 2016). Closer to Lake Superior, which is where our study takes place, literature has shown a net increase in DOM bioavailability during long-term photochemical incubations of deep and terrestrially-impacted waters in Lake Michigan and Lake Superior, but a net reduction in off-shore surface waters (Biddanda and Cotner, 2003). This research shows that understanding the photochemical processes in differentwaters that might be exposed to light is vital to defining the carbon cycle in aquatic systems across the globe. This study aims to understand how photochemical degradation of OM will change due to the increasing frequency and intensity of storm plumes in Lake Superior.

1.1 Organic Matter in Aquatic Ecosystems

Organic matter (OM) exists in aquatic ecosystems in the dissolved or particulate fraction. Dissolved organic matter (DOM) is often defined as the fraction of OM being able to pass through a 0.7 μm pore size filter, and the fraction that does not is defined as particulate organic matter (POM) (Zigah et al., 2014). The terms DOM and dissolved

organic carbon (DOC) are often used interchangeably, but DOC refers to the total dissolved concentration of carbon in a sample, where DOM also includes other elements such as nitrogen, oxygen, and phosphorus. Like DOM and POM, carbon exists in aquatic ecosystems as DOC and particulate organic carbon (POC), as well as in inorganic forms (DIC). Total organic carbon (TOC) is the combination of DOC and POC.

Dissolved organic carbon is a major reservoir of carbon on Earth, and acts as an important part of the carbon cycle and aquatic ecosystem. Globally, aquatic environments host an average DOC concentration of 5.75 mg/L (Meybeck, 1982). The dissolved carbon fraction outweighs the particulate fraction, with ratios of DOC:POC ranging from 6:1 to 10:1 across the globe (Wetzel, 2001). DOC acts as an important energy source for bacterial communities (Pérez and Sommaruga, 2006). The consumption of DOM by heterotrophic bacteria can then generate mineral nutrients to again be available for phytoplankton use, linking carbon and nutrient flows closely in what is known as the microbial loop (Azam et al., 1983). Adding an additional loop to the traditional food chain, the microbial loop must be considered when understanding the carbon cycle in aquatic systems, as it will be partially affected by its activity. In turn, the microbial loop itself will be influenced as quantity and quality of DOM will affect bacterial growth (Hiriart-Baer et al., 2011).

Characteristics of DOM vary depending on source. Allochthonous DOM is defined as coming from external sources from the surrounding watershed like landscape runoff, and is often abundant in streams, rivers, and coastal regions of large lakes. Autochthonous DOM comes from the primary production of in-system bacteriaand algae, and dominates in open waters of large lakes where allochthonous concentrations are low

(Hansell and Carlson, 2015). DOM has also been shown to be released from some species of phytoplankton, with the availability of nutrients influencing production (Azam et al., 1983). DOM release from phytoplankton can happen under varying circumstances, including sloppy feeding by heterotrophs, lytic viral infections, cell death, and direct release by living phytoplankton as waste (Thornton, 2014). Allochthonous DOM is usually more photochemically reactive, but can contribute to bacterial growth. In contrast, autochthonous DOM is thought to be more biologically labile (Berggren et al., 2010, Del Giorgio and Davis, 2003). In terms of composition, allochthonous DOM usually contains more humic substances, and appears more yellow due to the presence of conjugated double bonds and aromatics (Kirk, 2010). 'Humic substances' is a broad term for a complicated and varied group of compounds, but can be thought of as a group of polymers that consist of aromatic rings joined together via long-chain alkyl structures. They can be separated into three fractions: humin (the compounds that do not dissolve in dilute alkali), humic acids (the alkali-soluble fraction that precipates upon acidification), and fulvic acids (the alkali-soluble fraction that remains after acidification) (Kirk, 2010).

1.2 DOM and POM photodegradation under sunlight

Of particular interest to photochemists is chromophoric DOM (CDOM), which absorbs light in the ultraviolet (UV) and blue light regions of the electromagnetic spectrum. CDOM affects how much light can penetrate the water column, and is known to have both positive and negative effects on ecosystems (Kirk, 2010; Macdonald and Minor, 2013). It can act as a "sunscreen," shielding animals, plants, and microbes from UV light by absorbing it and therefore increasing ecosystem productivity (Hiriart-Baer,

2013). However, CDOM can also decrease productivity in water columns by absorbing light that is needed for photosynthesis, and its breakdown can create harmful reactive oxygen species, which can damage DNA, proteins, and lipids (Bracchini et al., 2004).

The photodegradation of organic matter occurs via direct or indirect pathways (Li et al., 2017; Vione et al., 2014). In direct photolysis, light is absorbed directly by a chromophore (like CDOM), which then undergoes a chemical change due to the radiation absorption (Vione et al., 2014; Zafiriou et al., 1984). Indirect photolysis occurs when a photosensitizer absorbs light and produces a reactant transient species, which can go on to react with DOM that may or may not have been initially chromophoric (Goldstone, 2002; Remucal, 2014; Vione et al., 2014). Photolysis can result in either partial or complete remineralization of DOM (Hansell and Carlson, 2014). Photomineralization leads to the production of dissolved inorganic carbon (DIC), and represents a source of CO_2 to the atmosphere. Incomplete photolysis of DOM can cause photobleaching and can yield low molecular weight (LMW) compounds that are biologically available to the food web (Hansell and Carlson, 2014).

POM photodegradation is significantly less studied than DOM photodegradation due to difficulties in separating biological and photochemical degradation processes. In DOM photodegradation studies, water samples are usually sterilized by filtration through a 0.22 μm pore size filter, but this technique is not perfect. Previous studies have shown that bacteria passing through 0.1 μm filters were able to assimilate organic carbon with relatively high specific growth rates (Wang et al., 2007). While filtering can eliminate a large fraction of the bacterial population from the sample, it also removes POM from the sample. While the discipline still lacks a good way to repress biological activities in a

sample containing POM without interfering with the original characteristics, POM is important to include in studies because POM is also susceptible to photochemical alteration, and can exist in large quantities in the environment (Zafiriou, 2002). Additionally, studies have shown that some decreases in DOC concentrations in filtered water irradiations can be accompanied by increases in POC concentrations, indicating the photochemically-induced formation of POC (Porcal et al., 2013).

Not only does the inclusion of particles complicate the sterilization of water samples, but particles also affect light attenuation in the water column, absorbing and scattering light (Schwarzenbach et al., 1993). Depending on the predominant effect, rates of direct photolysis of co-occurring dissolved OM can increase or decrease. A previous study in the Mackenzie River demonstrated that high particulate load can result in a reduction in CDOM photodegradation by comparing decreases of absorbance coefficients at 330 nm and DOC concentrations of filtered water irradiations to those of a photodegradation model based on light attenuation values (k_d) (Osburn et al., 2009). They found that the model showed lower losses of absorbance and DOC concentration than the irradiations on the same samples, suggesting that the high light attenuation the water columns resulted in a reduction of photodegradation (Osburn et al., 2009).

Other considerations that must be made when irradiating whole water samples are sorption mechanisms and the composition of POM. Particles adsorb organic molecules at their surfaces, and a sorbed species may undergo photolysis differently from when it is in the dissolved state (Schwarzenbach et al., 1993). Additionally, photoreactive metals such as iron, copper, and manganese are often found in particles, both in the POM and in the inorganic particulate components (Zafiriou, 2002). If trace metal photocycling such as

photo-Fenton chemistry is occurring, then the light absorption of the minerals in POM is as important to study as carbon absorption (Estapa and Mayer, 2010). More recently, studies have begun including particles in the interest of furthering understanding of how POM photodegrades. It has been hypothesized that the absorption of light by particles may lead to the decrease of direct photolysis of DOC into DIC, but that it could also change the amount of indirect DIC production because photodegradation of POC can result in the production of highly-oxygenated DOC. This DOC may have an altered bioavailibity, and any subsequent uptake by microbial populations could lead to the indirect production of DIC(Estapa and Mayer, 2010). Considerations like this show how interconnected DOC and POC photodegradation and processes such as photosynthesis and respiration are, and how complicated it is to study them as a whole.

When dealing with individual known chemical species, the efficiency of a photochemical reaction can be measured by calculating its quantum yield, which represents the number of moles of species created or photolyzed per the number of moles of photons absorbed by the chromophore of the process (Hansell and Carlson, 2014). When working with DOM or POM, it is difficult to identify one specific chromophore, so the apparent quantum yield (AQY) is used instead. For DOM, the AQY typically divides the change in absorption or DOC concentration by number of photons absorbed (Osburn et al., 2009).

1.3 Photochemically Produced Reactive Intermediates (PPRI)

In indirect photodegradation, DOM transformation is initiated by a photosensitizer, which produces a reactive transient species (Vione et al., 2014). These

transient species include reactive oxygen species (ROS) and electronically excited molecules, and are collectively referred to as photochemically produced reactive intermediates (PPRI) (McNeill and Canonica, 2016). CDOM itself has the capacity to form photochemically produced reactive intermediates (PPRI) in sunlit waters (Haag and Hoigné, 1985; McNeill and Canonica, 2016). PPRIs can then degrade many organic molecules that otherwise would not be photochemically reactive (Boreen et al., 2003; Remucal, 2014). PPRIs can be detected through direct or indirect methods. Direct methods like spectroscopy are often difficult to use because most of these species exist on very small timeframes. Indirect methods are more effective, and involve the use of a probe molecule to react with a particular ROS to form a more stable analyte (Burns et al., 2012).

PPRI include triplet excited states of CDOM (^{3}CDOM), singlet oxygen ($^1O_2$), hydroxyl radicals ($^{\bullet}OH$), hydrogen peroxide (H_2O_2), and carbonate radicals ($CO_3^{\bullet-}$). PPRI vary in their selectivity in reactions with substrates. For example, $^{\bullet}OH$ is very unselective and will react at rates controlled mainly by diffusion, while H_2O_2 is very selective and reacts at a much slower rate (Lundeen et al., 2014; Shemer et al., 2006). Quantum yields for individual PRRI species vary depending on DOM composition, with increasing $^1O_2$ quantum yields being found in waters with more saturated formulas and higher $^{\bullet}OH$ quantum yields in less saturated, more oxygenated waters (Berg et al., 2019).

^{3}CDOM is an important species to study due to its position as a precursor of other PPRI (such as $^1O_2$) and the fact that it is not very well-defined (McNeill and Canonica, 2016; Zepp et al., 1977). It exists as a mixture of different excited states with subsequently varying energy levels and redox potentials (McNeill and Canonica, 2016).

This creates issues when attempting to study ^{3}CDOM, even through indirect methods using chemical probes. An additional complication is that ^{3}CDOM compositions will vary for different sampling locations based on differing sources of organic matter. Methods that are being developed for detecting ^{3}CDOM include using singlet oxygen as a proxy, using energy transfer quenchers with different energies such as HDA (2,4-hexadienoate, or sorbic acid) isomerization or using TMP (trimethylphenol, a probe molecule for triplet oxidants) oxidation (McNeill and Canonica, 2016). HDA isomerization uses an energy transfer reaction to probe ^{3}CDOM, and TMP oxidation uses an oxidation mechanism, which potentially means that the two methods target different subpopulations of ^{3}CDOM (McNeill and Canonica, 2016). In the future, methods such as these should be detailed more specifically to understand ^{3}CDOM compositions and populations.

1.4 Kinetics of DOM Photodegradation

Photodegradation rates are difficult to study in natural environments, as they will vary as DOM composition changes and with the quality and quantity of light (Berg et al., 2019). Photochemically mediated decreases in CDOM have previously been modelled with a first order kinetics equation as a function of light dose rather than time. k_{ABS} was calculated using the following equation where E represents the cumulative energy (MJ/m^2) received during irradiation, $\sum ABS_0$ represents the integration of the absorption curve in the initial sample, and $\sum ABS$ represents the integration of the absorption curve after irradiation (Porcal et al., 2013).

$$\sum ABS = \sum ABS_0 e^{-k_{ABS} * E} \qquad \text{Equation 1.1 (Porcal et al., 2013)}$$

The first order kinetics rate constant at a specific wavelength (k_λ) could also be calculated by modeling the decrease of the absorption coefficient using Equation 1.2, where $a_{0\lambda}$ represents the initial absorption coefficient and a_λ represents the absorption coefficient after irradiation (Porcal et al., 2013).

$$a_\lambda = a_{0\lambda} * e^{-k_\lambda * E} \qquad \text{Equation 1.2 (Porcal et al., 2013)}$$

The photodegradation rate constant for loss of DOC (k_{DOC}) can be calculated similarly as shown in Equation 1.3, where DOC_E is the concentration of DOC after exposure to the cumulative energy, E, and DOC_0 is the initial concentration of DOC (Porcal et al., 2013).

$$DOC_E = DOC_0 * e^{-k_{DOC} * E} \qquad \text{Equation 1.3 (Porcal et al., 2013)}$$

In this study (Porcal et al., 2013), data from photochemical irradiations of filtered stream was paired with the k_{DOC} rate constant plotted against cumulative irradiation energy, and the two curves overlapped within the data's 95% confidence interval.

1.5 Nutrient release from photodegradation of DOM

Other important nutrients in aquatic ecosystems besides carbon include nitrogen and phosphorus, both of which exist in organic and inorganic forms. Inorganic nitrogen forms include nitrate (NO_3^-), nitrite (NO_2^-), and ammonia (NH_3). Total nitrogen (TN) refers to the sum of organic and inorganic forms, and total dissolved nitrogen (TDN) refers to the dissolved fraction of TN. Inorganic phosphorus forms commonly found in freshwaters include orthophosphates (PO_4^{3-}, $H_2PO_4^-$, and HPO_4^{2-}), which are measured as soluble reactive phosphorus (SRP) (Meybeck, 1982). Total dissolved phosphorus (TDP) includes these orthophosphates as well as any other dissolved forms, including organic P, and total phosphorus (TP) includes TDP and the particulate forms.

The forms these nutrients are in will affect their bioavailabilty for phytoplankton and other microbes. For example, phytoplankton exhibit a preferential uptake of ammonium relative to nitrate (McCarthy and Goldman, 1979). When ammonia is present, there can be an inhibition for nitrate uptake, so it is important to understand potential sources and fates of both nutrients (Procházková et al., 1970). As for phosphorus, soluble orthophosphates are usually the most readily taken up by aquatic biota (Tonello et al., 2019). Additionally, organic nutrients have been shown to be bioavailable, including low molecular weight DON compounds such as amino acids, sugar amines, and urea, as well as some higher molecular weight compounds (Berman and Chava, 1999; Bronk et al., 2006). Some DOP compounds have also been shown to be bioavailable (Diaz et al., 2018).

Recent studies have shown that sediment resuspended in water releases phosphorus under sunlight conditions (Li et al., 2017; Southwell et al., 2010). Phosphorus is often a limiting reagent in freshwater systems, where limitation is defined as the reduction of a growth rate of a community due to the lack of the relevant nutrient (Sterner et al., 2004). Thus the possible release of orthophosphates from photochemical reactions could help to determine community growth rates.Previous studies have also demonstrated the photochemical production of ammonium in natural waters (Aarnos et al., 2012; Stedmon et al., 2007). However, not all DOM studies show this photochemical liberation of ammonium, indicating that this process is likely highly dependent on the composition of the DOM (Stedmon et al., 2007). The release of bioavailable nutrients under photochemical irradiation could have important implications for primary production,

especially in oligotrophic systems like Lake Superior, where the possibility of this nutrient release has not yet been studied.

1.6 Storm Events

One effect of climate change in certain areas of the world has been the increase in large storm events, bringing increasing amounts of heavier precipitation (Walsh et al., 2014). Increasing intensity and frequency of storm events cause flooding, leading to severe damages to infrastructure like buildings, roads, and dams. Additionally, these floods cause changes to the environment, eroding soil and bringing increased amounts of debris and contaminants into watersheds (Cooney et al., 2018). The Midwest and Northeast in particular have experienced an increase in flooding events over the last century (Walsh et al., 2014). In recent years, Lake Superior's southwestern watershed has been subject to two "500-year" flood events that resulted in an increased input of CDOM, total nitrogen, and total phosphorus to the lake (Cooney et al., 2018; Minor et al., 2014). These additional inputs made up around seven percent of the lake's annual phosphorus budget during the 2012 plume (Cooney et al., 2018).

These two recent events are not unique; storm plume waters often contain high concentrations of CDOM and suspended particulate organic matter. The photochemistry of organic matter from plumes from large storm events has not yet been extensively studied, as large storms are difficult to predict far enough in advance for coordinated sampling across a relatively large spatial scale. It is reasonable to assume that DOM originating from storm-plumes will be mainlt terrestrially derived, or allochthonous, DOM. Allochthonous DOM is well known to have higher levels of aromaticity, a higher

average molecular weight, and be more photoreactive compared to autochthonous, as discussed in Section 1.1.

While the photochemistry of storm-events has not been extensively studied, CDOM variability in saltwater environments was shown to be dominated by storms (Boss et al., 2001). Another study was able to show that CDOM fluorescence was significantly altered during three storm events on the Southern West Florida Shelf, but further studies including more parameters and in freshwater systems are needed (Conmy et al., 2009). There have been multiple studies irradiating resuspended sediments, which could give some indication of how photochemistry in storm plumes may progress, as both situations would result in a higher organic matter content in the sample. These experiments have shown that irradiated resuspended sediment samples result in the photorelease of DOC and Fe (Hu et al., 2021; Kieber et al., 2006). They are also expected to have less direct photochemical DIC production compared to samples with less suspended POC(Estapa and Mayer, 2010).

1.7 Goals of This Study

This study investigated the photoreactivity of natural organic matter (both particulate and dissolved) in Lake Superior in open water and in coastal water before and after a storm event. Natural light irradiations spanning three days each were performed and natural organic matter and nutrient composition were characterized before and after photodegradation. Analyses included UV-Visible spectroscopy, total organic carbon/dissolved organic carbon (TOC/DOC), total nitrogen/total dissolved nitrogen

(TN/TDN), soluble reactive phosphorus (SRP), total dissolved phosphorus (TDP), and ammonia (NH_3). It was hypothesized that:

1. Photodegradation would result in the release of ammonia and dissolved phosphorus. This was particularly expected in the storm-impacted, whole water samples, because past experiments had shown a release of nutrients in resuspended sediment samples, which a storm plume-impacted sample may be compared to.
2. Whole water samples would undergo more photodegradation than filtered water samples as measured by total and percent changes in UV-Vis parameters, DOC, and nutrient concentrations due to the inclusion of POM resulting in increased chances for UV light to be absorbed by chromophores.
3. Plume waters (post-storm coastal water) would undergo more photodegradation than open lake waters in terms of total and percent changes in UV-Vis parameters, DOC and nutrient concentrations due to the fact that its DOM has spent less time in situ being photodegraded.

Chapter 2. Sampling and Methods

2.1 Sampling Locations

Water samples were collected from Lake Superior in August 2020. Two sample sites were chosen based on differing percent transmittance via a Wetlab CStar on the R/V *Blue Heron* on August 7th, 2020. The first site (P1) had 88.8% transmittance and was deemed the open lake water site, and the second (P2) had 41.5% transmittance (both at 1.96 m) and was deemed the storm plume impacted site. However, it should be noted this site was extremely close to the Superior Entry Channel and that the last storm was on July 21st, 2020 with a mean precipitation of 0.76 inches in the Duluth Area, MN (NOAA Online Weather Data, accessed January 21, 2021). Therefore, it might be that the site could be more accurately described as terrestrially impacted instead of storm plume impacted. A larger storm occurred on August 7-9, 2020 (mean precipitation totaling 1.48 inches), so an additional water sample (WP) was collected from the shore of Wisconsin Point, Superior, WI on August 10, 2020.

Lake Superior is the largest freshwater lake (by area) on Earth, holding about 10% of the world's freshwater that is not frozen in a glacier or ice-cap (Habermann et al., 2012). With a surface area of 82,100 km^2 and a volume of 12,230 km^3, it is the third largest freshwater lake in the world by volume (Assel, 1986; Habermann et al., 2012). It is an oligotrophic system with water column production ranging from 200 to 350 mg C m^{-2} d^{-1} (Sterner, 2010). The organic carbon pool is mostly made up of DOM with a ratio of DOC to POC of more than 10:1 (Biddanda et al., 2001). DOC values typically range from 80 to 210 μmol/L in Lake Superior while POC values are only around 2 to 17 μmol/L (Cooney et al., 2018; Zigah et al., 2012). This is a larger ratio of DOC to POC

compared to average open ocean values, which have a DOC concentration of 37 μmol/L and a DOC:POC ratio of about 9:1 (Wetzel 2001). Eutrophic lakes typically show a 6:1 ratio of DOC to POC, with DOC values averaging around 858 μmol/L Wetzel 2001).

Lake Superior is known for its low phosphorus concentrations (Anagnostou and Sherrell, 2008), which makes nitrogen concentrations very high with respect to the amount of phosphorus (Sterner, 2011). There are also low levels of dissolved iron, and this results in algal growth being limited by phosphorus and iron concentrations (Sterner et al., 2004). Therefore, the potential release of bioavailable phosphorus via photochemical processes could be an important source of this nutrient, which could increase primary productivity in the lake. Despite this, light and temperature remain the most important factors affecting primary production in Lake Superior, accounting for 93% of the variance of the volumetric production of carbon in the system (Sterner, 2010).

Figure 2.1. Lake Superior sampling locations.

2.2 Sample Collection and Processing

Lake Superior whole water was collected on August 7th, 2020 on the R/V *Blue Heron* via a rosette mounted with a Seabird Monel 911 Plus Conductivity, Temperature, and Depth (CTD) package. The CTD notes conductivity, temperature, depth, chlorophyll-A fluorescence (Wetlab Wetstar, mg/m^3), and percent transmittance (Wetlab CStar, %). The open lake sample (P1) was collected from 46.889°N, 91.763°W and the in-plume sample (P2) was collected from 46.708°N, 92.012°W. The samples were collected at a 2 m depth, and stored in 10 L jerrycans that were previously cleaned in soap and water, then soaked in 10% HCl for 2 hours, and rinsed with deionized water. Just before sample collection, the jerrycans were rinsed with sample water that was discarded. An additional surface water sample (WP) was collected using acid soaked jerrycans rinsed with sample and was taken the shore of Wisconsin Point after a precipitation event (Table 2.1).

After being transported to the laboratory, the water needed for filtered water portions of irradiations was filtered using a 0.8/0.2 μm Whatman capsule filter (which was reused between samples and back-flushed with deionized water for 1 hour prior to use with each new sample). The whole water portions of the sample were autoclaved in a Steris AMSCO Lab 250 for 30 minutes at 121°C in 1 L glass Nalgene bottles. All processed water was stored at 4°C in the dark until irradiation. If more than 14 days passed with the water samples in storage, the filtering and autoclaving processes were repeated.

Table 2.1. Sample collection dates and CTD data.

Site	Date of Sampling	Coordinates	Depth of Sample (m)	Temperature (°C)	Percent transmittance
Photochemistry Blue (P1)	8/7/20	46.889°N, 91.7627°W	1.96	20.9	88.777%
Photochemistry Brown (P2)	8/7/20	46.707933°N, 92.0125°W	1.96	19.6	41.4806%
Wisconsin Point (WP)	8/10/20	46.706497°N, 92.013625°W	0.42	21.8	Not taken

Natural light irradiations were performed, starting with the WP sample due to its more visible brown coloring and sediment loading relative to the other samples. Filtered and whole water samples for the same site were irradiated simultaneously. A small volume of each fraction was saved to take initial UV-Vis, organic carbon and nutrient samples as described in Section 2.3 the morning of irradiation.

2.3 Natural Light Irradiations

Initial aliquots were taken from the stored samples the day of the irradiations (before they began) and included a TOC/TN (for whole water samples), DOC/TDN, and a UV-Vis sample (for both filtered and whole water portions). These samples were placed in 40 mL amber vials rinsed once with sample, then stored at 4°C in the dark until analysis. All TOC/TN and DOC/TDN samples were immediately acidified with 40 μL

(or 20 μL if filled halfway) of 6M HCl (ACS Plus Grade). Initial SRP, TDP and NH_3 were also taken from both the filtered and whole water portions, and a TP sample was taken from the whole water portion. All nutrient samples were stored in 500 mL Nalgene bottles that had been soaked in 10% HCl for 2 hours, rinsed with deionized water, and rinsed three times with sample water before use. Nutrient samples were stored frozen until analysis.

Natural light irradiations were performed in August and September 2020 from the hours of 9AM-4PM in Duluth, Minnesota at the Large Lakes Observatory (46.8118° N, 92.07676° W). Whole water and filtered water from each site were irradiated simultaneously for three days with three light samples and three dark samples in acid washed Pyrex baking pans. The sides of the light treatment baking pans were covered with black electrical tape to only allow light to pass through the top of the pans, and the sides and bottoms of the dark treatment pans were completely covered in the tape. The light treatments were covered in Saran wrap tightly held down by electrical tape, and the dark treatments were covered in aluminum foil. Two ferrioxalate actinometer samples were also occasionally included for short time periods when convenient to insure accurate measurement of the radiant flux (Montalti et al., 2006). The pans were kept in an ambient water bath that was refreshed with cold water every hour. Every 60 minutes during the irradiation, the temperature of the ambient water was taken along with a spectrum of the natural light from 200 to 850 nm using a StellarNet Black Comet Spectrometer. The sensor of the spectrometer was covered in the same Cling wrap used on the top of the baking pans to correct for any wavelengths of light that may not completely travel through the Cling wrap.

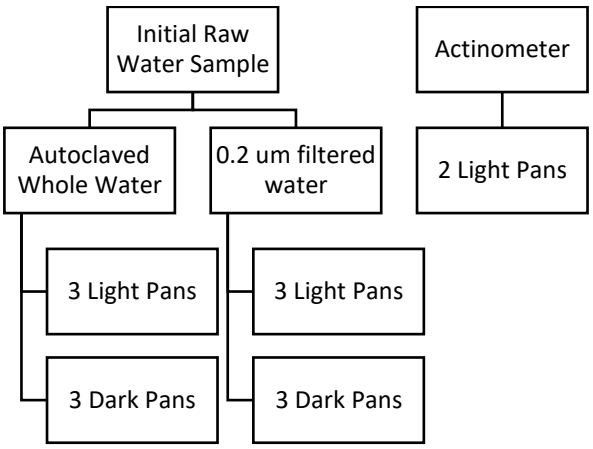

Figure 2.2. Flowchart showing how many pans of each type were irradiated during natural light irradiations.

After the irradiation was finished on Days 1 and 2, TOC/TN and UV-Vis samples were taken directly from the pans using an acid-washed pipette tip. On the final day of irradiation, these samples were taken along with TP (for whole water pans), and the rest of the water was filtered through 0.2 μm PES Millipore filters for DOC/TDN, NH_3, SRP, and TDP samples. Vacuum flasks were rinsed three times with Milli Q water and once with sample water to conserve volume.

Figure 2.3. Natural Light Irradiation setup.

2.4 Sample Analysis

a. Radiant Flux and Chemical Actinometry

The amount of UV light that samples are exposed to over the irradiation was calculated by taking the sum of the watts per meter squared (i.e., $J/(s \cdot m^2)$) per nanometer over the 250-400 nm wavelengths interpolated over the multiple scans taken every hour during the irradiation. These were all added up to give the total amount of joules per meter squared the sample received over the irradiation period. The same calculation was done over the 400-700 nm range to determine the amount of visible light the sample is exposed to. These values (in J/m^2) make it possible to compare the SpectraWiz measurements to the actinometer ones.

$$\text{Total irradiance} = \Delta t * \sum_{n=250}^{400} \frac{Watts}{m^2} \qquad \text{Equation 2.1}$$

A ferrioxalate actinometer was also used intermittently during the irradiations according to the Handbook of Photochemistry (Montalti et. al, 2006)'s recommended procedure to attempt to correct for any condensation that occurred on the Cling wrap. A ferrioxalate solution (0.012 M) was prepared from solid potassium ferrioxalate in sulfuric acid (0.05 M). Additionally, a buffered phenanthroline solution (0.1%) was prepared from $CH_3COONa \cdot 3H_2O$ (225 g) and phenanthroline (1 g) in sulfuric acid (1 L, 0.5 M). Light and dark actinometer samples were prepared in smaller glass dishes similar to the baking pans used for samples. The dishes were wrapped in black electrical tape and covered the same way as the sample baking pans. 30 mL of the ferrioxalate solution was irradiated at a time. These dishes contained less volume (only 30 mL compared to 1.3 L) and a lower depth (by 2.94 cm) than the sample baking pans, but the depth of the actinometer was measured and corrected for in the actinometer calculations. Under light excitation, this solution decomposes according to the following equations:

$$Fe(C_2O_4)_3^{3-} \xrightarrow{hv} Fe^{2+} + C_2O_4^{\cdot -} + 2C_2O_4^{2-} \qquad \text{Equation 2.2 (Montalti et al., 2006)}$$

$$Fe(C_2O_4)_3^{3-} + C_2O_4^{\cdot -} \xrightarrow{\Delta} Fe^{2+} + 2CO_2 + 3C_2O_4^{2-} \qquad \text{Equation 2.3 (Montalti et al., 2006)}$$

Once taken out of the light, 5 mL of buffered phenanthroline solution was added to react with the ferrous ions to form a colored tris-phenanthroline complex. The complex's absorbance is measured at 510 nm using UV-Visible spectroscopy, and then the moles of ferrous ions are calculated using the following equation where V_1 is the

irradiated volume (30mL), V_2 is the portion of solution taken for measurement in the UV-Visible spectrometer, V_3 is the final volume of the solution after addition of phenanthroline (35 mL), l is the optical pathlength of the cell, ΔA is the difference in absorption at 510 nm between the dark and light solutions, and ε is the molar absorptivity of the tris-phenanthroline complex (11100 L mol^{-1} cm^{-1} at λ_{max}=510 nm).

$$moles\ Fe^{2+} = \frac{V_1 * V_3 * \Delta A(510\ nm)}{10^3 * V_2 * l * \varepsilon(510\ nm)}$$ Equation 2.4 (Montalti et al., 2006)

From this value, the moles of photons absorbed by the irradiated solution per time unit (Nhv/t) is calculated using the following equation:

$$\frac{Nhv}{t} = \frac{moles\ of\ Fe^{2+}}{\Phi_y * t * F}$$ Equation 2.5 (Pitre et al., 2015)

Where Φ_y is the quantum yield of ferrous ion production at the irradiation wavelength, t is the irradiation time, and F is the mean fraction of light absorbed by the ferrioxalate solution. This value was divided by the volume of the sample, multiplied by the depth of the solution in the baking dishes to convert m^3 to surface area (m^2), and converted from moles of photons to Joules by calculating the sum of the energies of photons from 250 to 400 nm and multiplying by the number of photons per m^2 in order to compare the values in J/m^2 s to the values obtained from the SpectraWiz.

b. TOC/DOC and TN/TDN

As stated in the irradiation methods, each TOC/TN (or DOC/TDN depending on if the sample is filtered or not) sample was acidified with 40 μL (or 20 μL if filled halfway) of 6M HCl (ACS Plus Grade) to remove inorganic carbon. Samples were stored in amber vials at 4°C until analysis, which was carried out within one week of irradiation.

The analysis of OC was performed on a Shimadzu Total Organic Carbon-VSCH Analyzer coupled with an autosampler (Figure 4). The organic carbon samples were measured as non-purgeable organic carbon (NPOC) and the total nitrogen samples were measured as total nitrogen (TN). First the column was purged by running at least eight Milli Q blanks. The instrument was found to have an average detection limit over the three runs of 0.309 mg/L for carbon, and 0.010 mg/L for nitrogen (found by taking the average blank concentration plus three standard deviations, which were taken from the multiple injections taken of the lowest concentration standard). Then the analyzer was calibrated using a combined potassium hydrogen phthalate (KHP) and potassium nitrate standard acidified to 0.05 HCl as in Cooney et al., 2018 (Cooney et al., 2018). Calibration curves included 10 standards covering the range of anticipated sample concentrations. A Hansell Lab Deep Sea Reference (DSR) was used as a check standard for the TOC/DOC analyses. The accepted values for the DSR were within the standard deviation of the measured values, except for the P1 site, which was 0.12 mg higher than the accepted value This indicates that the P1 TOC/DOC values may be slightly overestimated. In-house standards of KHP were also measured three times at the beginning, middle, and end of each run, and were considered acceptable if within 10% of the known concentrations. All sites, including P1, met this requirement. Each sample was injected three to five times until the standard deviation was <2.5%. The organic carbon or nitrogen concentration was calculated using the calibration curves and corrected by subtracting the average concentration of Milli Q blanks dispersed throughout the run.

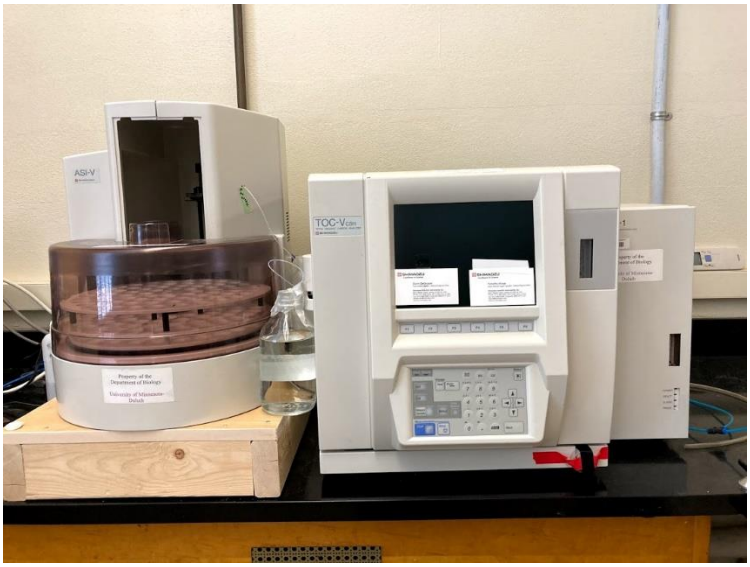

Figure 2.4. Shimadzu Total Organic Carbon-VSCH Analyzer and autosampler (University of Minnesota Duluth).

c. UV-Vis Parameters

UV-Visible light absorption spectra were taken on a Genesys 10s UV-Vis spectrophotometer using 5cm quartz cuvettes. Measurements were performed within 24 hours of sampling. Samples were scanned from 800 to 200 nm, with blanks taken at the beginning, end, and between every 6 samples. Cuvettes were rinsed three times with Milli Q water and at least once with sample prior to analysis of each new measurement. The spectra were blank corrected by subtracting the average of the blanks, then corrected for backscatter and refractive index mis-matches by subtracting the average absorbance from 700-800 nm from blank corrected absorbances (Green and Blough, 1994; Whitmire et al., 2007). After all wavelengths of all spectra were corrected, the absorption coefficient was calculated using Equation 2.1.

$$\frac{2.303 * Backscatterd\ Corrected\ Absorbances}{Cuvette\ pathlength\ (0.05\ m)}$$ Equation 2.1 (Helms et al., 2008)

Using the absorption coefficient data, the e2/e3 ratios is calculated by dividing the absorption coefficient at 250 nm (e2) by the absorption coefficient at 365 nm (e3) (De Haan and De Boer, 1987; Helms et al., 2008). This ratio is useful due to the fact that it has been shown to be inversely proportional to molecular size or aromaticity (Dalzell et al., 2009). CDOM absorbance is calculated by integrating the absorption coefficients from 250 to 400 nm (Kruger et al., 2011). For the whole water irradiations, absorbance was calculated the same way as CDOM absorbance, but the measurement includes any chromophoric particulates. Finally, $SUVA_{254}$ is calculated using Equation 2 and the data from the TOC/DOC runs. This value utilizes the DOC concentration to normalize the UV-absorption coefficient at 254 nm. Increases in $SUVA_{254}$ have been correlated to increases in aromaticity of the sample (Weishaar et al., 2003). For the whole water irradiations, $SUVA_{254}$ was calculated using the TOC concentration instead of DOC because the absorption coefficient was measured on a whole water sample.

$$SUVA_{254} = \frac{Absorption\ Coefficient\ at\ 254\ nm}{Organic\ carbon\ concentration\ (\frac{mg}{L})}$$ Equation 2.2 (Minor and Stephens, 2008)

d. Ammonium (NH_4^+)

Frozen samples were thawed within one day prior to analysis. Ammonium was analyzed utilizing the methods established in Holmes et al., 1999 and modified by Taylor et al., 2007 (Holmes et al., 1999; Taylor et al., 2007). The working reagent consists of sodium tetraborate (40 g/L, 21 mM), sodium sulfite (40 g/L, 0.063 mM), and *o*-

phthaldialdehyde (50 mL/L) which has been allowed to age for at least 2 weeks. On the day of analysis, an ammonium sulfate standard was made to spike prepared samples. Fifteen samples were run at a time, with each having duplicates of 0, 25, 50, and 100 μL NH_4SO_4 spikes. 2.5 mL of the working reagent was added to each test tube with 10 mL of sample. Samples were incubated in the dark at room temperature for at least 18 hours prior to analyses via fluorometer (AquaFluor Handheld Fluorometer, Turner Designs). The fluorometer utilizes a 375 nm LED light, has an excitation wavelength of 350/80 nm, measures emission at ≥420 nm, and has a method detection limit of 0.1 μM. Additionally, initial background fluorescence was measured before the incubation by combining 5 mL of sample with 1.25 mL of working reagent in the dark to account for interactions between the working reagent and the sample (Taylor et al., 2007). This allows the samples to be corrected for background fluorescence before addition of ammonium sulfate standard and incubation. After 18 to 24 hours, the samples were measured in the dark. The average background fluorescence was subtracted from each sample fluorescence, which was plotted versus concentration (μM) of the NH_4SO_4 spike. The intercept of the resulting curve was used to find the absolute value of the concentration of ammonia at the x-axis intercept $|c_x| = {}^{b}/_{m}$, where b is the y-axis intercept and m is the slope) (Taylor et al., 2007).

Samples that had too high ammonium concentrations (WP whole water samples) for the benchtop method as described above were analyzed on a Seal Analytical AQ400 Discrete Analyzer instead. The EPA-103-A (Rev. 10) method was followed for these samples (WP Whole water NH_3 samples), and has a detection limit of 0.004 mg N/L. For

this method, ammonia reacts with hypochlorite at a pH greater than 12 to form chloramine, which then reacts with alkaline phenol in the presence of nitroferricyanide. When incubated at 40°C, a blue indophenol dye forms, which is photometrically measured at 660 nm by the AQ400 Discrete Analyzer (*EPA-103-A Rev. 10. Ammonia-N in Drinking and Surface Waters, Domestic and Industrial Wastes*, 2012).

e. TP/TDP

TP and TDP analyses were performed as in Cooney et al., 2018 on a Seal Analytical AQ400 Discrete Analyzer (Cooney et al., 2018). Each run consisted of 4 blanks, 16 standards, and 20 samples. The standards were made of a phosphorus standard solution (HACH NIST standard #21092-10) with a final concentration range from 0.0001 to 1.0000 mg/L PO_4-P, with the majority of standards with concentrations below 0.4 mg/L. For a single analysis, 10 mL of blank, standard, or sample was added to each 21-150mm screw cap tube. Then 10 mL of potassium persulfate solution (0.05g/mL, Baker 3239-05) was added to each tube. All standards, blanks, and samples were digested by autoclaving on a Steris AMSCO Lab 250 for 30 minutes at 121°C (Liquid 30 cycle), which allows total conversion of all phosphorus forms to orthophosphate. Samples were allowed to cool overnight before analyzing on a Seal Analytical AQ400 Discrete Analyzer (Method 119A). The orthophosphates were reacted with potassium antimony tartrate, and ammonium molybdate (Wetzel and Likens, 1991) in the AQ400 Discrete Analyzer. The resulting antimony-phospho-molybdate complex is reduced with ascorbic acid to form a blue colored solution that is proportional to the concentration of total phosphorus. This method has a reported detection limit of 0.003 mg P/L.

f. SRP

Soluble reactive phosphorus samples were analyzed using the molybdate method as in Cooney et al., 2018. SRP samples were freeze-dried and reconstituted to a tenth of the original volume using Milli Q water (using an Explorer Pro EP2102C balance to measure volume). This was done because Lake Superior is known to have very low SRP concentrations. Samples were analyzed in a similar manner to TP/TDP, but without the potassium persulfate digestion step. All orthophosphate in the sample was converted to the blue colored complex as described above and in Wetzel and Likens, 1991. Sample reactions and analyses were performed on a Seal Analytical AQ400 Discrete Analyzer (Method 119A), which has a method detection limit of 0.0006 mg P/L.

2.5 Statistical Analyses

To determine how each variable was affected by site location, fraction, and light treatment, a three-way ANOVA analysis (or two-way for TOC, TN, and TP) was performed using a Standard Least Squares fit in JMP Pro. Using the p-values generated from this analysis, we were able to see if site location, filtered vs. autoclaved whole water, and light vs. dark treatment resulted in a significant difference in the variable being studied (i.e., DOC concentration). The interactions between variables were also viewed, including the two-way interactions between Site Location*Fraction, Site Location*Light Treatment, Fraction*Light Treatment, and the three-way interaction Site Location*Fraction*Light Treatment. A significant interaction, for example Site Location*Fraction, would mean that the effect of Site Location is different for the filtered

and whole fractions. Note that this was only done for samples taken on Day Three of irradiations.

After the ANOVA tests were performed, a Tukey HSD was performed using JMP Pro to test differences between sample means. For example, the light and dark treatment means for each variable were compared to see if light treatment resulted in a significant difference for that specific variable. Again, note that this was only done for samples taken on Day Three of irradiations.

Finally, to compare individual values, for example, the light and dark concentrations of a variable on Day 1 of the irradiation for a specific site, t-tests were performed using the Data Analysis Toolpack in Excel. To decide which kind of t-test was correct (Equal or Unequal Variances), an F-test was performed between the light and dark samples for each day, as well as between the initial and Day 3 light and dark values, using the three irradiation replicates. Depending on the result, the variances between samples were determined to be either equal or unequal, and the corresponding t-test (α=0.05) was performed.

To graph changes between light and dark treatments for the UV-Vis parameters, percent change was calculated by taking the [light treatment – dark treatment]/dark treatment *100. Errors for each variable were propagated using the following formula (where l refers to the light treatment and d refers to the dark treatment) and included on plots to show significance.

$$Error = \%\ change * \sqrt{\frac{\sqrt{\partial_l^2+\partial_d^2}^2}{l-d} + \frac{\partial_d}{d}^2} \qquad \text{Equation 2.3}$$

For the nutrient concentration changes, instead of graphing percent changes like the UV-Vis parameters, total changes (light – dark) were plotted instead due to small concentration changes leading to misleading percent changes.

Chapter 3. Results

3.1. Radiant Flux

The total irradiance each experiment received is shown in Table 3.1 and is calculated as described in Section 2.5a. Each experiment took place at 46.8118 N, 92.07676 W. While it was attempted to perform the irradiations on the sunniest days with the least cloud cover, this goal was difficult to achieve due to the three-day irradiation period and the limited time for sample storage. The P1 site, or open water site, received the least amount of irradiation, with two cloudy and foggy days (Figure 3.1). The samples were protected from the environment with saran wrap or aluminum foil, and any condensation or light rain was wiped off the light treatment samples, but refraction from condensed water on the saran wrap or the saran wrap itself could have affected irradiance levels. To correct for the saran wrap, radiometer measurements were also taken through it, but this does not account for any potential condensation that may have occurred on its surface. Ferrioxalate actinometer experiments were performed to verify radiometer measurements, and these experiments would correct for the condensation on the saran wrap as the light treatments were under the same conditions as the samples. However, in the actinometer experiments, there was some issue with flocculation happening upon addition of buffered phenanthroline solution; the resulting particles settled to the bottom and made absorbance measurements of the light treatments particularly difficult. Due to this problem, and potential breakdown of the stock solutions despite our best efforts to keep them in the dark, the actinometer experiments only performed as expected for the WP irradiations. The other irradiations' actinometer calculations were unable to be performed correctly due to the ΔA (A_{light}-A_{dark}) in Equation 2.4 being negative, which

meant that the total amount of photons received could not be calculated. Only the results for the actinometer experiments that correctly performed are shown in Table S-1. For a actinometer experiments during the WP irradiation the total amount of light received by the sample as determined by actinometry was 93-97% higher than the dose over the same time frame as determined using radiometer measurements Appendix S-1). This was likely due to light reflection and refraction happening on condensation on the saran wrap covering the light treatments, as well as any reflection, refraction or upwelling irradiance happening within the actual solution itself. Therefore, the radiometer measurements are likely underestimating the cumulative irradiance energy received by the samples, but these measurements are used to keep irradiance measurements consistent across the experiments.

Table 3.1. Measured radiant fluxes received from natural light for each experiment using the SpectraWiz radiometer.

Site Irradiated	Date of Sampling	Dates of Irradiation	Sample Exposure Time (hr)	Total Irradiance (J/m^2) over 250-400 nm	Total Irradiance (J/m^2) over 400-700 nm	Total Irradiance (J/m^2) over 250-700 nm
Photochemistry Blue (P1)	8/7/20	8/19/20-8/21/20	18.85	2.85E+06	9.48E+06	1.23E+07
Photochemistry Brown (P2)	8/7/20	9/2/20-9/4/20	18.83	6.08E+06	9.79E+06	1.59E+07
Wisconsin Point (WP)	8/10/20	8/16/20-8/18/20	19.25	7.47E+06	1.08E+07	1.82E+07

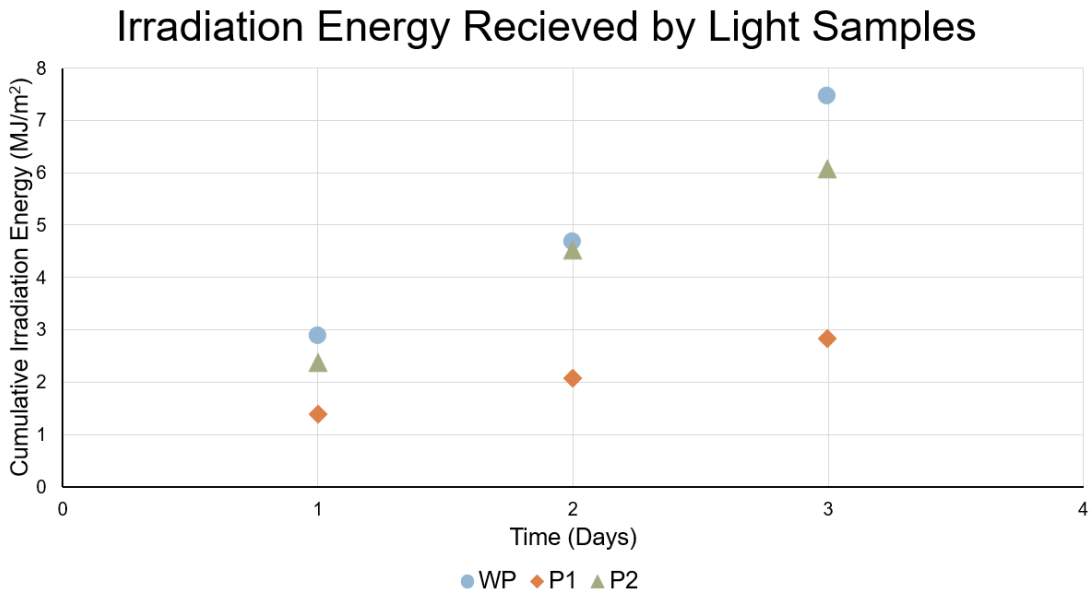

Figure 3.1. Irradiation energy received by light samples plotted against time. Note that samples were only exposed to light from around 9am to 4pm, then kept in the dark overnight.

3.2 Initial values

Trends among initial values for UV-Vis parameters and nutrient concentrations were mostly as predicted, with the post-storm, plume-impacted site, WP, generally having higher nutrient concentrations, larger average molecular weights and amounts of aromaticity of organic matter than the open lake site, P1. The terrestrially-impacted site, P2, mostly had values between these two extremes.

The e2/e3 ratios were calculated as described in Section 2.5c, and are used as surrogates for the average molecular weight and average aromaticity of DOM, with a lower e2/e3 ratio representing DOM with a higher molecular weight (De Haan and De Boer, 1987; Hiriart-Baer, 2013). For the filtered water fraction, the open lake samples (P1) had the highest e2/e3 ratios, which correspond with the lowest average molecular weights of DOM. Both terrestrially impacted sites (post-storm and pre-storm) sites (WP,

P2) had similar, lower e2/e3 ratios, indicating a higher average molecular weight and a higher aromaticity compared to DOM in open lake waters (Figure 3.2). When measuring the UV-Vis parameters for the autoclaved, whole water fraction, it is important to note that samples were note filtered and can thus be impacted by particulate material. The whole water fraction e2/e3 ratios followed the same inter-sample trend as the filtered water fraction. Compared to the filtered water e2/e3 ratios, the scatter-corrected whole water ratios were smaller, indicating that when POM was included in the measurement, there was a higher average molecular weight, which makes sense as larger molecules might be excluded in the filtered water fractions.

CDOM absorbances, which were calculated as described in Section 2.5c, are used to estimate CDOM content, where a higher value corresponds to a higher concentration of CDOM in the sample (Helms et al., 2008). As expected, the post-storm plume-impacted WP had the highest CDOM absorbance, followed by P2 and the open water site, P1 (Figure 3.2). Despite similar inter-site trends, the whole water samples have much higher backscatter-corrected particle absorbances compared to the filtered water samples, indicating particles make up a large percentage of the material absorbing UV and blue light, highlighting its importance to study.

As described in Section 2.5c, $SUVA_{254}$ is defined as the UV-absorbance at 254 nm divided by the DOC concentration in mg/L, and is used as a surrogate measurement for DOC aromaticity (Weishaar et al., 2003). An increase in $SUVA_{254}$ indicates an increase in the aromaticity of the sample. The open lake site, P1, had the lowest $SUVA_{254}$ values, meaning the DOC was the least aromatic in these samples compared to the in-plume sites. For the filtered water fraction, P2 and WP had similar $SUVA_{254}$ values, with

the P2 site (which was sampled before the storm) having slightly higher DOC aromaticity (Figure 3.2). For the whole water fraction, because the UV-Vis measurements were performed on whole water samples (so POM was included in the absorbance measurements), TOC concentration was used instead of DOC. Compared to the respective filtered water samples, all whole water $SUVA_{254}$ values were higher, indicating a larger degree of OM aromaticity when POM was included.

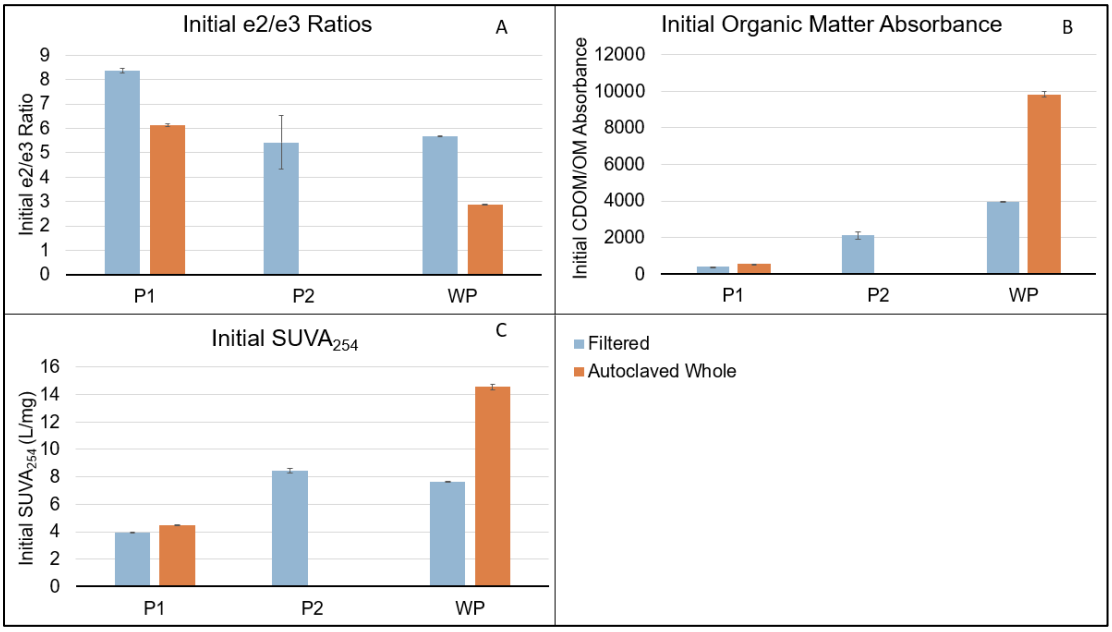

Figure 3.2. Initial UV-Vis parameters. (A) shows initial e2/e3 ratios for filtered and autoclaved whole fractions at each site. (B) shows initial organic matter absorbance from 250 nm to 400 nm for each fraction, and (C) shows initial $SUVA_{254}$ values. Error bars shown are calculated from the standard deviations of three replicates taken. The whole autoclaved P2 initial values are not shown due to an insufficient volume.

Initial nutrient samples also followed the hypothesized trends that the storm-impacted site would have the highest concentrations and the open-lake water site the lowest. For DOC initial concentrations, this held true for both filtered and autoclaved, then filtered water samples (Figure 3.3A) As was expected due to the low transparency of

the sample, DOC values were the highest for WP, the plume-impacted site that was sampled following a storm. P2, the plume-impacted site sampled before the storm, had the next highest DOC concentrations, and the open lake water site, P1, had the lowest DOC values (Figure 3.3A). When comparing the whole water vs the filtered water treatments from each site, the DOC concentrations for the whole water irradiations were similar to those of the filtered water irradiations. TOC concentrations were also quite close to the corresponding DOC concentrations for each sample, indicating that the majority of OC concentration can be attributed to the dissolved fraction.

TDN values for all sites ranged from 0.37 to 0.50 mg/L for the filtered water treatments and 0.38 to 0.57 mg/L for the whole water treatment. The WP plume-impacted site again had the highest concentrations and the open lake water site (P1) had the lowest concentrations (Figure 3.3B).The autoclaved, then filtered initial TDN concentrations are on average higher than the initials that were just filtered. It is possible that this is due to the autoclaving process, in which heat might have resulted in some particulate nitrogen breaking down into TDN or some desorption from the POM may have occurred.

Initial TN values in the whole water samples were also the highest at the storm-impacted site, and had values ranging from 0.38 to 0.53 mg/L for all three sampling sites (Figure 3.3B). There was one outlier, one of the dark replicates for WP Day 1, possibly due to contamination or sample heterogeneity.

Initial ammonium concentrations in the whole water samples were highest at the terrestrially-impacted site, P2, and lowest for the open lake site, P1 (Figure 3.3C). Unlike the previous nutrient concentration trends, the storm-impacted site, WP, did not have the highest ammonium concentration, potentially indicating that the storm runoff of the

August 5-7 storm did not contribute to an increase in ammonium to the lake. All sites that were able to be measured showed higher concentrations in the whole water samples compared to the corresponding filtered water samples.

Initial TDP concentrations for all three samples were consistently low, remaining below 0.013 mg/L, which is typical for Lake Superior samples, and close to the detection limit of the analytical method (0.003 mg/L). On average, P2 showed the highest initial concentrations of TDP in both filtered and whole water fractions (Figure 3.3D). The whole water TDP concentrations are higher in the plume-impacted sites compared to the filtered water values, which may indicate a release of TDP during the autoclaving process.

Initial TP concentrations in the whole water samples were the highest for the storm-impacted site, WP, by far, indicating a significant input of phosphorus to the lake during the August 5-7 storm event (Figure 3.3D). This differs from the filtered water samples, whose trend is difficult to discern due to low concentrations and overlapping precisions.

Initial SRP values during the filtered water irradiations were approximately 0.001 mg/L for all three sites (LOD = 0.0006 mg P/L). The initial SRP values in the whole water samples remained relatively consistent around 0.002 mg/L, which was slightly higher than the filtered water values, again potentially indicating a phosphorus release during the autoclaving process (Figure 3.3D).

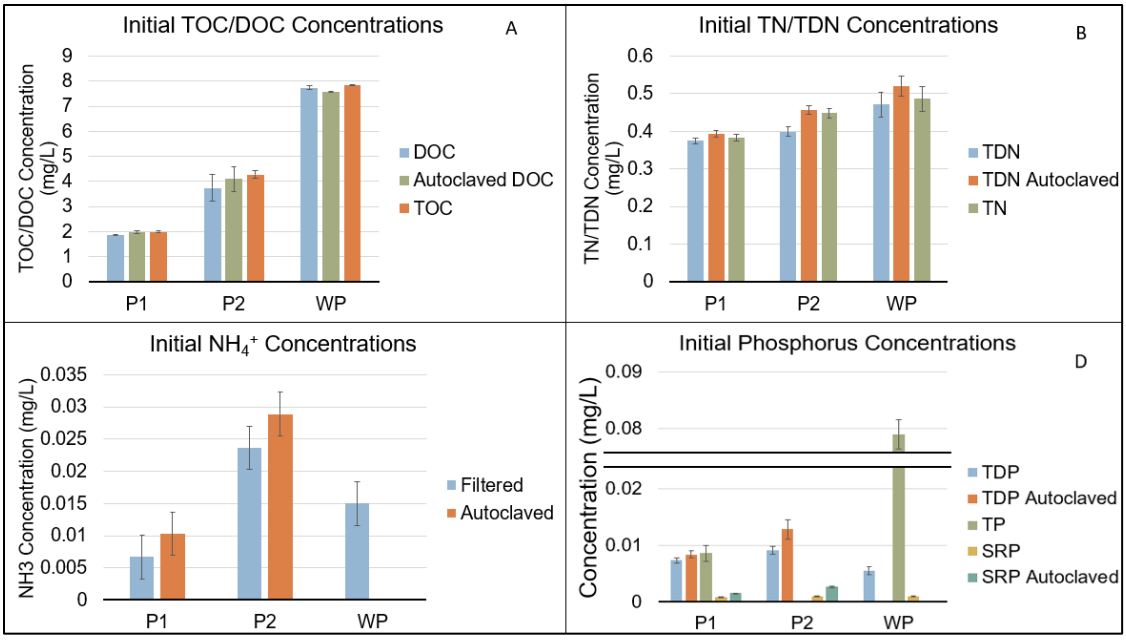

Figure 3.3. Initial values of nutrient concentrations in the filtered, autoclaved, thenfiltered, and autoclaved whole fractions. (A) shows initial DOC or TOC concentrations for filtered and whole fractions, respectively. (B) The error bars for A and B are calculated from the standard deviation of the three injections the Shimadzu took. (C) shows initial ammonia concentrations, with standard deviations taken from a representative Lake Superior sample run 14 times using the same method. (D) shows initial phosphorus concentrations, including TDP for both filtered and filtered autoclaved initial samples, TP for autoclaved whole initial samples, and SRP for both filtered and filtered autoclaved initial samples. Error bars shown are taken from the standard deviation of the three injections the AQ400 took. Some values are missing due to insufficient volume.

3.3 Nutrient Concentrations

a. DOC

The three-way ANOVA test for DOC concentrations only showed a significant one-way interaction with Site Location. DOC concentrations for samples during irradiations showed the same trend as the initial concentrations, with the storm-impacted site WP having the highest concentration and the open-water site, P1, having the lowest concentrations. The Tukey HSD tests confirmed these significant differences between site locations (Table S-53). According to these results, it is unlikely that any significant

changes in DOC are occurring in the filtered water irradiations for any of the sampling sites, and that the major factor determining DOC concentration is where the water is in the lake and any runoff events that have previously happened.

For the individual site analyses, only the DOC concentration of the P2 whole water DOC showed a significant increase in the dark treatment compared to both the light treatment and the initial sample, indicating a potential release of DOC from particles in the dark and, if the same process happens in the light, concurrent degradation of the DOC in the light sample. However, the extent to which this happened overall at all three sites appears to be insignificant.

Table 3.2. Three-way or two-way ANOVA p-values for DOC and TOC concentrations, respectively, on Day 3 of the irradiations.

Source	**DOC p-value**	**TOC p-value**
Site Location	<0.0001	<0.0001
Fraction	0.0725	
Light Treatment	0.9779	0.8715
Site Location*Fraction	0.0919	
Site Location*Light Treatment	0.4053	0.7597
Fraction*Light Treatment	0.2568	
Site Location*Fraction*Light Treatment	0.4608	

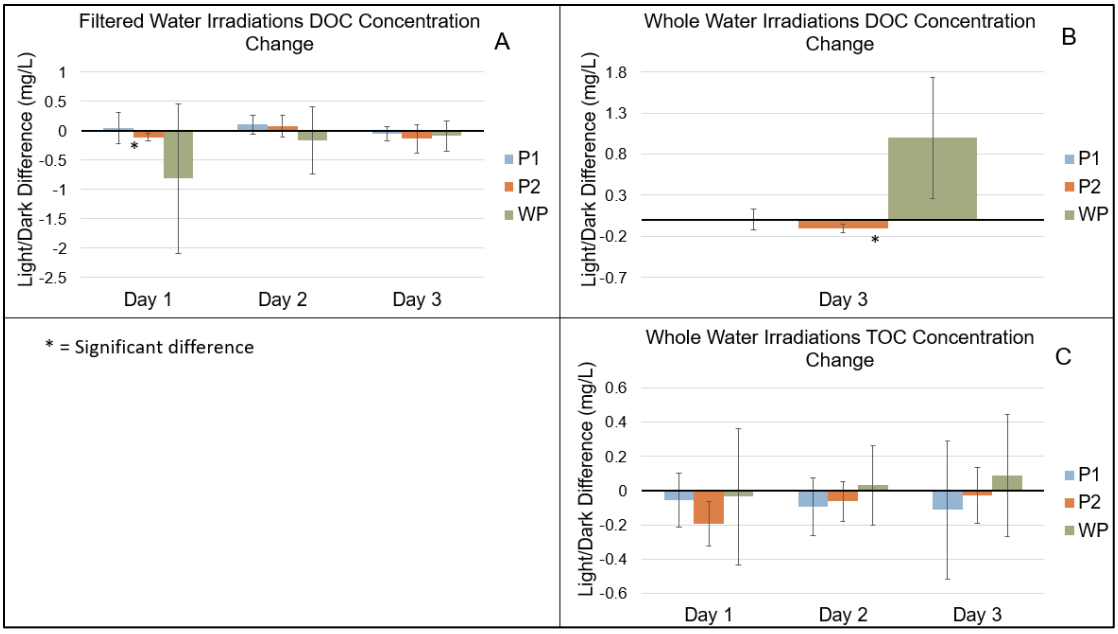

Figure 3.4. Total DOC/TOC concentration changes ([Light OC] – [Dark OC]) over irradiations for all three sites. (A) shows DOC concentration changes for the filtered water irradiations. (B) shows DOC concentration changes for the whole water irradiations, and (C) shows their TOC concentration changes. An asterisk indicates a significant difference between light and dark values as determined by a t-test. The error bars shown are calculated by propagating the errors of the original samples.

b. TDN/TN

The three-way ANOVA analysis for TDN showed significant contributions from each individual factor except for Site Location. This indicates that TDN concentrations were primarily determined by filtered vs. whole fraction and light vs. dark treatment, not where the sample was taken from. The presence of two-way and three-way interactions shows that effects on concentration varied depending upon all three different factors. Despite the ANOVA analysis showing significant interactions among factors, the Tukey HSD test indicated no honestly significant differences between any of the means, proving that TDN concentrations were not significantly altered over the course of irradiation. This also seen in individual t-tests as described in Section 2.5 (Figure 3.5). One important nuance to mention is that for the filtered water irradiations, samples were filtered before

irradiations had begun, as previous experiments had seen no significant difference between samples that were additionally filtered at the end of the irradiation versus ones that were not. For the whole water irradiations, TDN samples were filtered at the end of the experiment.

For the TN 2-way ANOVA analysis, a significant one-way interaction for Site Location but not Light Treatment was found, indicating TN concentrations were mainly determined by where the sample was taken. The Tukey HSD test further confirmed this, showing that there were significant differences between each site's TN concentrations. However, irradiations resulted in no significant concentration change for this variable (Figure 3.5).

Table 3.3. Three-way or two-way ANOVA p-values for TDN and TN concentrations, respectively, on Day 3 of the irradiations.

Source	**TDN p-value**	**TN p-value**
Site Location	0.2315	<0.0001
Fraction	0.0024	
Light Treatment	0.0009	0.1528
Site Location*Fraction	0.0145	
Site Location*Light Treatment	0.0001	0.5548
Fraction*Light Treatment	0.0006	
Site Location*Fraction*Light Treatment	<0.0001	

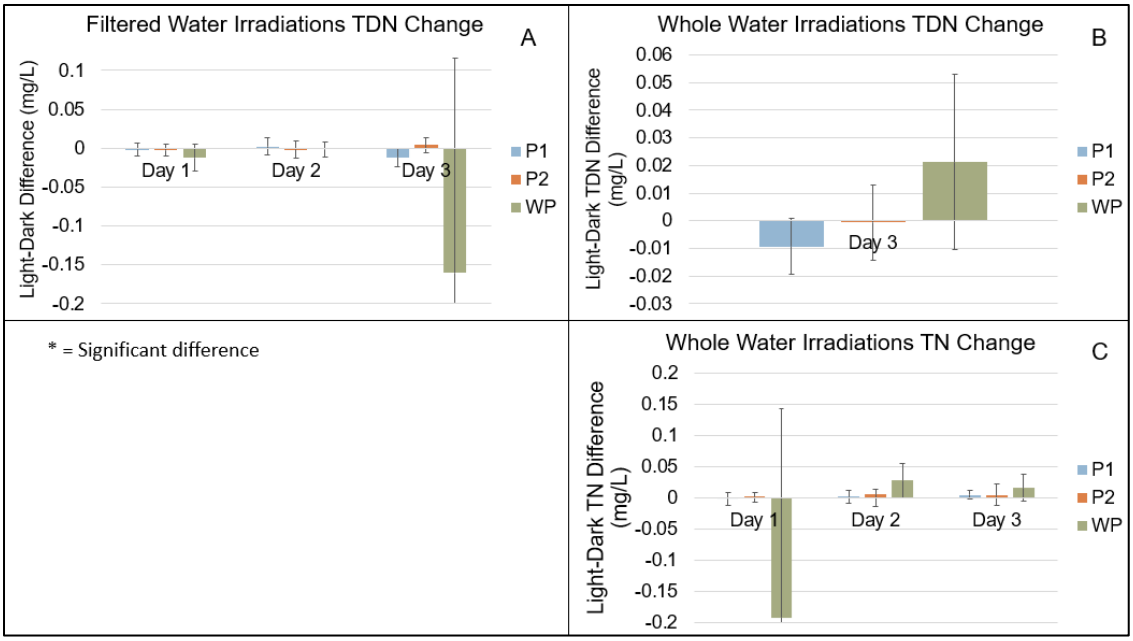

Figure 3.5. Total TDN/TN concentration changes over irradiations for all three sites ([Light] – [Dark]). (A) shows TDN concentration changes for the filtered water irradiations. (B) shows TDN concentration changes for the whole water irradiations, and (C) shows their TN concentration changes. An asterisk indicates a significant difference between light and dark values as determined by a t-test. The error bars shown are calculated by propagating the errors of the original samples.

c. UV-Visible spectroscopy:e2/e3 ratio

Three way ANOVA analyses for the e2/e3 ratios showed that all interactions for the three factors were significant, except for the two-way interaction between Site Location and Light Treatment (Table 3.4). This indicates that the effect that Site Location had on the ratios was the same between light and dark treatments. The Tukey HSD test found significant differences between all paired means for Site Location and Fraction, but not for Light Treatment, which means that overall, these former two factors have the most effect on e2/e3 ratios across the entire data set.

When individual t-tests were performed for the filtered water irradiations, a significant difference was found between all light and dark samples for P2 and WP, but

not for P1 (Figure 3.6). These tests show that e2/e3 ratios increased in both irradiation sites affected by storm plumes or terrestrial runoff in the light replicates compared to the dark controls, which corresponds to a decrease in molecular weight and aromaticity of the CDOM in the sample over the irradiation period. Additionally, a significant difference was found between initial and final (both light and dark) samples for WP, indicating that some other process in addition to UV exposure is affecting e2/e3 ratios.

For the whole water irradiations, significant increases in the light sample values compared to dark treatments were found for all samples except the first two days of irradiation of WP using the t-tests described in Section 2.5. This indicates that for whole water irradiations, all sites, including the open water site, showed signs of decreasing CDOM molecular weight and aromaticity (Figure 3.6). There was also a significant difference between initial and final dark samples for the P1 site, showing that in addition to UV exposure, some other factor was affecting e2/e3 ratios in the whole water open lake sample.

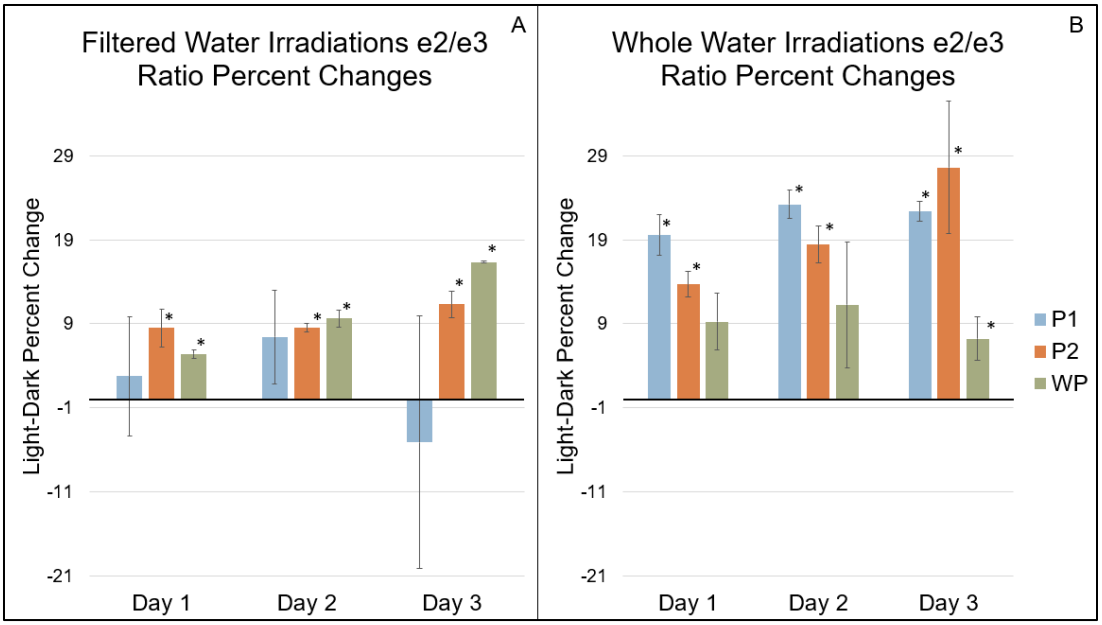

Figure 3.6. Percent changes of e2/e3 ratios ([{light-dark}/dark]*100) over irradiations for all three sites. (A) shows percent changes for the filtered water irradiations, and (B) shows percent changes for the whole water irradiations. An asterisk indicates a significant difference between light and dark values for the original values (not the percent change) as determined by a t-test. The error bars shown are calculated by propagation as described in Equation 2.3.

d. UV-Visible Spectroscopy: OM Absorbance

The three-way ANOVA analysis for OM absorbance showed significant interactions for all combinations of factors except for the three-way interaction (Table 3.4). The Tukey HSD tests found significant differences between paired means for Site Location and Fraction, but not for Light Treatment, mirroring findings for the e2/e3 ratios (Section 3.4c).

For the filtered water irradiations, the t-tests described in Section 2.5 found significant decreases in CDOM absorbance in the light compared to dark samples for sites WP and P2 on each day of the irradiation. For site P1, only the second day of sampling showed a significant difference between light and dark samples (Figure 3.7). For the whole water irradiations, a significant decrease in light samples compared to the

dark controls was shown for all samples except the first two days of the WP irradiation. This indicates that for the whole water fraction, OM was being significantly photobleached in all irradiations, including the open lake site, P1.

For the filtered water irradiation, when comparing the final light and dark samples to the initial samples, WP showed a significant difference between initial and light, and initial and dark pairs. Since there was a significant difference between the final light and dark samples, it was expected there would also be a significant difference between the final light and initial samples. However, the significant increase between the initial and final dark sample indicates that some other process other than UV exposure is affecting CDOM at this site. For the whole water irradiations, a significant difference between the initial P1 sample and the final dark control was found, showing that some other factor was affecting the open lake whole water sample's OM.

Also interesting to note was the OM absorbance trend for the WP whole water site. For the first two days, it appears that both light and dark values decrease compared to the initial sample, and then increase. However, additional F- and t-tests between the Day 2 samples and the initial reveal that there is a significant difference between the initial and Day 2 light, but not between the initial and Day 2 dark sample. In other words, there is a significant decrease of OM absorbance in the light sample over the first 2 days of the irradiation. Comparing the Day 2 and Day 3 light samples reveals a significant increase in OM absorbance. Therefore, for WP's OM rich sample, there is a decrease in absorbance over the first two days of irradiation, but during the third, some other process, perhaps coagulation of DOM, attributed to an increase in OM absorbance (Chin et al., 1998).

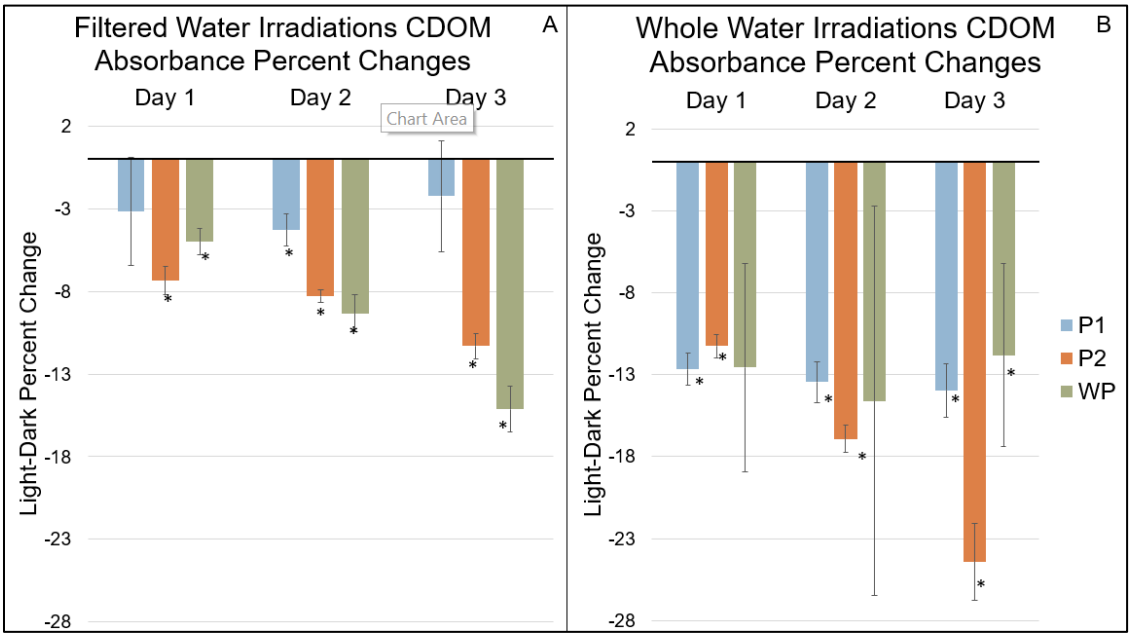

Figure 3.7. Percent changes of OM absorbance over irradiations for all three sites ([{light-dark}/dark]*100). (A) shows percent changes for the filtered water irradiations, and (B) shows percent changes for the whole water irradiations. An asterisk indicates a significant difference between light and dark values for the original values (not the percent change) as determined by a t-test. The error bars shown are calculated by propagation as described in Equation 2.3.

e. UV-Visible Spectroscopy: $SUVA_{254}$

For $SUVA_{254}$, the three-way ANOVA analysis revealed significant interactions between all factors except for the three-way interaction and the two-way interaction between Fraction and Light Treatment. This means that the effect of filtered vs. whole water fractions was the same for light and dark treatments. The Tukey HSD test showed that there was no significant difference between $SUVA_{254}$ values for the WP and P2 sites, but there was between these sites and the open-lake site, P1. There was also a significant difference between paired means for the filtered vs. whole water fraction, but not the light vs. dark treatment.

Using the same F and t-tests as described in Section 2.5, site WP's filtered light irradiation saw a significant decrease in $SUVA_{254}$ on Day 3 of the experiment compared to the dark control, indicating a decrease in DOM aromaticity for this site (Figure 3.8). Both dark and light endpoints were also significantly different than the initial value, which further supports the suspicion that some other factor beside UV treatment (sorption, perhaps?) is affecting DOM in this sample.

For the whole water irradiations, a significant difference was found between the light and dark treatments for site P2 for days 2 and 3, but without the initial sample, which was not taken due to volume constraints, it is impossible to tell for sure whether this was an increase or decrease from the original sample. It appears, however, that over the irradiation, light values continued decreasing compared to the dark controls, with a -9.69% change on Day 2 and a -13.1% change on Day 3 of the irradiation. Finally, there was a significant decrease in WP's final light sample compared to the initial, indicating a decrease in DOM aromaticity in this site's light treatment.

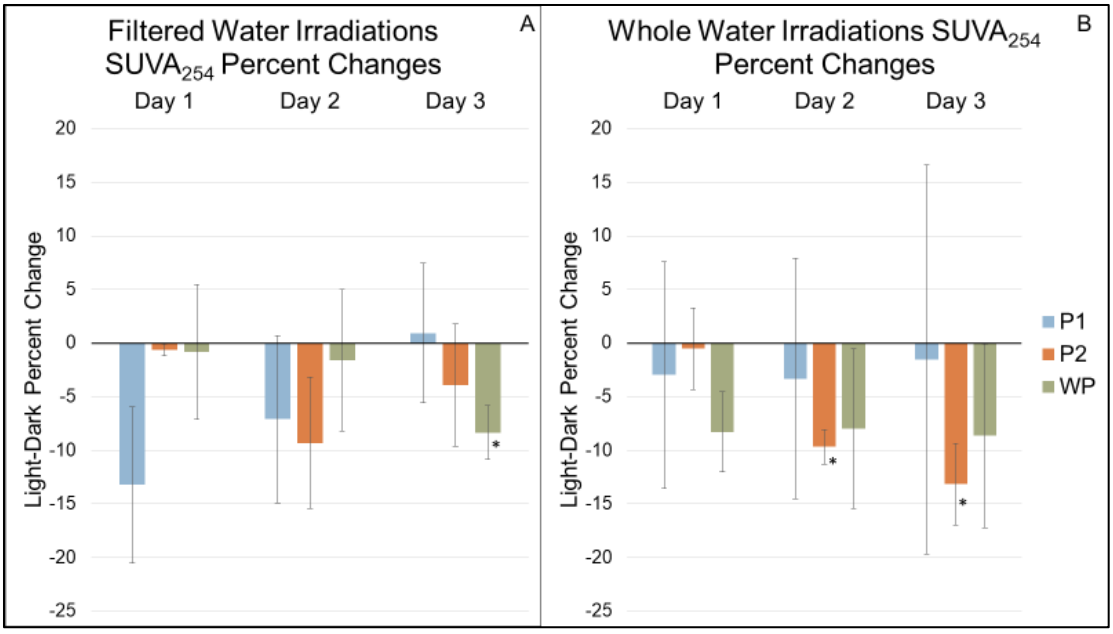

Figure 3.8. Percent changes of $SUVA_{254}$ over irradiations for all three sites ([{light-dark}/dark]*100). (A) shows percent changes for the filtered water irradiations, and (B) shows percent changes for the whole water irradiations. An asterisk indicates a significant difference between light and dark values for the original values (not the percent change) as determined by a t-test. The error bars shown are calculated by propagation as described in Equation 2.3.

Table 3.4. Three-way ANOVA p-values for UV-Vis parameters on Day 3 of the irradiations.

Source	**e2/e3 p-value**	**CDOM p-value**	**$SUVA_{254}$ p-value**
Site Location	<0.0001	<0.0001	<0.0001
Fraction	<0.0001	<0.0001	<0.0001
Light Treatment	<0.0001	<0.0001	0.0009
Site Location*Fraction	<0.0001	<0.0001	<0.0001
Site Location*Light Treatment	0.1403	<0.0001	0.0478
Fraction*Light Treatment	0.0053	0.0037	0.0812
Site Location*Fraction*Light Treatment	0.0001	0.1704	0.5394

f. Ammonium

The three-way ANOVA analysis for ammonium showed that there were significant one-way interactions for Site Location and Fraction, but not for Light

Treatment. Tukey HSD tests, which included both filtered and whole water treatments, found significant differences between paired means for P1-WP and P1-P2, but not for P2-WP. The paired means between the whole water vs. filtered water treatments were also significantly different, but not those between the light and dark treatment (Table S-53).

Using the F- and t-tests as described in Section 2.5, there are no significant differences between light and dark samples in the filtered water irradiations except for the P1 site. At the end of the irradiation, the P1 light sample had significantly less NH_3 than the dark treatment. At first glance, it appears that ammonia concentration may be increasing in the dark treatment, but there was no significant difference found between the initial sample and the dark final sample. Additionally, there was no significant difference between the initial sample and light final sample either.

For the whole water irradiations, there was a significant increase in ammonia concentrations in the P2 light treatment compared to the dark control. This indicates a release in ammonia in P2's light treatment during the irradiation. The rest of the sites showed no significant differences between light and dark treatments or initial and final samples. However, it is important to note that because WP's whole water samples were above the maximum fluorescence that the benchtop method could detect, a different method had to be used (as described in Section 2.5d). This method, using the AQ400, was not as precise as can be seen from the error bars on the WP points (Figure 3.16). The detection limit of this methods has been reported to be 0.004 mg N/L, where the benchtop method has a detection limit of 0.001 mg N/L (*EPA-103-A Rev. 10. Ammonia-N in Drinking and Surface Waters, Domestic and Industrial Wastes*, 2012; Taylor et al., 2007). Still, the change in methods was not expected to make this much of a difference.

The larger error in replicates of the AQ400 method could be from the change in technique or could possibly indicate that the WP whole water sample was quite heterogenous despite being shaken before analysis. In either case, a possible light-induced increase in ammonia for site WP may have been obscured by the precision of the method used to analyze these samples.

Table 3.5. Three-way ANOVA p-values for NH_3 concentrations on Day 3 of the irradiations.

Source	**NH_3 p-value**
Site Location	0.0021
Fraction	0.0008
Light Treatment	0.6992
Site Location*Fraction	0.0882
Site Location*Light Treatment	0.6536
Fraction*Light Treatment	0.7413
Site Location*Fraction*Light Treatment	0.9135

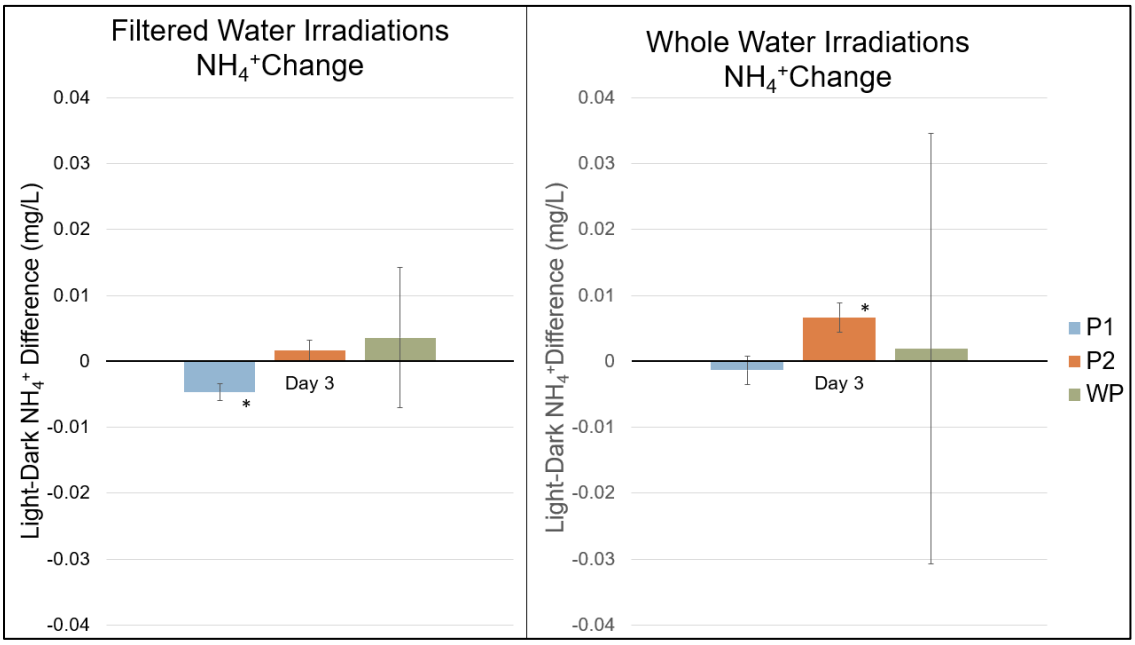

Figure 3.9. Light-dark differences of NH_4^+ over irradiations for all three sites. (A) shows total changes for the filtered water irradiations, and (B) shows total changes for the whole water irradiations. An asterisk indicates a significant difference between light and dark

values as determined by a t-test. The error bars shown are calculated by propagating the errors of the original samples.

g. TDP

Three-way ANOVA analyses revealed significant one-way interactions for TDP's Site Location and Fraction, as well as a significant two-way interaction for Site Location*Fraction. TP's two way-ANOVA test, on the other hand, only had a significant one-way interaction for Site Location. Tukey HSD tests indicated that TP had significant differences between paired means for all three sites, but TDP only had a significant difference between P1-WP and P1-P2. There was also a significant difference between paired means for the filtered vs whole water treatments for TDP. These results indicate that the most important factors influencing TDP concentrations were whether the site was terrestrially-impacted or not, and the filtering process that the sample went through.

When comparing light and dark samples for TDP using the same F and t-tests as in Section 2.5, there were no significant differences for any of the sites. There were also no significant differences between any of the initial and final values, indicating that any TDP changes are negligible during irradiations.

For TP (whole water) concentrations, both the P1 and P2 sites showed no significant differences between light and dark treatments or initial and final samples. For site WP, a significant decrease in TP concentration was found between the initial and final samples for both light and dark treatments, but it is suspected that this is due to the large amounts of sediment in this sample settling over the three-day irradiation and insufficient shaking prior to analysis.

Table 3.6. Three-way and two-way ANOVA p-values for TDP and TP concentrations, respectively, on Day 3 of the irradiations.

Source	TDP p-value	TP p-value
Site Location	<0.0001	<0.0001
Fraction	<0.0001	
Light Treatment	0.1257	0.6559
Site Location*Fraction	<0.0001	
Site Location*Light Treatment	0.1740	0.5126
Fraction*Light Treatment	0.7368	
Site Location*Fraction*Light Treatment	0.6036	

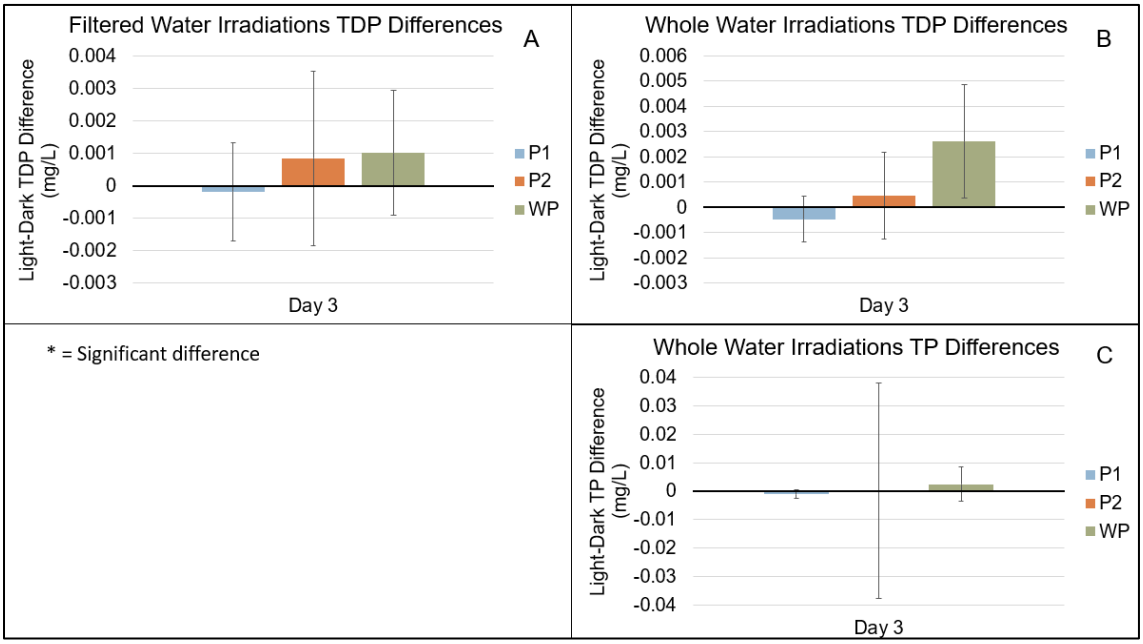

Figure 3.10. Total TDP/TP concentration changes (light-dark) over irradiations for all three sites. (A) shows TDP concentration total changes for the filtered water irradiations. (B) shows TDP concentration total changes for the whole water irradiations, and (C) shows their TP concentration total changes. An asterisk indicates a significant difference between light and dark values as determined by a t-test. The error bars shown are calculated by propagating the original concentration errors.

h. SRP

For the SRP concentrations at the end of irradiations, fraction appeared to play the most important role. The three-way ANOVA found that there were significant

interactions for Fraction and the two-way interactions Fraction*Light Treatment and Site Location*Fraction. Tukey HSD tests saw no significant differences between paired means except for the filtered vs. wholetreatments.

T-tests showed no significant differences between light and dark treatments for whole water irradiations, and there were no significant differences between initial and final samples, indicating no significant changes in SRP concentrations over the irradiation for any of the sampling sites. These findings, combined with those from the three-way ANOVA, show that fraction is the most important factor influencing SRP concentration. The fact that the whole water concentrations were overall higher than the filtered water values could support the theory that there was some phosphorus release during the autoclaving process.

Table 3.7. Three-way ANOVA p-values for SRP concentrations on Day 3 of the irradiations.

Source	**SRP p-value**
Site Location	0.3407
Fraction	<0.0001
Light Treatment	0.3105
Site Location*Fraction	0.0137
Site Location*Light Treatment	0.0940
Fraction*Light Treatment	0.0483
Site Location*Fraction*Light Treatment	0.6110

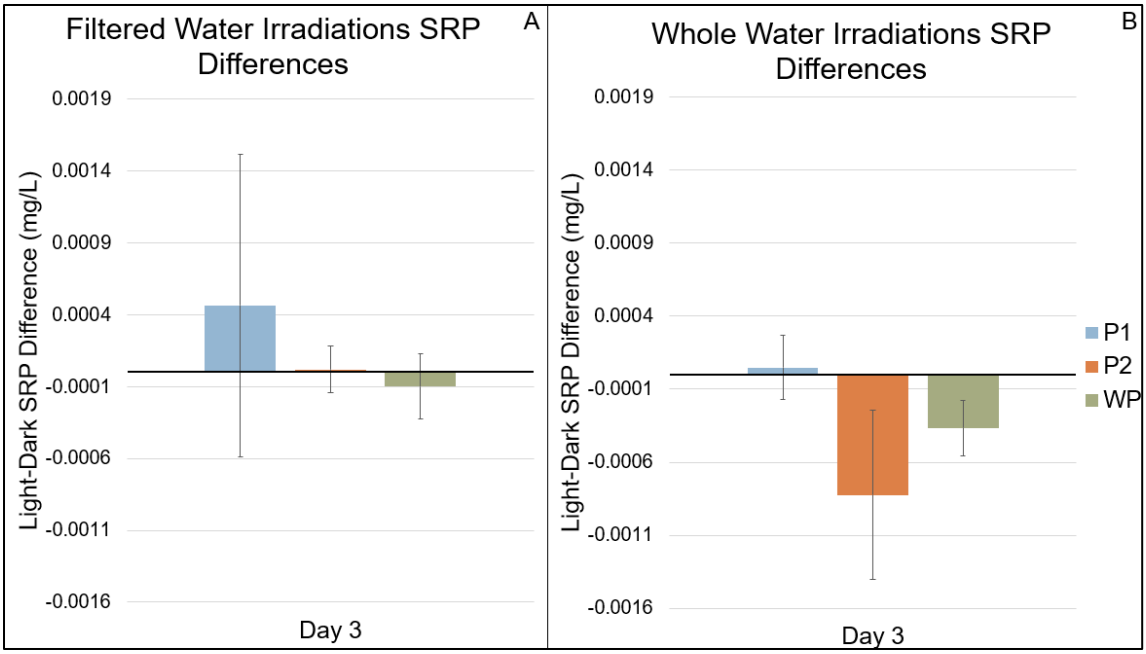

Figure 3.11. Light-dark differences of SRP over irradiations for all three sites. (A) shows total changes for the filtered water irradiations, and (B) shows total changes for the whole water irradiations. An asterisk indicates a significant difference between light and dark values as determined by a t-test. The error bars shown are calculated by propagating the errors of the original samples.

3.4 Kinetics Calculations

As described in Section 1.4, the kinetics of CDOM decrease as a function of light dose were able to be modeled using Equations 1.1 and 1.2. These values were calculated for our experiments, although it should be noted that for the whole water irradiations, the UV-Vis samples were not filtered but were corrected for particle effects, so absorbances include all absorbing matter, not just dissolved, and which we assume to be mainly organic matter(Table 3.8). For k_{ABS}, the absorption coefficients for the initial and final light samples were integrated from 250 to 400 nm using the UV-Vis samples, which was the same range used for CDOM absorbance (Kruger et al., 2011). The cumulative energy

received during the irradiation (E) was taken from the radiometer data from 250 to 700 nm shown in Table 3.1.

Table 3.8. k_{ABS} rate constants for filtered and whole water irradiations. The rate constants for the P2 whole water irradiation were unable to be calculated due to a lack of initial replicates.

Site	**Filtered Water Irradiations k_{ABS} (m^2/MJ)**	**Filtered Water Irradiations Average k_{ABS} (m^2/MJ)**	**Whole Water Irradiations k_{ABS} (m^2/MJ)**	**Whole Water Irradiations Average k_{ABS} (m^2/MJ)**
Photochemistry Blue (P1)	0.002528 0.004988 0.004825	0.004 ± 0.001	0.01410 0.01497 0.01600	0.015 ± 0.001
Photochemistry Brown (P2)	0.01614 0.006870 0.006374	0.009 ± 0.006		
Wisconsin Point (WP)	0.007717 0.007676 0.008178	0.0079 ± 0.0003	0.006652 0.005245 0.005764	0.0059 ± 0.0007

Equation 1.2 was used to calculate k_λ from 200 to 450 nm (Figures 3.12 and 3.13). Again, the cumulative energy received during the irradiation (E) was found using the radiometer data from 250-700 nm (Table 3.1). The three initial values were paired with the three final light samples on Day 3 to calculate three k_λ values, which were averaged. The standard deviations are indicated by the error bars, and show that uncertainty in the measurement increases as wavelength increases.

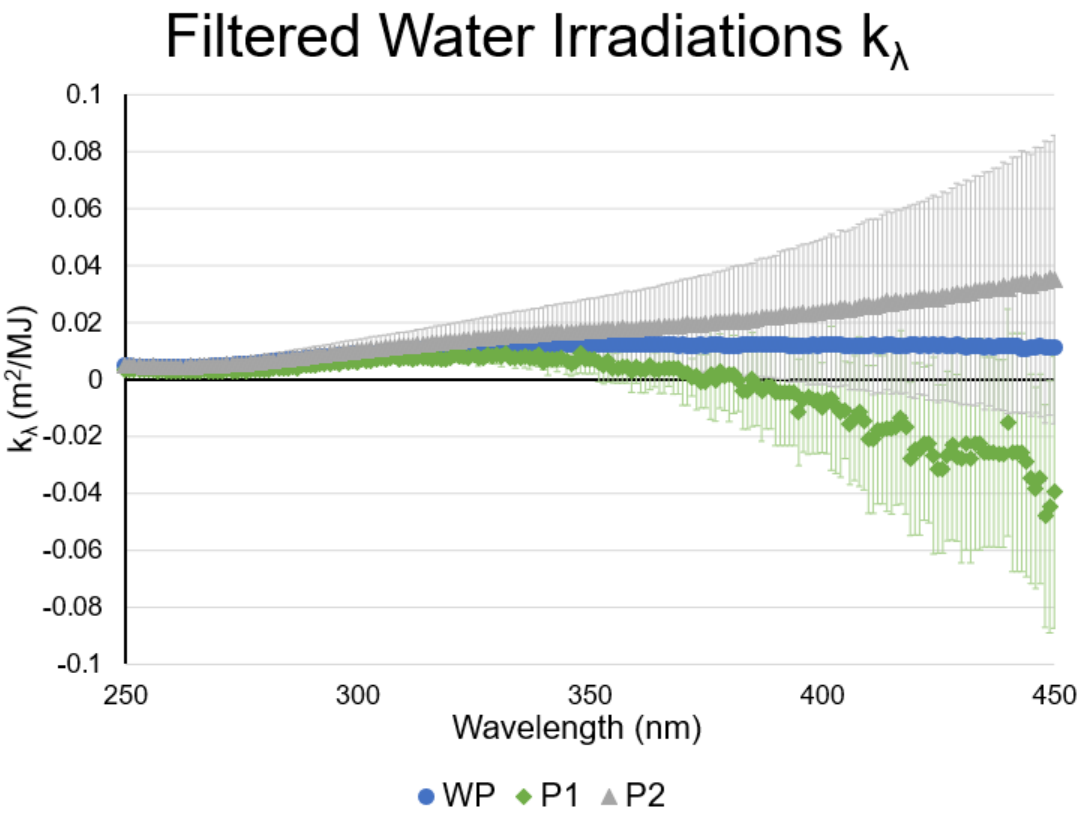

Figure 3.12. Filtered water irradiations k_λ rate constants averages from 200 to 450 nm. Error bars shown are calculated from the three k_λ values calculated from the three UV-Vis replicates.

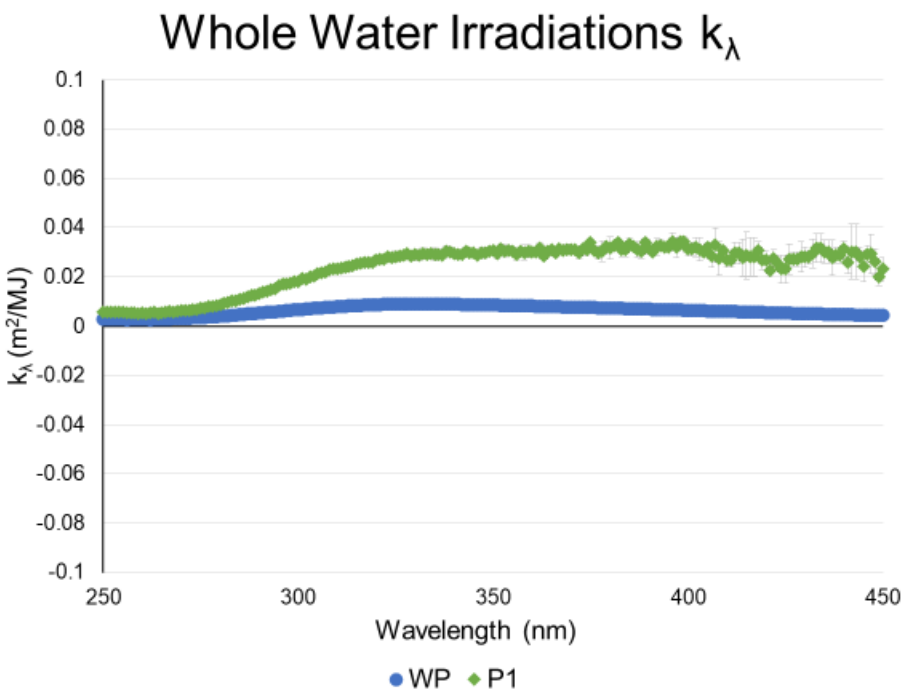

Figure 3.13. Whole water irradiations k_λ rate constants averages from 200 to 450 nm. Error bars shown are calculated from the three k_λ values calculated from the three UV-Vis replicates.

Chapter 4. Discussion

4.1 Photochemical Release of Nutrients

It was hypothesized that photodegradation would result in the release of bioavailable nutrients, specifically ammonia and dissolved phosphorus. It was expected that this might occur to a greater extent in the storm-impacted and terrestrially-impacted site compared to the open-lake water site. While no dissolved or soluble reactive phosphorus releases were found due to light treatment, there was an ammonium release found in the whole water, terrestrially-impacted site sampled before the storm.

Potential mechanisms that could lead to a change in ammonium concentration include nitrification and photoammonification. Nitrification was not expected to occur in our samples due to the fact that the majority of bacteria were removed. Photoammonification, as discussed in Section 4.2, occurs when CDOM is photodegraded under UV light, releasing ammonium. Previous studies have found ammonium to be photoproduced in areas such as the Baltic Sea (Aarnos et al., 2012; Stedmon et al., 2007).At a high enough pH can become ammonia and leave the sample as a gas, reducing TDN concentrations, but the pH of our samples was likely not high enough for this to happen because there were no significant losses of TDN (Tarr et al., 2001; Zhang et al., 2013).

For the whole water irradiations, a significant increase in ammonium concentration was observed in the P2 light treatment compared to the dark control. Additionally, there is a possibility that a similar increase could have occurred in WP that is obscured by the lack of precision of the alternative method used as discussed in Section 3.3f. It is not completely clear what caused this increase in ammonium concentration. As

discussed in Section 4.2, photoammonification of DOM is unlikely as there are no significant increases in ammonium concentrations in filtered water samples. Because POM is included in the whole water samples, it is also possible that ammonium could have been released directly from these particles or by interactions of DOM with components of these particles. As discussed before, it is suspected that WP could have had a higher iron concentration due to runoff following the storm. Previous literature has shown that metal cations such as iron are important for DOM aggregate's integrity (Chin et al., 1998). During photodegradation, the binding strength of organic ligands to iron decreases (Powell and Wilson-Finelli, 2003). If these bonds in POM were to break apart, and then iron was precipitated, preventing reaggregation (as iron has been shown to flocculate with DOM to produce POM), it is possible that ammonium could be part of the ligands now free in the solution (He et al., 2016). Another study also showed that photolysis of DOM can result in the reduction of iron, which causes disaggregation (Voelker et al., 1997). Again, if ammonium was trapped in POM particles, this could explain the release in only the whole water irradiations. It is not possible to tell from this data if these processes were occurring; future studies should measure iron to determine if there were high enough concentrations for this to occur. Another possibility is that with iron present, there could have been direct photolysis of Fe-CDOM carboxylate complexes via a ligand-to-metal charge transfer. This reaction creates ROS, which could have oxidized OM to form products such as ammonium. Previous studies have demonstrated the photorealease of ammonium under similar conditions with naturally occurring iron (Gao and Zepp, 1998). However, this is the first study to the author's knowledge that

demonstrates that a photorelease of ammonium may be happening in Lake Superior in terrestrially-impacted waters.

For both TP/TDP and SRP measurements, all the irradiations showed no significant changes between light and dark treatments, indicating that phosphorus is minimally effected by UV irradiation in these Lake Superior samples. Previous studies have shown an increase in PO_3^{4-} concentrations when autoclaved resuspended sediment was exposed to UV irradiation (Li et al., 2017). Another study also showed the release of TDP from photodegraded CDOM but remarked that phenomenon was not widespread across all lake types, and that it seemed to be observed in humic-rich lakes more often (Zhang et al., 2013). Lake Superior, with its low phosphorus concentrations, probably does not have enough phosphorus incorporated into CDOM to cause a substantial increase in concentrations upon photodegradation.

For the whole water irradiations, a significant decrease in TP concentration for the storm-impacted site (WP) was found between the initial and final samples for both light and dark treatments. This is most likely due to the sediment settling in the storm-impacted WP whole water samples and insufficient mixing, as TP concentrations are not expected to change over an irradiation.

4.2 Whole vs. Filtered Water Treatments

The second hypothesis to consider was that whole water samples would undergo more photodegradation than filtered water samples as measured by total and percent changes in UV-Vis parameters and DOC concentrations due to the inclusion of POM. For the UV-Vis parameters, generally a larger percent change was found in whole water

samples for all sites expect for the storm-impacted site, WP. For the most part, there were not significant changes in the DOC concentrations due to light treatment.

a. DOC/TOC

With the inclusion of POM in the whole water irradiations, there are a few mechanisms in which DOC concentrations might change in light exposed or dark control samples Mechanisms through which POC produces DOC are through dissolution, desorption, photo-dissolution, and biodegradation (He et al., 2016). DOC can also produce POC via aggregation, coagulation, adsorption, and photo-flocculation (He et al., 2016). Photo-flocculation and photo-dissolution are of the most interest in this experiment since they would be expressed in the differences between light and dark treatments.

During the irradiations, there was little change in DOC or TOC concentrations. DOC concentrations might be expected to decrease as DOC was photodegraded into DIC, as previous literature has often shown a decrease in DOC concentrations over similar filtered water irradiations (Larson et al., 2007; Macdonald and Minor, 2013; Minor and Stephens, 2008; Porcal et al., 2013). The only significant DOC concentration decreases occurred in the Day 3 whole water and Day 1 of the filtered fraction for Site P2. These findings indicate that light exposure may be affecting both filtered and whole water treatments, but not to a large enough extent that it is able to be seen with the precision of current instrumentation.

b. TN/TDN

TOC concentrations would change if any organic carbon in the sample was converted to inorganic carbon. Again, this process does not seem to be occurring to a significant extent

for this study. As the Tukey HSD tests showed, site location and whether the water is whole or filtered plays a much larger role in determining DOC concentrations.

None of the irradiations in this study resulted in a significant difference of TN or TDN concentrations between light and dark treatments. No TN changes were expected because the total amount of nitrogen is unlikely to change in an oxic sample. Potential routes of TN loss include denitrification, which occurs when organic matter is oxidized via the reduction of NO_3^- or NO_2^- and yields a comparable energy to aerobic respiration for bacteria, but this process requires anaerobic conditions (Valiela, 1995). In oxic environments aerobic respiration dominates, and because our samples were kept open to the air (albeit covered), it is unlikely that denitrification would be leading to a loss of TN.

Another mechanism that might cause a loss of TN and TDN that has been suggested is photoammonification, in which CDOM is photodegraded to form the ammonium ion. Ammonium exists in equilibrium with ammonia if pH is high enough, and ammonia can then be released into the atmosphere as a gas (Tarr et al., 2001; Zhang et al., 2013). Photoammonification results in an increase in ammonium concentration accompanied by a decrease in TDN concentration, and was observed in humic water samples and samples from China's Lake Taihu watershed (Tarr et al., 2001; Zhang et al., 2013). Our study did not observe a significant decrease in any TDN concentrations. It's is likely that the pH of Lake Superior is not high enough for ammonia to be present, and therefore escape into the atmosphere. It can also be noted that the Lake Taihu nitrogen concentrations were much higher than Lake Superior's, at concentrations of 1.2 to 5.1 mg/L, where Lake Superior's did not exceed 0.6 mg/L for the most part. It is possible that Lake Superior concentrations are too low for this mechanism to have a significant impact, especially

since the majority of TDN in this lake is made up of nitrate, not ammonium (J. B. Cotner et al., 2004; Sterner et al., 2019). Future studies may benefit from including nitrate/nitrite measurements in addition to other nitrogen parameters.

c. UV-Vis parameters

e2/e3 ratios have been shown to be inversely proportional to molecular size and aromaticity of the DOM being measured (Dalzell et al., 2009). An increase in the e2/e3 ratio over an irradiation period implies that DOM with higher molecular weights and higher aromaticity is being preferentially photodegraded by UV light, leaving behind a DOM population with a lower average molecular weight and aromaticity. Almost all irradiations in this study showed an increase in e2/e3 ratios in the light treatment compared to the dark controls, except for the filtered water P1 site. Therefore, in all of the irradiations except for the filtered open water sample, UV irradiation led to a decrease in molecular weight and aromaticity of the CDOM or OM in the sample. Comparing the whole water treatment to the filtered water one, both P1 (Filtered: -5.1%, Whole: 22.3%) and P2 (Filtered: 11.3%, Whole: 27.6%) experienced larger percent changes in the whole water irradiations as predicted. WP experienced larger percent changes in the filtered water irradiations (Filtered:16.3%, Whole: 7.2%). This is hypothesized to be because of the larger, visible particles in the whole water, storm-impacted samples. The amount and size of the particles most likely impaired UV-light penetration into the sample via absorption, reflection, and refraction, resulting in a smaller percent change of e2/e3 ratios (Osburn et al., 2009).

OM absorbance calculations confirmed the conclusions from the e2/e3 data, with almost all of the irradiations showing a significant decrease in CDOM absorbance in the

light treatments compared to the dark controls, indicating the photodegradation of CDOM (or OM for the whole water) over the irradiation. The only site that did not exhibit a significant decrease was the filtered P1, the open water site. Both P2 (Filtered: -11.3%, Whole –24.4%), and P1 (Filtered: -2.29%, Whole: -14.0%) had higher percent changes for the whole water irradiations as expected. However, the storm-impacted site, WP, exhibited the opposite relationship: the whole water irradiation had a smaller percent change than the filtered water (Filtered: -15.1%, Whole: -11.8%). This finding further indicates that POM in the storm-impacted site shielded DOM from further photodegradation via altering the light penetration via absorption, reflection, and refraction.

A significant decrease in $SUVA_{254}$ values occurred during the irradiation of P2, indicating a decrease in OM aromaticity for this site. The same trend was not found in the storm-impacted site, WP. This, along with the significant decrease in WP in the filtered treatment, is alsoconsistent with the hypothesis that light attenuation led to the reduction of photodegradation in this sample as has been shown in previous studies of particle-rich waters (Osburn et al., 2009).

4.3 Plume vs. Open Lake Waters

The final hypothesis that was considered was that plume waters would undergo more photodegradation than open lake waters in terms of total and percent changes in UV-Vis parameters, DOC and nutrient concentrations. This hypothesis was mostly proven to be true in terms of percent changes in UV-Vis parameters, expect for in the case of the storm-impacted whole water irradiation (WP).

As stated in Section 4.2, there were few cases of significant differences in DOC concentrations. This was unexpected for the P2 and WP sites, as previous literature has often shown a decrease in DOC concentrations over similar filtered water irradiations (Larson et al., 2007; Macdonald and Minor, 2013; Minor and Stephens, 2008; Porcal et al., 2013). Previous studies in our lab have shown decreases in DOC concentrations in photodegradation experiments for Lester River mouth (located on Lake Superior's shore) samples and five trout streams in the Lake Superior watershed (Macdonald and Minor, 2013; Minor and Stephens, 2008). Therefore, while it was hypothesized that the open lake sample, P1, would not have a significant difference in DOC concentrations, it was thought that the storm-impacted WP sample would be similar in DOM composition to these terrestrially-impacted samples in previous studies and would thus exhibit similar photodegradation. However, this was not shown by our data.

There are a few potential explanations for the absence of DOC loss in the filtered water irradiations, the most likely being that there was not enough photodegradation of DOC into DIC happening to register as significant on our instrumentation. The total irradiance received by the samples was smaller than the aforementioned studies: our irradiations received 9.48 to 10.8 MJ/m^2 over the experiment (400-700 nm), and the Macdonald and Minor 2013 study irradiations received 16.8 to 20.1 MJ/m^2 (400-1,110 nm). Therefore, it is possible that the MacDonald and Minor irradiations experienced more irradiance from light in the UV-light region as well, but that data was not reported. However, the Porcal et al. 2013 study (which used a Suntest XLS+ solar simulator to simulate irradiation at sea level with an intensity of 700 W/m^2) was able to show a decrease in DOC concentration by the time their experiments reached our cumulative

irradiation energies. There are several possible reasons for this. One, their simulator may have provided a larger proportion of UV-light than was available at ~47°N during our natural light irradiations. Two, our sample containers for the irradiation had longer pathlengths for light into the samples. The Porcal study used Teflon tubes with a smaller diameter, which compared to our baking pans, may have had more light penetration. Three, our samples' organic matter characteristics and inorganic light sensitive components may have differed in quantity and quality. For example, the DOC in this study's samples may have been less oxidized than previous studies, which could result in the irradiations only causing photodegradation into LMW species without actually releasing DIC.

As for the UV-Vis parameters, as stated in Section 4.2, e2/e3 ratios almost always increased and OM absorbances decreased, regardless of the site location. This agrees with previous literature findings, including studies in Lake Superior's western arm (Macdonald and Minor, 2013; Minor and Stephens, 2008). These aforementioned studies, as discussed in Section 4.1, took samples from terrestrially-impacted sites such as stream waters and plume-impacted lake sites similar to P2 and WP. In our study, the addition of the open lake water sample, P1, and its comparative lack of photodegradation shows that photodegradation of CDOM is more substantial and important to study on Lake Superior's shorelines and under storm-impacted circumstances. Furthermore, Tukey HSD tests showed significant interactions for site location, highlighting the differences between sites. It appears that as DOM moves out into the open lake and spends more time being photodegraded, it becomes less reactive to further photodegradation. This trend has been shown in previous studies that have irradiated samples from upstream to

downstream locations, indicating that as DOM is photodegraded upstream, it undergoes molecular changes that make it resemble the DOM in downstream samples (Dalzell et al., 2009). Indirect photodegradation pathways also change travelling downstream, with the highly reactive hydroxyl radical having the highest quantum yields upstream (Berg et al., 2019). For these reasons, the sampling location (upstream to downstream) is one of the most important factors in determining how photoreactive the DOM will be.

4.4 Other Observations between Initial and Final Samples

Other observations that were made in this study involve the comparison of initial and final samples. In general, the final dark samples were expected to be the same as the initials taken at the beginning of irradiation, but this was not always the case. For example, the P2 whole water treatment showed a significant increase in DOC concentration in the dark treatment compared to the initial values. It is not completely clear which mechanism led to this, but we hypothesize that there was a desorption from the POM in both light and dark samples, but that in the light sample, a slightly higher standard deviation prevented the data from showing a significant increase in DOC concentration.

For the UV-Vis parameters, the dark WP filtered site experienced a significant decrease in e2/e3 ratios and a significant increase in CDOM absorbance over the irradiation period compared to the initial values. This probably indicates aggregation of DOM into particles, thereby increasing molecular size and causing an e2/e3 ratio decrease. DOM has been shown to spontaneously assemble into polymers, acting as an important step in the transformation of DOM to POM (Chin et al., 1998). One

mechanism that has been proposed for this transformation is the binding of soluble metal species onto anionic sites on DOC (Duan and Gregory, 2003), and WP likely had these metal species from terrestrial runoff after the storm.

Additionally, the P1 whole water irradiation experienced a decrease in e2/e3 ratios and an increase of OM absorbance in the dark controls compared to the initial sample. This indicates that a decrease in molecular size and aromaticity of DOM was occurring in the dark for this sample. This is most likely due to a sorption issue: as previously stated DOM has been shown to spontaneously assemble, so that is most likely happening in this dark sample (Chin et al., 1998).

4.5 PPRI

While this study did not include any measurement of PPRI concentrations, a previous study in the Lake Superior watershed found that ^{3}DOM and $^{1}O_2$ quantum yields were the highest downstream and $^{\bullet}$OH quantum yields were the highest farther upstream (Berg et al., 2019). This study also took DOC, $SUVA_{254}$, and e2/e3 ratios for each of their sites. Using this information, we can compare our study's samples and make some estimates of how PPRI quantum yields may compare between the storm plume impacted, terrestrially-impacted, and open lake water samples. In the Berg et al. 2019 study, whole water e2/e3 ratios increased farther downstream, ranging from 4.32 to 5.78 (excluding a wastewater treatment effluent). DOC concentrations and $SUVA_{254}$ values were the highest upstream, with DOC values ranging from 69 to 3.45 mg/L. In this study, the storm-impacted site, WP had the lowest e2/e3 ratios and the highest DOC and $SUVA_{254}$ values, where the open lake sample had the highest e2/e3 ratio and the lowest DOC

concentrations and $SUVA_{254}$ values. Our whole water e2/e3 values from lake waters bracketed these values from a Lake Superior watershed transect, ranging from 2.88 to 6.13 moving from the storm-impacted site to open water. Our DOC values overlapped the lower concentrations from the Berg et al study and extended to lower values more representative of open lake water, ranging from 7.73 mg/L to 1.86 mg/L from storm-impacted site to open lake water (Berg et al., 2019; Seekell et al., 2015; Zigah et al., 2011). Looking at the trends established in the Berg study, we can hypothesize that $^{\bullet}OH$ have higher quantum yields in storm-plume impacted waters, and ^{3}DOM and $^{1}O_2$ have higher quantum yields and play a more important role in open lake waters. Future studies should test this hypothesis by calculating the quantum yields of different PPRI species in plume-impacted versus open lake samples.

4.6 Kinetics of CDOM decrease

Compared to the Porcal et al. 2013 study, the k_{ABS} and k_{λ} rate constants for this study were substantially lower, indicating either an innate difference in CDOM photoreactivity in Lake Superior samples compared to the tributaries of Plastic Lake in Ontario, Canada or that a difference in the light source (natural light for this study versus a Xenon lamp for the Porcal study) within the two sets of irradiations plays a role in CDOM fate. The previous study had k_{ABS} rate constants ranging from 0.047 to 0.073 m^2/MJ, where our study's values ranged from 0.004 to 0.015 m^2/MJ (Porcal et al., 2013). The k_{λ} rate constants for our filtered water irradiations peaked at 0.0091 m^2/MJ and 0.0126 m^2/MJ for the P1 and WP sites, respectively. The uncertainty of constants increased as wavelength increased for the P1 and P2 sites. The whole water irradiations

exhibited higher k_λ rate constants for the P1 site, peaking at 0.029 m^2/MJ, compared to the WP site, which had a maximum at 0.0091 m^2/MJ. This provides further evidence that the inclusion of particles in the storm-impacted site resulted in a decreased rate of photodegradation. For the open lake water site, the whole water irradiations had a higher k_λ rate constant than the filtered water, indicating that when the particulate load is not large enough to attenuate light, the inclusion of particles may result in a faster rate of photodegradation. The Porcal et al. 2013 study's values exhibited a maximum of k_λ around 300 nm with a rate constant around 0.8 m^2/MJ, where our study shows maxima around 330 – 344 nm except for the P2 filtered water site, which does not exhibit a maximum likely due to higher uncertainty at higher wavelengths. Again, this study showed much smaller rate constants, which could be due to the DOM composition of the samples differing from that of the Porcal et al. study. The Porcal study took their water samples from a headwater stream in Ontario, so it is likely that this study's Lake Superior samples were much less aromatic and photoreactive due to more time spent in situ being photodegraded. This would explain our study's lower k_{ABS} and k_λ constants.

Chapter 5. Conclusion

This study investigated differences between the photodegradation of whole and filtered water samples, as well as between open water, terrestrially impacted, and storm-plume impacted samples. In the filtered water irradiations, UV-Vis measurements indicated decreasing molecular weight and aromaticity of CDOM, with storm-impacted sites having the highest percent change, followed by the terrestrially-impacted site, and then the open lake water site as hypothesized. The whole water irradiations also showed that chromophoric OM saw decreasing molecular weight and aromaticity, but the storm-impacted site (WP) had the least percent changes, indicating the DOM rich and sediment rich sample was likely subject to light limitation due to self-shading. The calculation of absorbance rate constants further confirmed this, indicating a slower rate of photodegradation in the whole water storm-impacted irradiations compared to its filtered replicate and the open lake water site. No change in DOC concentration was found in the filtered water irradiations, but an increase in DOC concentration was found in the dark sample for the whole water irradiation of P2, indicating when POM is included, other processes such as desorption can play a role in changing dissolved organic carbon concentrations. No significant trends were found in TN/TDN or phosphorus measurements over the irradiations. However, an increase in ammonium concentration was found for P2's whole water irradiation, potentially due to interactions between particulate iron and either POM or DOM, releasing ammonium. This finding may point towards another previously unstudied ammonium source in Lake Superior.

Future studies should focus on improving methods of studying whole water photodegradations; this study used autoclaving to sterilize whole water samples and the

changes in temperature and pressure may alter the initial DOM used for irradiations.. This study showed that the presence of POM at naturally occurring levels (even relatively low levels as seen at our open water site) leads to different photo-mediated trends in UV-Vis parameters and nutrient concentrations. While autoclaving whole water samples to kill bacterial populations allows the study of photochemical changes, it is also appears to alter phosphorus forms. A different approach that does not affect nutrient concentrations could provide key insights into light-mediated natural processes. It would also be beneficial to study how quickly bacteria might regrow in the sample after autoclaving to establish a shelf life of the sample. Additional irradiation studies of storm plume-impacted samples taken farther offshore would also be valuable to determine over what areal extent of the plume, and over what time frame, the changes we identify are relevant.

Works Cited

Aarnos, H., Ylöstalo, P., Vähätalo, A. V., 2012. Seasonal phototransformation of dissolved organic matter to ammonium, dissolved inorganic carbon, and labile substrates supporting bacterial biomass across the Baltic Sea. J. Geophys. Res. Biogeosciences 117, 1–14. https://doi.org/10.1029/2010JG001633

Alin, S.R., Johnson, T.C., 2007. Carbon cycling in large lakes of the world: A synthesis of production, burial, and lake-atmosphere exchange estimates. Global Biogeochem. Cycles 21, 1–12. https://doi.org/10.1029/2006GB002881

Anagnostou, E., Sherrell, R.M., 2008. MAGIC method for subnanomolar orthophosphate determination in freshwater. Limnol. Oceanogr. Methods 6, 64–74. https://doi.org/10.4319/lom.2008.6.64

Anderson, T.R., Rowe, E.C., Polimene, L., Tipping, E., Evans, C.D., Barry, C.D.G., Hansell, D.A., Kaiser, K., Kitidis, V., Lapworth, D.J., Mayor, D.J., Monteith, D.T., Pickard, A.E., Sanders, R.J., Spears, B.M., Torres, R., Tye, A.M., Wade, A.J., Waska, H., 2019. Unified concepts for understanding and modelling turnover of dissolved organic matter from freshwaters to the ocean: the UniDOM model. Biogeochemistry 146, 1–19. https://doi.org/10.1007/s10533-019-00621-1

Assel, R.A., 1986. Fall and Winter Thermal Structure of Lake Superior. J. Great Lakes Res. 12, 251–262. https://doi.org/10.1016/S0380-1330(86)71725-5

Atilla, N., McKinley, G.A., Bennington, V., Baehr, M., Urban, N., DeGrandpre, M., Desai, A.R., Wu, C., 2011. Observed variability of Lake Superior pCO2. Limnol. Oceanogr. 56, 775–786. https://doi.org/10.4319/lo.2011.56.3.0775

Azam, F., Fenchel, T., Field, J.G., Gray, J.S., Meyer-Reil, L.A., Thingstad, F., 1983. The

Ecological Role of Water-Column Microbes in the Sea. Mar. Ecol. - Prog. Ser. 10, 257–263. https://doi.org/10.1021/acs.joc.6b00938

Berg, S.M., Whiting, Q.T., Herrli, J.A., Winkels, R., Wammer, K.H., Remucal, C.K., 2019. The Role of Dissolved Organic Matter Composition in Determining Photochemical Reactivity at the Molecular Level. Environ. Sci. Technol. 53, 11725–11734. https://doi.org/10.1021/acs.est.9b03007

Berggren, M., Laudon, H., Haei, M., Ström, L., Jansson, M., 2010. Efficient aquatic bacterial metabolism of dissolved low-molecular-weight compounds from terrestrial sources. ISME J. 4, 408–416. https://doi.org/10.1038/ismej.2009.120

Berman, T., Chava, S., 1999. Algal growth on organic compounds as nitrogen sources. J. Plankton Res. 21, 1423–1437. https://doi.org/10.1111/j.1529-8817.1978.tb02449.x

Biddanda, B.A., Cotner, J.B., 2003. Enhancement of dissolved organic matter bioavailability by sunlight and its role in the carbon cycle of Lakes Superior and Michigan. J. Great Lakes Res. 29, 228–241. https://doi.org/10.1016/S0380-1330(03)70429-8

Biddanda, B.A., Ogdahl, M., Cotner, J.B., 2001. Dominance of Bacterial Metabolism in Oligotrophic Relative to Eutrophic Waters. Limnol. Oceanogr. 46, 730–739.

Boreen, A.L., Arnold, W.A., McNeill, K., 2003. Photodegradation of pharmaceuticals in the aquatic environment: A review. Aquat. Sci. 65, 320–341. https://doi.org/10.1007/s00027-003-0672-7

Boss, E., Pegau, W.S., Zaneveld, J.R. V., Barnard, A.H., 2001. Spatial and temporal variability of absorption by dissolved material at a continental shelf. J. Geophys. Res. Ocean. 106, 9499–9507. https://doi.org/10.1029/2000jc900008

Bracchini, L., Loiselle, S., Dattilo, A.M., Mazzuoli, S., Cózar, A., Rossi, C., 2004. The Spatial Distribution of Optical Properties in the Ultraviolet and Visible in an Aquatic Ecosystem¶. Photochem. Photobiol. 80, 139. https://doi.org/10.1562/2004-01-26-ra-063.1

Bronk, D.A., See, J.H., Bradley, P., Killberg, L., 2006. DON as a source of bioavailable nitrogen for phytoplankton. Biogeosciences Discuss. 3, 1247–1277. https://doi.org/10.5194/bgd-3-1247-2006

Burns, J.M., Cooper, W.J., Ferry, J.L., King, D.W., DiMento, B.P., McNeill, K., Miller, C.J., Miller, W.L., Peake, B.M., Rusak, S.A., Rose, A.L., Waite, T.D., 2012. Methods for reactive oxygen species (ROS) detection in aqueous environments. Aquat. Sci. 74, 683–734. https://doi.org/10.1007/s00027-012-0251-x

Cao, F., Medeiros, P.M., Miller, W.L., 2016. Optical characterization of dissolved organic matter in the Amazon River plume and the Adjacent Ocean: Examining the relative role of mixing, photochemistry, and microbial alterations. Mar. Chem. 186, 178–188. https://doi.org/10.1016/j.marchem.2016.09.007

Chin, W.-C., Orellana, M., Verdugo, P., 1998. Spontaneous assembly of marine dissolved organic matter into polymer gels. Nature 391, 568–572. https://doi.org/10.1038/246170a0

Cole, J.J., Prairie, Y.T., Caraco, N.F., Mcdowell, W.H., Tranvik, L.J., Striegl, R.G., Duarte, C.M., Kortelainen, P., Downing, J.A., Middelburg, J.J., Melack, J., 2007. Plumbing the Global Carbon Cycle : Integrating Inland Waters into the Terrestrial Carbon Budget 171–184. https://doi.org/10.1007/s10021-006-9013-8

Conmy, R.N., Coble, P.G., Cannizzaro, J.P., Heil, C.A., 2009. Influence of extreme storm

events on West Florida Shelf CDOM distributions. J. Geophys. Res. Biogeosciences 114. https://doi.org/10.1029/2009JG000981

Cooney, E.M., McKinney, P., Sterner, R., Small, G.E., Minor, E.C., 2018. Tale of Two Storms: Impact of Extreme Rain Events on the Biogeochemistry of Lake Superior. J. Geophys. Res. Biogeosciences 123. https://doi.org/10.1029/2017JG004216

Cory, R.M., Harrold, K.H., Neilson, B.T., Kling, G.W., 2015. Controls on dissolved organic matter (DOM) degradation in a headwater stream: The influence of photochemical and hydrological conditions in determining light-limitation or substrate-limitation of photo-degradation. Biogeosciences Discuss. 12, 9793–9838. https://doi.org/10.5194/bgd-12-9793-2015

Cory, R.M., Ward, C.P., Crump, B.C., Kling, G.W., 2014. Sunlight controls water column processing of carbon in arctic fresh waters 345.

Cotner, J., Biddanda, B., Makino, W., Stets, E., 2004. Organic carbon biogeochemistry of Lake Superior. Aquat. Ecosyst. Heal. Manag. 7, 451–464. https://doi.org/10.1080/14634980490513292

Cotner, J.B., Biddanda, B.A., Makino, W., Stets, E., 2004. Organic carbon biogeochemistry of Lake Superior. Aquat. Ecosyst. Heal. Manag. 7, 451–464. https://doi.org/10.1080/14634980490513292

Dalzell, B.J., Minor, E.C., Mopper, K.M., 2009. Photodegradation of estuarine dissolved organic matter: a multi-method assessment of DOM transformation. Org. Geochem. 40, 243–257. https://doi.org/10.1016/j.orggeochem.2008.10.003

De Haan, H., De Boer, T., 1987. Applicability of Light Absorbance and Fluorescence as Measures of Concentration and Molecular Size of Dissolved Organic Carbon in

Humic Lake Tjeukemeer. Water Res. 21, 731–734.

Del Giorgio, P.A., Cole, J.J., Caraco, N.F., Peters, R.H., 1999. Linking planktonic biomass and metabolism to net gas fluxes in northern temperate lakes. Ecology 80, 1422–1431. https://doi.org/10.1890/0012-9658(1999)080[1422:LPBAMT]2.0.CO;2

Diaz, J.M., Holland, A., Sanders, J.G., Bulski, K., Mollett, D., Chou, C.W., Phillips, D., Tang, Y., Duhamel, S., 2018. Dissolved organic phosphorus utilization by phytoplankton reveals preferential degradation of polyphosphates over phosphomonoesters. Front. Mar. Sci. 5, 1–17. https://doi.org/10.3389/fmars.2018.00380

Duan, J., Gregory, J., 2003. Coagulation by hydrolysing metal salts. Adv. Colloid Interface Sci. 100–102, 475–502. https://doi.org/10.1016/S0001-8686(02)00067-2

EPA-103-A Rev. 10. Ammonia-N in Drinking and Surface Waters, Domestic and Industrial Wastes, 2012.

Estapa, M.L., Mayer, L.M., 2010. Photooxidation of particulate organic matter, carbon/oxygen stoichiometry, and related photoreactions. Mar. Chem. 122, 138–147. https://doi.org/10.1016/j.marchem.2010.06.003

Gao, H., Zepp, R.G., 1998. Factors influencing photoreactions of dissolved organic matter in a coastal river of the southeastern United States. Environ. Sci. Technol. 32, 2940–2946. https://doi.org/10.1021/es9803660

Goldstone, J.V., 2002. Direct and Indirect Photoreactions of Chromophoric Dissolved Organic Matter: Roles of Reactive Oxygen Species and Iron.

Green, S.A., Blough, N. V., 1994. Optical absorption and fluorescence properties of chromophoric dissolved organic matter in natural waters. Limnol. Oceanogr. 39,

1903–1916. https://doi.org/10.4319/lo.1994.39.8.1903

Haag, W.R., Hoigné, J., 1985. Photo-sensitized oxidation in natural water via OH radicals. Chemosphere 14, 1659–1671. https://doi.org/10.1016/0045-6535(85)90107-9

Habermann, R., Moen, S., Stykel, E., 2012. Superior Facts. Minnesota Sea Grant (pub. S25).

Hanson, P.C., Bade, D.L., Carpenter, S.R., Kratz, T.K., 2003. Lake metabolism: Relationships with dissolved organic carbon and phosphorus. Limnol. Oceanogr. 48, 1112–1119. https://doi.org/10.4319/lo.2003.48.3.1112

He, W., Chen, M., Schlautman, M.A., Hur, J., 2016. Dynamic exchanges between DOM and POM pools in coastal and inland aquatic ecosystems: A review. Sci. Total Environ. 551–552, 415–428. https://doi.org/10.1016/j.scitotenv.2016.02.031

Hedges, J.I., 1992. Global biogeochemical cycles: progress and problems. Mar. Chem. 39, 67–93. https://doi.org/10.1016/0304-4203(92)90096-S

Hedges, J.I., Keil, R.G., Benner, R., 1997. What happens to terrestrial organic matter in the ocean? Org. Geochem. 27, 195–212. https://doi.org/10.1016/S0146-6380(97)00066-1

Helms, J.R., Stubbins, A., Ritchie, J.D., Minor, E.C., Kieber, D.J., Mopper, K., 2008. Absorption Spectral Slopes and Slope Ratios As Indicators of Molecular Weight,Source,and Photobleaching of Chromophoric Dissolved Organic Matter. Limnol. Oceanogr. 53, 955–969. https://doi.org/doi: 10.4319/lo.2008.53.3.0955

Hiriart-Baer, V., 2013. Dissolved organic matter quantity and quality in Lake Simcoe compared to two other large lakes in southern Ontario. Inl. Waters 3, 139–152.

https://doi.org/10.5268/IW-3.2.535

Hiriart-Baer, V.P., Milne, J.E., Marvin, C.H., 2011. Temporal trends in phosphorus and lacustrine productivity in Lake Simcoe inferred from lake sediment. J. Great Lakes Res. 37, 764–771. https://doi.org/10.1016/j.jglr.2011.08.014

Holmes, R.M., Aminot, A., Kérouel, R., Hooker, B.A., Peterson, B.J., 1999. A simple and precise method for measuring ammonium in marine and freshwater ecosystems. Can. J. Fish. Aquat. Sci. 56, 1801–1808. https://doi.org/10.1139/f99-128

Hu, B., Wang, P., Bao, T., Qian, J., Wang, X., 2021. Mechanisms of photochemical release of dissolved organic matter and iron from resuspended sediments. J. Environ. Sci. (China) 104, 288–295. https://doi.org/10.1016/j.jes.2020.12.002

Kieber, R.J., Whitehead, R.F., Skrabal, S.A., 2006. Photochemical Production of Dissolved Organic Carbon from Resuspended Sediments. Limnol. Oceanogr. 51, 2187–2195.

Kirk, J.T.O., 2010. The underwater light field, in: Light and Photosynthesis in Aquatic Ecosystems. pp. 1–262.

Kruger, B.R., Dalzell, B.J., Minor, E.C., 2011. Effect of organic matter source and salinity on dissolved organic matter isolation via ultrafiltration and solid phase extraction. Aquat. Sci. 73. https://doi.org/10.1007/s00027-011-0189-4

Larson, J.H., Frost, P.C., Lodge, D.M., Lamberti, G.A., 2007. Photodegradation of dissolved organic matter in forested streams of the northern Great Lakes region. J. North Am. Benthol. Soc. 26, 416–425. https://doi.org/10.1899/06-097.1

Li, X., Zhou, Y., Liu, G., Lei, H., Zhu, D., 2017. Mechanisms of the photochemical release of phosphate from resuspended sediments under solar irradiation. Sci. Total

Environ. 595, 779–786. https://doi.org/10.1016/j.scitotenv.2017.04.039

Lundeen, R.A., Janssen, E.M.L., Chu, C., McNeill, K., 2014. Environmental photochemistry of amino acids, peptides and proteins. Chimia (Aarau). 68, 812–824. https://doi.org/10.2533/chimia.2014.812

Macdonald, M.J., Minor, E.C., 2013. Photochemical degradation of dissolved organic matter from streams in the western Lake Superior watershed. Aquat. Sci. 75, 509–522. https://doi.org/10.1007/s00027-013-0296-5

McCarthy, J.J., Goldman, J.C., 1979. Nitrogenous Nutrition of Marine Phytoplankton in Nutrient-Depleted Waters. Science (80-.). 203, 670–672.

McNeill, K., Canonica, S., 2016. Triplet state dissolved organic matter in aquatic photochemistry: Reaction mechanisms, substrate scope, and photophysical properties. Environ. Sci. Process. Impacts 18, 1381–1399. https://doi.org/10.1039/c6em00408c

Meybeck, M., 1982. Carbon, Nitrogen, and Phosphorus Transport by World Rivers. Am. J. Sci. 282, 401–450.

Minor, E., Stephens, B., 2008. Dissolved organic matter characteristics within the Lake Superior watershed. Org. Geochem. 39, 1489–1501. https://doi.org/10.1016/j.orggeochem.2008.08.001

Minor, E.C., Forsman, B., Guildford, S.J., 2014. The effect of a flood pulse on the water column of western Lake Superior, USA. J. Great Lakes Res. 40, 455–462. https://doi.org/10.1016/j.jglr.2014.03.015

Osburn, C.L., Retamal, L., Vincent, W.F., 2009. Photoreactivity of chromophoric dissolved organic matter transported by the Mackenzie River to the Beaufort Sea.

Mar. Chem. 115, 10–20. https://doi.org/10.1016/j.marchem.2009.05.003

Pérez, M.T., Sommaruga, R., 2006. Differential effect of algal- and soil-derived dissolved organic matter on alpine lake bacterial community composition and activity. Limnol. Oceanogr. 51, 2527–2537. https://doi.org/10.4319/lo.2006.51.6.2527

Pitre, S.P., McTiernan, C.D., Vine, W., Dipucchio, R., Grenier, M., Scaiano, J.C., 2015. Visible-Light Actinometry and Intermittent Illumination as Convenient Tools to Study Ru(bpy)3Cl2 Mediated Photoredox Transformations. Sci. Rep. 5, 1–10. https://doi.org/10.1038/srep16397

Porcal, P., Dillon, P.J., Molot, L.A., 2013. Photochemical production and decomposition of particulate organic carbon in a freshwater stream. Aquat. Sci. 75, 469–482. https://doi.org/10.1007/s00027-013-0293-8

Powell, R.T., Wilson-Finelli, A., 2003. Photochemical degradation of organic iron complexing ligands in seawater. Aquat. Sci. 65, 367–374. https://doi.org/10.1007/s00027-003-0679-0

Procházková, L., Blažka, P., Králová, M., 1970. Chemical Changes Involving Nitrogen Metabolism in Water and Particulate Matter During Primary Production Experiments. Limnol. Oceanogr. 15, 797–807. https://doi.org/10.4319/lo.1970.15.5.0797

Remucal, C.K., 2014. The role of indirect photochemical degradation in the environmental fate of pesticides: A review. Environ. Sci. Process. Impacts 16, 628–653. https://doi.org/10.1039/c3em00549f

Seekell, D.A., Lapierre, J.F., Ask, J., Bergstreom, A.K., Deininger, A., Rodriguez, P.,

Karlsson, J., 2015. The influence of dissolved organic carbon on primary production in northern lakes. Limnol. Oceanogr. 60, 1276–1285. https://doi.org/10.1002/lno.10096

Shemer, H., Sharpless, C.M., Elovitz, M.S., Linden, K.G., 2006. Relative rate constants of contaminant candidate list pesticides with hydroxyl radicals. Environ. Sci. Technol. 40, 4460–4466. https://doi.org/10.1021/es0602602

Southwell, M.W., Kieber, R.J., Mead, R.N., Avery, G.B., Skrabal, S.A., 2010. Effects of sunlight on the production of dissolved organic and inorganic nutrients from resuspended sediments. Biogeochemistry 98, 115–126. https://doi.org/10.1007/s10533-009-9380-2

Stedmon, C.A., Markager, S., Tranvik, L., Kronberg, L., Slätis, T., Martinsen, W., 2007. Photochemical production of ammonium and transformation of dissolved organic matter in the Baltic Sea. Mar. Chem. 104, 227–240. https://doi.org/10.1016/j.marchem.2006.11.005

Sterner, R., 2011. C:N:P stoichiometry in Lake Superior: freshwater sea as end member. Inl. Waters 1, 29–46. https://doi.org/10.5268/iw-1.1.365

Sterner, R.W., 2021. The laurentian great lakes: A biogeochemical test bed. Annu. Rev. Earth Planet. Sci. 49, 201–229. https://doi.org/10.1146/annurev-earth-071420-051746

Sterner, R.W., 2010. In situ-measured primary production in Lake Superior. J. Great Lakes Res. 36, 139–149. https://doi.org/10.1016/j.jglr.2009.12.007

Sterner, R.W., Smutka, T.M., Mckay, R.M.L., Xiaoming, Q., Brown, T., Sherrell, R.M., Limnology, S., Mar, N., Sterner, R.W., Smutka, T.M., Mckay, R.M.L., Xiaoming,

Q., Brown, E.T., Sherrell, R.M., 2019. Phosphorus and Trace Metal Limitation of Algae and Bacteria in Lake Superior Published by : Wiley Stable URL : https://www.jstor.org/stable/3597859 Phosphorus and trace metal limitation of algae and bacteria in Lake Superior 49, 495–507.

Sterner, R.W., Smutka, T.M., Mckay, R.M.L., Xiaoming, Q., Brown, T., Sherrell, R.M., Limnology, S., Mar, N., Sterner, R.W., Smutka, T.M., Mckay, R.M.L., Xiaoming, Q., Brown, E.T., Sherrell, R.M., 2004. Phosphorus and Trace Metal Limitation of Algae and Bacteria in Lake Superior. Limnol. Oceanogr. 49, 495–507.

Tarr, M.A., Wang, W., Bianchi, T.S., Engelhaupt, E., 2001. Mechanisms of ammonia and amino acid photoproduction from aquatic humic and colloidal matter. Water Res. 35, 3688–3696. https://doi.org/10.1016/S0043-1354(01)00101-4

Taylor, B.W., Keep, C.F., Hall, R.O., Koch, B.J., Tronstad, L.M., Flecker, A.S., Ulseth, A.J., 2007. Improving the fluorometric ammonium method: Matrix effects, background fluorescence, and standard additions. J. North Am. Benthol. Soc. 26, 167–177. https://doi.org/10.1899/0887-3593(2007)26[167:ITFAMM]2.0.CO;2

Thornton, D.C.O., 2014. Dissolved organic matter (DOM) release by phytoplankton in the contemporary and future ocean. Eur. J. Phycol. 49, 20–46. https://doi.org/10.1080/09670262.2013.875596

Tonello, M.S., Hebner, T.S., Sterner, R.W., Brovold, S., Tiecher, T., Bortoluzzi, E.C., 2019. Geochemistry and mineralogy of southwestern Lake Superior sediments with an emphasis on phosphorus lability.

Tranvik, L.J., Kaplan, L.A., Battin, T.J., Richter, A., Aufdenkampe, A.K., Luyssaert, S., 2009. The boundless carbon cycle. Nat. Geosci. 2, 598–600.

https://doi.org/10.1038/ngeo618

Urban, N.R., Auer, M.T., Green, S.A., Lu, X., Apul, D.S., Powell, K.D., Bub, L., 2005. Carbon cycling in Lake Superior. J. Geophys. Res., [Oceans] 110, C06S90/1-C06S90/17. https://doi.org/10.1029/2003jc002230

Vione, D., Minella, M., Maurino, V., Minero, C., 2014. Indirect photochemistry in sunlit surface waters: Photoinduced production of reactive transient species. Chem. - A Eur. J. 20, 10590–10606. https://doi.org/10.1002/chem.201400413

Voelker, B.M., Morel, F.M.M., Sulzberger, B., 1997. Iron redox cycling in surface waters: Effects of humic substances and light. Environ. Sci. Technol. 31, 1004–1011. https://doi.org/10.1021/es9604018

Walsh, J., Wuebbles, D., Hayhoe, K., Kossin, J., Kunkel, K., Stephens, G., Thorne, P., Vose, R., Wehner, M., Willis, J., Anderson, D., Doney, S., Feely, R., Hennon, P., Kharin, V., Knutson, T., Landerer, F., Lenton, T., Kennedy, J., Somerville, R., 2014. Chapter 2: Our Changing Climate, in: Climate Change Impacts in the United States: The Third National Climate Assessment. pp. 19–67.

Wang, Y., Hammes, F., Boon, N., Egli, T., 2007. Quantification of the filterability of freshwater bacteria through 0.45, 0.22, and 0.1 μm pore size filters and shape-dependent enrichment of filterable bacterial communities. Environ. Sci. Technol. 41, 7080–7086. https://doi.org/10.1021/es0707198

Weishaar, J.L., Aiken, G.R., Bergamaschi, B.A., Fram, M.S., Fujii, R., Mopper, K., 2003. Evaluation of specific ultraviolet absorbance as an indicator of the chemical composition and reactivity of dissolved organic carbon. Environ. Sci. Technol. 37, 4702–4708. https://doi.org/10.1021/es030360x

Wetzel, R.G., Likens, G.E., 1991. Limnological Analyses, Springer Science+Business Media, LLC. https://doi.org/10.1046/j.1440-1770.2002.01722.x

Whitmire, A.L., Boss, E., Cowles, T.J., Pegau, W.S., 2007. Spectral variability of the particulate backscattering ratio. Opt. Express 15, 7019–7031.

Zafiriou, O.C., 2002. Sunburnt Organic Matter: Biogeochemistry of Light-Altered Substrates. Limnol. Oceanogr. Bull. 11, 69–88. https://doi.org/10.1002/lob.200211469

Zafiriou, O.C., Joussot-Dubien, J., Zepp, R.G., Zika, R.G., 1984. Photochemistry of natural waters: Many compounds and environments are affected by sunlight-induced photochemistry. Environ. Sci. Technol. 18, 358A-371A. https://doi.org/10.1021/es00130a711

Zepp, R.G., Wolfe, N.L., Baughman, G.L., Hollis, R.C., 1977. Singlet oxygen in natural waters. Nature 267, 421–423.

Zhang, Y., Liu, X., Osburn, C.L., Wang, M., Qin, B., Zhou, Y., 2013. Photobleaching Response of Different Sources of Chromophoric Dissolved Organic Matter Exposed to Natural Solar Radiation Using Absorption and Excitation-Emission Matrix Spectra. PLoS One 8. https://doi.org/10.1371/journal.pone.0077515

Zigah, P.K., Minor, E.C., Abdulla, H.A.N., Werne, J.P., Hatcher, P.G., 2014. An investigation of size-fractionated organic matter from Lake Superior and a tributary stream using radiocarbon, stable isotopes and NMR. Geochim. Cosmochim. Acta 127. https://doi.org/10.1016/j.gca.2013.11.037

Zigah, P.K., Minor, E.C., Werne, J.P., 2012. Radiocarbon and stable-isotope geochemistry of organic and inorganic carbon in Lake Superior. Global

Biogeochem. Cycles 26. https://doi.org/10.1029/2011GB004132

Zigah, P.K., Minor, E.C., Werne, J.P., McCallisterd, S.L., 2011. Radiocarbon and stable carbon isotopic insights into provenance and cycling of carbon in Lake Superior. Limnol. Oceanogr. 56, 867–886. https://doi.org/10.4319/lo.2011.56.3.0867

Supplementary Information

Table S-1. Comparisons of actinometer data to total irradiance as measured by the SpectraWiz radiometer. Only the successful actinometer experiments during the WP irradiation are shown. Actinometer start and end times show when the actinometer light and dark samples were placed outside in the sun. The radiometer irradiance was calculated using the integration of radiometer measurements taken during the same time the actinometer was out, and are not representative of the total amount of irradiance the Lake Superior samples received. They should only be directly compared to the actinometer irradiance for each time period.

Site	Date	Actinometer Start Time	Actinometer End Time	Total Time (min)	Actinometer irradiance (J/m^2)	Radiometer irradiance (J/m^2)
Wisconsin Point (WP)	8/16/20	9:45	13:45	240	5.36E7	3.58E6
Wisconsin Point (WP)	8/16/20	14:09	16:00	111	2.65E7	1.85E6
Wisconsin Point (WP)	8/18/20	9:30	10:30	60	2.70E7	7.94E5

Table S-2. DOC values before and after filtered water irradiations. The errors shown in this table are from the standard deviation from the multiple injections the Shimadzu takes as described in Section 2.5b.

Site	Initial DOC (mg/L)	Day 1 DOC Light (mg/L)	Day 1 DOC Dark (mg/L)	Day 2 DOC Light (mg/L)	Day 2 DOC Dark (mg/L)	Day 3 DOC Light (mg/L)	Day 3 DOC Dark (mg/L)
Photochemistry Blue (P1)	1.86 ± 0.04	2.02 ± 0.01 1.76 ± 0.03 2.14 ± 0.02	1.92 ± 0.02 2.11 ± 0.03 1.75 ± 0.03	1.87 ± 0.02 1.78 ± 0.03 1.95 ± 0.02	1.92 ± 0.01 1.64 ± 0.02 1.73 ± 0.01	1.98 ± 0.02 1.92 ± 0.03 1.77 ± 0.06	1.89 ± 0.02 1.99 ± 0.02 1.95 ± 0.02
Photochemistry Brown (P2)	3.74 ± 0.53	3.72 ± 0.50 3.67 ± 0.52 3.72 ± 0.52	3.84 ± 0.51 3.74 ± 0.50 3.86 ± 0.51	3.96 ± 0.53 3.77 ± 0.57 3.85 ± 0.51	3.87 ± 0.50 3.88 ± 0.53 3.59 ± 0.50	3.82 ± 0.52 3.71 ± 0.51 3.78 ± 0.53	3.74 ± 0.49 4.17 ± 0.54 3.79± 0.49
Wisconsin Point (WP)	7.73 ± 0.08	7.65 ± 0.08 8.10 ± 0.05 7.97 ± 0.08	8.35 ± 0.13 7.70 ± 0.02 10.12 ± 0.14	7.92 ± 0.13 7.57 ± 0.09 8.51 ± 0.04	8.33 ± 0.09 7.79 ± 0.11 8.37 ± 0.06	7.92 ± 0.07 8.22 ± 0.02 8.10 ± 0.01	8.07 ± 0.02 8.41 ± 0.08 8.02 ± 0.08

Table S-3. TDN values before, during, and after filtered water irradiations. The errors shown in this table are from the standard deviation from the multiple injections the Shimadzu takes as described in Section 2.5b.

Site	Initial TDN (mg/L)	Day 1 TDN Light (mg/L)	Day 1 TDN Dark (mg/L)	Day 2 TDN Light (mg/L)	Day 2 TDN Dark (mg/L)	Day 3 TDN Light (mg/L)	Day 3 TDN Dark (mg/L)

Photochemistry Blue (P1)	0.38 ± 0.01	0.37 ± 0.01 0.38 ± 0.01 0.38 ± 0.01	0.38 ± 0.01 0.39 ± 0.01 0.38 ± 0.01	0.37 ± 0.01 0.37 ± 0.01 0.38 ± 0.01	0.38 ± 0.01 0.37 ± 0.01 0.38 ± 0.01	0.38 ± 0.01 0.39 ± 0.02 0.37 ± 0.01	0.39 ± 0.01 0.39 ± 0.01 0.38 ± 0.01
Photochemistry Brown (P2)	0.40 ± 0.01	0.40 ± 0.01 0.40 ± 0.01 0.41 ± 0.01	0.40 ± 0.01 0.41 ± 0.01 0.41 ± 0.01	0.41 ± 0.01 0.40 ± 0.01 0.40 ± 0.01	0.41 ± 0.01 0.42 ± 0.01 0.40 ± 0.01	0.42 ± 0.01 0.40 ± 0.01 0.42 ± 0.01	0.41 ± 0.01 0.41 ± 0.01 0.41 ± 0.01
Wisconsin Point (WP)	0.47 ± 0.03	0.47 ± 0.02 0.47 ± 0.03 0.47 ± 0.03	0.50 ± 0.03 0.48 ± 0.03 0.47 ± 0.03	0.48 ± 0.03 0.48 ± 0.03 0.48 ± 0.03	0.48 ± 0.03 0.49 ± 0.03 0.48 ± 0.03	0.50 ± 0.03 0.48 ± 0.03 0.47 ± 0.03	0.48 ± 0.03 0.48 ± 0.03 0.96 ± 0.03

Table S-4. e2/e3 ratios during the filtered water irradiations. Two samples instead of three were taken for Days 1 and 2 due to volume constraints.

Site	Initial e2/e3 Ratio (dimensionless)	Day 1 e2/e3 Ratio Light	Day 1 e2/e3 Ratio Dark	Day 2 e2/e3 Ratio Light	Day 2 e2/e3 Ratio Dark	Day 3 e2/e3 Ratio Light	Day 3 e2/e3 Ratio Dark
Photochemistry Blue (P1)	8.339 8.496 8.303	8.580 9.289	8.438 8.951	8.948 9.575	8.750 8.496	7.382 9.147 8.714	9.270 8.972 8.362
Photochemistry Brown (P2)	4.167 6.065 6.074	6.271 6.325	5.892 5.717	6.529 6.570	6.031 6.042	6.625 6.750 6.666	5.964 6.033 6.008
Wisconsin Point (WP)	5.646 5.704 5.671	5.918 5.879	5.598 5.592	6.205 6.123	5.623 5.622	6.450 6.449 6.568	5.585 5.571 5.576

Table S-5. CDOM Absorbances during the filtered water irradiations. Two samples instead of three were taken for Days 1 and 2 due to volume constraints.

Site	Initial CDOM Absorbance (dimensionless)	Day 1 CDOM Absorbance Light	Day 1 CDOM Absorbance Dark	Day 2 CDOM Absorbance Light	Day 2 CDOM Absorbance Dark	Day 3 CDOM Absorbance Light	Day 3 CDOM Absorbance Dark
Photochemistry Blue (P1)	417.3 404.4 413.7	390.3 381.5	406.6 390.5	385.9 380.6	399.8 400.9	404.4 380.4 389.8	395.2 399.4 407.0
Photochemistry Brown (P2)	2357 2014 2017	1934 1924	2070 2093	1876 1855	2023 2045	1824 1805 1823	2037 2051 2059
Wisconsin Point (WP)	3955 3944 3926	3743 3781	3971 3948	3580 3608	3936 3992	3437 3430 3383	3984 4078 4015

Table S-6. $SUVA_{254}$ values before and after filtered water irradiations. Two samples instead of three were taken for Days 1 and 2 due to volume constraints.

Site	Initial $SUVA_{254}$ $(mg/L)^{-1}$	Day 1 $SUVA_{254}$ Light $(mg/L)^{-1}$	Day 1 $SUVA_{254}$ Dark $(mg/L)^{-1}$	Day 2 $SUVA_{254}$ Light $(mg/L)^{-1}$	Day 2 $SUVA_{254}$ Dark $(mg/L)^{-1}$	Day 3 $SUVA_{254}$ Light $(mg/L)^{-1}$	Day $SUVA_{254}$ Dark $(mg/L)^{-1}$

Photochemistry Blue (P1)	3.98 3.91 9.96	3.50 3.25	3.74 4.05	3.76 3.57	3.75 4.14	3.58 3.63 3.99	3.80 3.60 3.70
Photochemistry Brown (P2)	8.65 8.24 8.36	8.22 8.19	8.29 8.23	7.60 7.74	8.10 8.81	7.71 7.88 7.78	8.38 7.59 8.37
Wisconsin Point (WP)	7.66 7.66 7.62	7.65 8.10	7.12 7.67	7.07 7.42	7.07 7.66	6.90 6.63 6.68	7.36 7.22 7.47

Table S-7. NH_4^+ values before and after irradiation of filtered samples.

Site	Initial NH_4^+ (mg/L)	Day 3 NH_4^+ Light (mg/L)	Day 3 NH_4^+ Dark (mg/L)
Photochemistry Blue (P1)	0.0067	0.0055 0.0072 0.0067	0.0105 0.0122 0.0106
Photochemistry Brown (P2)	0.0024	0.0206 0.0226 0.0212	0.0193 0.0190 0.0213
Wisconsin Point (WP)	0.0150	0.0293 0.0110 0.0109	0.0134 0.0132 0.0139

Table S-8. TDP values before and after irradiation of filtered samples. The errors shown in this table are taken from the standard deviation of the three injections performed on the AQ400 Discrete Analyzer.

Site	Initial TDP (mg/L)	Day 3 TDP Light (mg/L)	Day 3 TDP Dark (mg/L)
Photochemistry Blue (P1)	0.0074 ± 0.0005	0.0069 ± 0.0010 0.0082 ± 0.0009 0.0079 ± 0.0010	0.0089 ± 0.0059 0.0083 ± 0.0012 0.0063 ± 0.0010
Photochemistry Brown (P2)	0.0091 ± 0.0007	0.0090 ± 0.0004 0.0129 ± 0.0050 0.0084 ± 0.0003	0.0086 ± 0.0006 0.0105 ± 0.0005 0.0086 ± 0.0021
Wisconsin Point (WP)	0.0056 ± 0.0007	0.0073 ± 0.0008 0.0090 ± 0.0020 0.0053 ± 0.0005	0.0055 ± 0.0004 0.0064 ± 0.0020 0.0067 ± 0.0003

Table S-9. SRP values before and after irradiation of filtered samples. The errors shown in this table are taken from the standard deviation of the three injections performed on the AQ400 Discrete Analyzer.

Site	Initial SRP (μg/L)	Day 3 SRP Light (μg/L)	Day 3 SRP Dark (μg/L)
Photochemistry Blue (P1)	0.80 ± 0.06	2.67 ± 1.56 0.88 ± 0.03 0.86 ± 0.01	1.22 ± 0.08 0.91 ± 0.05 0.88 ± 0.04
Photochemistry Brown (P2)	0.99 ± 0.11	0.81 ± 0.002 0.96 ± 0.003	0.93 ± 0.02 0.93 ± 0.07

		1.13 ± 0.014	0.99 ± 0.03
Wisconsin Point (WP)	1.07 ± 0.06	1.28 ± 0.20 0.86 ± 0.03 0.99 ± 0.07	1.08 ± 0.17 1.16 ± 0.03 1.20 ± 0.08

Table S-10. TOC values before and after whole water irradiations. The errors shown in this table are from the standard deviation from the multiple injections the Shimadzu takes as described in Section 2.5b.

Site	Initial TOC (mg/L)	Day 1 TOC Light (mg/L)	Day 1 TOC Dark (mg/L)	Day 2 TOC Light (mg/L)	Day 2 TOC Dark (mg/L)	Day 3 TOC Light (mg/L)	Day 3 TOC Dark (mg/L)
Photochemistry Blue (P1)	1.98 ± 0.04	1.91 ± 0.03 1.98 ± 0.02 1.86 ± 0.02	2.09 ± 0.02 2.01 ± 0.02 1.81 ± 0.02	2.05 ± 0.03 1.83 ± 0.01 1.83 ± 0.02	2.09 ± 0.03 2.02 ± 0.03 1.88 ± 0.04	1.95 ± 0.04 2.28 ± 0.04 1.84 ± 0.03	2.02 ± 0.02 2.51 ± 0.02 1.88 ± 0.02
Photochemistry Brown (P2)	4.27 ± 0.15	4.13 ± 0.15 4.15 ± 0.12 4.23 ± 0.17	4.34 ± 0.17 4.26 ± 0.18 4.49 ± 0.15	4.40 ± 0.14 4.21 ± 0.21 4.27 ± 0.19	4.40 ± 0.13 4.38 ± 0.18 4.28 ± 0.16	4.16 ± 0.16 4.29 ± 0.17 4.33 ± 0.14	4.45 ± 0.15 4.19 ± 0.17 4.23 ± 0.17
Wisconsin Point (WP)	7.84 ± 0.01	8.28 ± 0.06 8.14 ± 0.04 8.61 ± 0.04	8.27 ± 0.08 8.13 ± 0.13 8.74 ± 0.05	8.15 ± 0.11 7.97 ± 0.10 8.38 ± 0.09	8.03 ± 0.05 8.26 ± 0.01 8.12 ± 0.07	8.29 ± 0.00 8.23 ± 0.10 7.99 ± 0.05	8.35 ± 0.02 7.73 ± 0.09 8.17 ± 0.08

Table S-11. DOC values before and after whole water irradiations. The errors shown in this table are from the standard deviation from the multiple injections the Shimadzu takes as described in Section 2.5b.

Site	Initial DOC (mg/L)	Day 3 DOC Light (mg/L)	Day 3 DOC Dark (mg/L)
Photochemistry Blue (P1)	1.97 ± 0.04	1.75 ± 0.03 2.00 ± 0.02 1.83 ± 0.01	1.90 ± 0.03 1.83 ± 0.02 1.85 ± 0.01
Photochemistry Brown (P2)	4.10 ± 0.50	4.17 ± 0.54 4.13 ± 0.49 4.23 ± 0.53	4.30 ± 0.54 4.27 ± 0.49 4.23 ± 0.53
Wisconsin Point (WP)	7.57 ± 0.03	8.04 ± 0.09 7.99 ± 0.03 9.28 ± 0.00	8.16 ± 0.05 7.93 ± 0.10 8.07 ± 0.12

Table S-12. TN values before, during, and after whole water irradiations. The errors shown in this table are from the standard deviation from the multiple injections the Shimadzu takes as described in Section 2.5b.

Site	Initial TN (mg/L)	Day 1 TN Light (mg/L)	Day 1 TN Dark (mg/L)	Day 2 TN Light (mg/L)	Day 2 TN Dark (mg/L)	Day 3 TN Light (mg/L)	Day 3 TN Dark (mg/L)
Photochemistry Blue (P1)	0.38 ± 0.01	0.40 ± 0.01 0.41 ± 0.01 0.40 ± 0.01	0.40 ± 0.01 0.40 ± 0.01 0.40 ± 0.01	0.41 ± 0.01 0.40 ± 0.01 0.39 ± 0.01	0.40 ± 0.01 0.40 ± 0.01 0.40 ± 0.01	0.41 ± 0.01 0.40 ± 0.01 0.39 ± 0.01	0.40 ± 0.01 0.39 ± 0.01 0.40 ± 0.01
Photochemistry Brown (P2)	0.45 ± 0.01	0.46 ± 0.01 0.44 ± 0.01 0.45 ± 0.01	0.45 ± 0.01 0.44 ± 0.01 0.44 ± 0.01	0.47 ± 0.01 0.46 ± 0.01 0.44 ± 0.01	0.46 ± 0.01 0.44 ± 0.01 0.44 ± 0.02	0.44 ± 0.01 0.47 ± 0.01 0.45 ± 0.01	0.46 ± 0.01 0.44 ± 0.01 0.45 ± 0.01

Wisconsin Point (WP)	0.49 ± 0.03	0.50 ± 0.03 0.49 ± 0.02 0.50 ± 0.03	1.08 ± 0.04 0.49 ± 0.03 0.50 ± 0.03	0.53 ± 0.03 0.53 ± 0.03 0.56 ± 0.03	0.53 ± 0.03 0.49 ± 0.02 0.52 ± 0.03	0.51 ± 0.03 0.51 ± 0.03 0.53 ± 0.03	0.52 ± 0.03 0.48 ± 0.03 0.50 ± 0.03

Table S-13. TDN values before and after whole water irradiations. The errors shown in this table are from the standard deviation from the multiple injections the Shimadzu takes as described in Section 2.5b.

Site	Initial TDN (mg/L)	Day 3 TDN Light (mg/L)	Day 3 TDN Dark (mg/L)
Photochemistry Blue (P1)	0.39 ± 0.01	0.38 ± 0.01 0.40 ± 0.01 0.40 ± 0.01	0.40 ± 0.01 0.40 ± 0.01 0.40 ± 0.01
Photochemistry Brown (P2)	0.46 ± 0.01	0.47 ± 0.01 0.46 ± 0.02 0.46 ± 0.01	0.47 ± 0.01 0.45 ± 0.01 0.46 ± 0.01
Wisconsin Point (WP)	0.52 ± 0.03	0.54 ± 0.03 0.56 ± 0.03 0.56 ± 0.03	0.57 ± 0.03 0.52 ± 0.03 0.51 ± 0.03

Table S-14. e2/e3 ratios during irradiation of whole water samples. Two samples instead of three were taken for Days 1 and 2 due to volume constraints. Additionally, an initial sample for P2 was unable to be taken due to volume constraints.

Site	Initial e2/e3 ratio (dimensionless)	Day 1 e2/e3 ratio Light	Day 1 e2/e3 ratio Dark	Day 2 e2/e3 ratio Light	Day 2 e2/e3 ratio Dark	Day 3 e2/e3 ratio Light	Day 3 e2/e3 ratio Dark
Photochemistry Blue (P1)	6.119 6.072 6.195	7.440 7.294	6.084 6.238	8.430 8.273	6.768 6.787	8.349 8.451 8.355	6.856 6.795 6.908
Photochemistry Brown (P2)		5.284 5.346	4.714 4.635	5.923 5.982	5.099 4.956	6.213 6.616 5.998	5.171 4.807 4.779
Wisconsin Point (WP)	2.873 2.890 2.866	3.286 3.423	3.043 3.098	3.800 3.670	3.521 3.192	3.174 3.170 3.141	3.030 2.882 2.935

Table S-15. CDOM Absorbance for whole water samples before, during, and after irradiation. Two samples instead of three were taken for Days 1 and 2 due to volume constraints. Additionally, an initial sample for P2 was unable to be taken due to volume constraints.

Site	Initial CDOM Absorbance (dimensionless)	Day 1 CDOM Absorbance Light	Day 1 CDOM Absorbance Dark	Day 2 CDOM Absorbance Light	Day 2 CDOM Absorbance Dark	Day 3 CDOM Absorbance Light	Day 3 CDOM Absorbance Dark
Photochemistry Blue (P1)	555.1 551.2 553.1	486.0 493.0	562.4 558.7	463.5 462.2	530.3 539.4	466.7 458.5 454.3	529.1 533.3 541.0
Photochemistry Brown (P2)		2536 2508	2845 2838	2314 2285	2775 2761	2200 2107 2262	2786 2845 2855
Wisconsin Point (WP)	9862 9662 10001	8099 7645	9334 8670	6458 6804	7142 8387	8738 8782 9005	9427 10465 10190

Table S-16. $SUVA_{254}$ values (for OM) for each site before and after whole water irradiations. An initial sample for P2 was unable to be taken due to volume constraints.

Site	Initial $SUVA_{254}$ $(mg/L)^{-1}$	Day 1 $SUVA_{254}$ Light $(mg/L)^{-1}$	Day 1 $SUVA_{254}$ Dark $(mg/L)^{-1}$	Day 2 $SUVA_{254}$ Light $(mg/L)^{-1}$	Day 2 $SUVA_{254}$ Dark $(mg/L)^{-1}$	Day 3 $SUVA_{254}$ Light $(mg/L)^{-1}$	Day 3 $SUVA_{254}$ Dark $(mg/L)^{-1}$
Photochemistry Blue (P1)	4.49 4.44 4.48	4.39 4.57	4.28 4.95	4.05 4.52	4.17 4.69	4.27 3.61 4.43	4.31 3.49 4.71
Photochemistry Brown (P2)		9.24 8.95	9.34 8.94	8.27 8.46	9.21 9.32	8.46 8.00 8.27	9.18 9.69 9.61
Wisconsin Point (WP)	14.57 14.32 14.75	12.13 11.87	13.41 12.77	10.52 11.15	11.25 12.31	12.95 13.08 13.79	13.37 15.68 14.54

Table S-17. NH_4^+ values before and after irradiation of whole, autoclaved samples. The initial WP value is missing due to insufficient volume.

Site	Initial NH_4^+ (mg/L)	Day 3 NH_4^+ Light (mg/L)	Day 3 NH_4^+ Dark (mg/L)
Photochemistry Blue (P1)	0.0103	0.0162 0.0133 0.0136	0.0141 0.0160 0.0170
Photochemistry Brown (P2)	0.0288	0.0327 0.0337 0.0303	0.0241 0.0260 0.0265

Wisconsin Point (WP)		0.0539 0.0547 0.0105	0.0561 0.0417 0.0155

Table S-18. TP and TDP concentrations during whole water irradiations. The errors shown in this table are taken from the standard deviation of the three injections performed on the AQ400 Discrete Analyzer. An initial TP sample for P2 and an initial TDP sample for WP were unable to be taken due to volume constraints.

Site	Initial TP (mg/L)	Initial TDP (mg/L)	Day 3 TP Light (mg/L)	Day 3 TP Dark (mg/L)	Day 3 TDP Light (mg/L)	Day 3 TDP Dark (mg/L)
Photochemistry Blue (P1)	0.0086 ± 0.0014	0.0084 ± 0.0006	0.0081 ± 0.0012 0.0077 ± 0.0008 0.0073 ± 0.0001	0.0104 ± 0.0031 0.0076 ± 0.0006 0.0082 ± 0.0002	0.0084 ± 0.0007 0.0079 ± 0.0002 0.0088 ± 0.0017	0.0082 ± 0.0004 0.0097 ± 0.0004 0.0085 ± 0.0005
Photochemistry Brown (P2)		0.0128 ± 0.0017	0.0157 ± 0.0005 0.0175 ± 0.0020 0.0179 ± 0.0016	0.0181 ± 0.0017 0.0170 ± 0.0005 0.0153 ± 0.0016	0.0152 ± 0.0004 0.0127 ± 0.0026 0.0151 ± 0.0012	0.0150 ± 0.0006 0.0132 ± 0.0008 0.0135 ± 0.0021
Wisconsin Point (WP)	0.0789 ± 0.0026		0.0418 ± 0.0094 0.0492 ± 0.0058 0.0492 ± 0.0022	0.0470 ± 0.0030 0.0462 ± 0.0029 0.0394 ± 0.0012	0.0204 ± 0.0008 0.0205 ± 0.0005 0.0221 ± 0.0024	0.0208 ± 0.0006 0.0174 ± 0.0007 0.0171 ± 0.0009

Table S-19. SRP concentrations during whole water irradiations. The errors shown in this table are taken from the standard deviation of the three injections performed on the AQ400 Discrete Analyzer. An initial sample for WP was unable to be taken due to volume constraints.

Site	Initial SRP (μg/L)	Day 3 SRP Light (μg/L)	Day 3 SRP Dark (μg/L)

Photochemistry Blue (P1)	1.60 ± 0.02	1.74 ± 0.10 1.78 ± 0.05 1.57 ± 0.09	1.58 ± 0.08 1.86 ± 0.13 1.50 ± 0.02
Photochemistry Brown (P2)	2.66 ± 0.11	1.96 ± 0.06 2.03 ± 0.09 1.74 ± 0.07	2.28 ± 0.01 3.36 ± 0.16 2.57 ± 0.12
Wisconsin Point (WP)		1.52 ± 0.03 1.56 ± 0.02 1.73 ± 0.10	1.82 ± 0.14 1.96 ± 0.05 2.12 ± 0.05

Table S-20. DOC filtered water irradiation two-tailed t-test results (α=0.05) between light and dark treatments. Percent change is only shown for significant t-tests.

T tests between light and dark treatments	Photochemistry Blue (P1) Day 1	Photochemistry Brown (P2) Day 1	Wisconsin Point (WP) Day 1	Photochemistry Blue (P1) Day 2	Photochemistry Brown (P2) Day 2	Wisconsin Point (WP) Day 2	Photochemistry Blue (P1) Day 3	Photochemistry Brown (P2) Day 3	Wisconsin Point (WP) Day 3
F stat	1.14	5.89	29.22	2.94	2.85	2.16	4.52	18.59	2.02
F critical	39	39	39	39	39	39	39	39	39
Variances	Equal	Equal	Equal	Equal	Equal	Equal	Equal	Equal	Equal
T stat	0.29	2.84	1.11	0.89	0.74	0.50	0.75	0.96	0.59
T critical	2.78	2.78	2.78	2.78	2.78	2.78	2.78	2.78	2.78
p value	0.79	0.05	0.33	0.43	0.50	0.64	0.49	0.39	0.58
Significant?	No	Yes	No	No	No	No	No	No	No
Percent change (%)		-2.98							

Table S-21. DOC filtered water irradiation two-tailed t-test results (α=0.05) between initial and final Day 3 light and dark endpoints. The f-tests were not able to be performed for this set due to the initial DOC concentration only having one replicate. The t-test assuming equal variances was used. Percent change is only shown for significant t-tests.

T tests between initial and final samples	Photochemistry Blue (P1) Light	Photochemistry Brown (P2) Light	Wisconsin Point (WP) Light	Photochemistry Blue (P1) Dark	Photochemistry Brown (P2) Dark	Wisconsin Point (WP) Dark
T stat	0.30	1.96	0.39	1.51	0.58	1.76
T critical	4.30	4.30	4.30	4.30	4.30	4.30
p value	0.80	0.19	0.73	0.27	0.62	0.22
Significant?	No	No	No	No	No	No
Percent change (%)						

Table S-22. TDN filtered water irradiation two-tailed t-test results between light and dark treatments. Percent change is only shown for significant t-tests.

T tests between light and dark treatments	Photochemistry Blue (P1) Day 1	Photochemistry Brown (P2) Day 1	Wisconsin Point (WP) Day 1	Photochemistry Blue (P1) Day 2	Photochemistry Brown (P2) Day 2	Wisconsin Point (WP) Day 2	Photochemistry Blue (P1) Day 3	Photochemistry Brown (P2) Day 3	Wisconsin Point (WP) Day 3
F stat	1.28	10.71	34.88	2.77	2.00	2.87	1.83	5.59	465.28
F critical	39	39	39	39	39	39	39	39	39
Variances	Equal	Equal	Equal	Equal	Equal	Equal	Equal	Equal	Unequal

T stat	0.44	0.60	1.21	0.31	0.36	0.27	1.73	0.74	1.01
T critical	2.78	2.78	2.78	2.78	2.78	2.78	2.78	2.78	4.30
p value	0.68	0.58	0.29	0.76	0.74	0.80	0.16	0.50	0.42
Significant?	No	No	No	No	No	No	No	No	No
Percent change (%)									

Table S-23. TDN filtered water irradiation two-tailed t-test results (α=0.05) between initial and final Day 3 light and dark endpoints. The f-tests were not able to be performed for this set due to the initial DOC concentration only having one replicate. The t-test assuming equal variances was used. Percent change is only shown for significant t-tests.

T tests between initial and final samples	Photochemistry Blue (P1) Light	Photochemistry Brown (P2) Light	Wisconsin Point (WP) Light	Photochemistry Blue (P1) Dark	Photochemistry Brown (P2) Dark	Wisconsin Point (WP) Dark
T stat	0.20	1.40	0.68	1.73	2.33	0.54
T critical	4.30	4.30	4.30	4.30	4.30	4.30
p value	0.86	0.30	0.57	0.23	0.14	0.65
Significant?	No	No	No	No	No	No
Percent change (%)						

Table S-24. e2/e3 filtered water irradiation two-tailed t-test results between light and dark treatments. Percent change is only shown for significant t-tests.

T tests between light and dark treatments	Photochemistry Blue (P1) Day 1	Photochemistry Brown (P2) Day 1	Wisconsin Point (WP) Day 1	Photochemistry Blue (P1) Day 2	Photochemistry Brown (P2) Day 2	Wisconsin Point (WP) Day 2	Photochemistry Blue (P1) Day 3	Photochemistry Brown (P2) Day 3	Wisconsin Point (WP) Day 3
F stat	1.91	10.41	39.11	6.11	11.99	2.65E6	3.95	1.02	85.4
F critical	648	648	648	648	648	648	39	39	39
Variances	Equal	Equal	Equal	Equal	Equal	Unequal	Equal	Equal	Unequal
T stat	0.55	5.40	15.22	1.89	24.39	13.21	0.76	16.15	22.91
T critical	4.30	4.30	4.30	4.30	4.30	12.71	2.78	2.78	4.30
p value	0.64	0.03	0.004	0.20	0.002	0.05	0.49	8.59E-5	0.002
Significant?	No	Yes	Yes	No	Yes	Yes	No	Yes	Yes
Percent change (%)		8.50	5.42		8.50	9.63		11.31	16.35

Table S-25. e2/e3 filtered water irradiation two-tailed t-test results (α=0.05) between initial and final Day 3 light and dark endpoints. Percent change is only shown for significant t-tests.

T tests between initial and	Photochemistry Blue (P1) Light	Photochemistry Brown (P2) Light	Wisconsin Point (WP) Light	Photochemistry Blue (P1) Dark	Photochemistry Brown (P2) Dark	Wisconsin Point (WP) Dark

final samples						
F stat	80.69	295.75	5.74	20.44	995.24	14.87
F critical	39	39	39	39	39	39
Variances	Unequal	Unequal	Equal	Equal	Unequal	Equal
T stat	0.07	1.96	19.02	1.79	0.89	5.65
T critical	4.30	4.30	2.78	2.78	4.30	2.78
p value	0.95	0.19	4.50E-5	0.15	0.47	0.005
Significant?	No	No	Yes	No	No	Yes
Percent change (%)			14.37			1.73

Table S-26. Filtered water irradiation CDOM absorbance two-tailed t-test results between light and dark treaments. Percent change is only shown for significant t-tests.

T tests between light and dark treatments	Photochemistry Blue (P1) Day 1	Photochemistry Brown (P2) Day 1	Wisconsin Point (WP) Day 1	Photochemistry Blue (P1) Day 2	Photochemistry Brown (P2) Day 2	Wisconsin Point (WP) Day 2	Photochemistry Blue (P1) Day 3	Photochemistry Brown (P2) Day 3	Wisconsin Point (WP) Day 3
F stat	3.31	5.51	2.63	21.92	1.14	3.99	4.04	1.15	2.65
F critical	648	648	648	648	648	648	39	39	39
Variances	Equal	Equal	Equal	Equal	Equal	Equal	Equal	Equal	Equal

T stat	1.38	12.11	8.76	6.25	10.92	11.80	1.15	25.96	18.76
T critical	4.30	4.30	4.30	4.30	4.30	4.30	2.78	2.78	2.78
p value	0.30	0.007	0.01	0.02	0.008	0.007	0.31	1.31E-5	4.76E-5
Significant?	No	Yes	Yes	Yes	Yes	Yes	No	Yes	Yes
Percent change (%)		-7.32	-4.98	-4.27	-7.32	-9.33		-11.31	-15.12

Table S-27. Filtered water irradiation CDOM absorbance two-tailed t-test results (α=0.05) between initial and final Day 3 light and dark endpoints. Percent change is only shown for significant t-tests.

T tests between initial and final samples	Photochemistry Blue (P1) Light	Photochemistry Brown (P2) Light	Wisconsin Point (WP) Light	Photochemistry Blue (P1) Dark	Photochemistry Brown (P2) Dark	Wisconsin Point (WP) Dark
F stat	3.40	350.89	3.91	1.19	304.79	10.38
F critical	39	39	39	39	39	39
Variances	Equal	Unequal	Equal	Equal	Unequal	Equal
T stat	2.54	2.73	27.61	2.18	0.70	2.88
T critical	2.78	4.30	2.78	2.78	4.30	2.78
p value	0.06	0.11	1.02E-5	0.09	0.55	0.04

Significant?	No	No	Yes	No	No	Yes
Percent change (%)			-13.32			2.12

Table S-28. Filtered water irradiation $SUVA_{254}$ two-tailed t-test results between light and dark treatments. Percent change is only shown for significant t-tests.

T tests between light and dark treatments	Photochemistry Blue (P1) Day 1	Photochemistry Brown (P2) Day 1	Wisconsin Point (WP) Day 1	Photochemistry Blue (P1) Day 2	Photochemistry Brown (P2) Day 2	Wisconsin Point (WP) Day 2	Photochemistry Blue (P1) Day 3	Photochemistry Brown (P2) Day 3	Wisconsin Point (WP) Day 3
F stat	1.58	3.85	2.34	4.54	25.79	2.82	5.10	28.26	1.33
F critical	648	648	648	648	648	648	39	39	39
Variances	Equal	Equal	Equal	Equal	Equal	Equal	Equal	Equal	Equal
T stat	2.59	1.72	0.18	1.29	2.16	0.35	0.25	1.20	5.73
T critical	4.30	4.30	4.30	4.30	4.30	4.30	2.78	2.78	2.78
p value	0.12	0.23	0.87	0.33	0.16	0.76	0.82	0.30	0.005
Significant?	No	No	No	No	No	No	No	No	Yes
Percent change (%)									-8.34

Table S-29. Filtered water irradiation $SUVA_{254}$ two-tailed t-test results (α=0.05) between initial and final Day 3 light and dark endpoints. Percent change is only shown for significant t-tests.

T tests between initial and final samples	Photochemistry Blue (P1) Light	Photochemistry Brown (P2) Light	Wisconsin Point (WP) Light	Photochemistry Blue (P1) Dark	Photochemistry Brown (P2) Dark	Wisconsin Point (WP) Dark
F stat	38.78	4.20	36.46	7.61	6.73	27.49
F critical	39	39	39	39	39	39
Variances	Equal	Equal	Equal	Equal	Equal	Equal
T stat	1.68	5.84	11.12	4.20	1.20	4.16
T critical	2.78	2.78	2.78	2.78	2.78	2.78
p value	0.17	0.004	3.72E-4	0.01	0.30	0.01
Significant?	No	Yes	Yes	Yes	No	Yes
Percent change (%)		-7.79	-11.91	-6.38		-3.89

Table S-30. DOC whole water irradiation two-tailed t-test results (α=0.05) between light and dark treatments. Percent change is only shown for significant t-tests.

T tests between light and dark treatments	Photochemistry Blue (P1) Day 3	Photochemistry Brown (P2) Day 3	Wisconsin Point (WP) Day 3

F stat	12.32	10.03	42.00
F critical	39	39	39
Variances	Equal	Equal	Unequal
T stat	0.06	3.32	0.91
T critical	2.78	2.78	4.30
p value	0.95	0.03	0.46
Significant?	No	Yes	No
Percent change (%)		-2.78	

Table S-31. DOC whole water irradiation two-tailed t-test results (α=0.05) between initial and final Day 3 light and dark endpoints. The f-tests were not able to be performed for this set due to the initial DOC concentration only having one replicate. The t-test assuming equal variances was used. Percent change is only shown for significant t-tests.

T tests between initial and final samples	Photochemistry Blue (P1) Light	Photochemistry Brown (P2) Light	Wisconsin Point (WP) Light	Photochemistry Blue (P1) Dark	Photochemistry Brown (P2) Dark	Wisconsin Point (WP) Dark
T stat	0.74	1.33	1.03	2.71	9.72	3.68
T critical	4.30	4.30	4.30	4.30	4.30	4.30

p value	0.54	0.31	0.41	0.11	0.01	0.07
Significant?	No	No	No	No	Yes	No
Percent change (%)					4.45	

Table S-32. TOC whole water irradiation two-tailed t-test results (α=0.05) between light and dark treatments. Percent change is only shown for significant t-tests.

T tests between light and dark treatments	Photochemistry Blue (P1) Day 1	Photochemistry Brown (P2) Day 1	Wisconsin Point (WP) Day 1	Photochemistry Blue (P1) Day 2	Photochemistry Brown (P2) Day 2	Wisconsin Point (WP) Day 2	Photochemistry Blue (P1) Day 3	Photochemistry Brown (P2) Day 3	Wisconsin Point (WP) Day 3
F stat	5.69	4.91	1.72	1.43	2.26	3.28	2.10	2.52	3.89
F critical	39	39	39	39	39	39	39	39	39
Variances	Equal	Equal	Equal	Equal	Equal	Equal	Equal	Equal	Equal
T stat	0.60	2.60	0.16	0.98	0.92	0.22	0.48	0.30	0.42
T critical	2.78	2.78	2.78	2.78	2.78	2.78	2.78	2.78	2.78
p value	0.58	0.06	0.88	0.38	0.41	0.83	0.66	0.78	0.70
Significant?	No	No	No	No	No	No	No	No	No
Percent change (%)									

Table S-33. TOC whole water irradiation two-tailed t-test results (α=0.05) between initial and final Day 3 light and dark endpoints. The f-tests were not able to be performed for this set due to the initial TOC concentration only having one replicate. The t-test assuming equal variances was used. Percent change is only shown for significant t-tests.

T tests between initial and final samples	Photochemistry Blue (P1) Light	Photochemistry Brown (P2) Light	Wisconsin Point (WP) Light	Photochemistry Blue (P1) Dark	Photochemistry Brown (P2) Dark	Wisconsin Point (WP) Dark
T stat	0.17	0.12	1.80	0.41	0.10	0.68
T critical	4.30	4.30	4.30	4.30	4.30	4.30
p value	0.88	0.91	0.21	0.72	0.93	0.57
Significant?	No	No	No	No	No	No
Percent change (%)						

Table S-34. TDN whole water irradiation two-tailed t-test results between light and dark treatments. Percent change is only shown for significant t-tests.

T tests between light and dark treatments	Photochemistry Blue (P1) Day 3	Photochemistry Brown (P2) Day 3	Wisconsin Point (WP) Day 3
F stat	11.15	10.17	8.38

F critical	39	39	39
Variances	Equal	Equal	Equal
T stat	1.59	0.07	1.17
T critical	2.78	2.78	2.78
p value	0.19	0.95	0.31
Significant?	No	No	No
Percent change (%)			

Table S-35. TDN whole water irradiation two-tailed t-test results (α=0.05) between initial and final Day 3 light and dark endpoints. The f-tests were not able to be performed for this set due to the initial TDN concentration only having one replicate. The t-test assuming equal variances was used. Percent change is only shown for significant t-tests.

T tests between initial and final samples	Photochemistry Blue (P1) Light	Photochemistry Brown (P2) Light	Wisconsin Point (WP) Light	Photochemistry Blue (P1) Dark	Photochemistry Brown (P2) Dark	Wisconsin Point (WP) Dark
T stat	0.23	1.27	3.08	1.99	0.43	0.45
T critical	4.30	4.30	4.30	4.30	4.30	4.30
p value	0.84	0.33	0.09	0.18	0.71	0.70
Significant?	No	No	No	No	No	No
Percent change (%)						

Table S-36. TN whole water irradiation two-tailed t-test results (α=0.05) between light and dark treatments. Percent change is only shown for significant t-tests.

T tests between light and dark treatments	Photochemistry Blue (P1) Day 1	Photochemistry Brown (P2) Day 1	Wisconsin Point (WP) Day 1	Photochemistry Blue (P1) Day 2	Photochemistry Brown (P2) Day 2	Wisconsin Point (WP) Day 2	Photochemistry Blue (P1) Day 3	Photochemistry Brown (P2) Day 3	Wisconsin Point (WP) Day 3
F stat	4.09	4.19	5684	50.66	1.45	1.97	9.50	1.80	4.73
F critical	39	39	39	39	39	39	39	39	39
Variances	Equal	Equal	Unequal	Unequal	Equal	Equal	Equal	Equal	Equal
T stat	0.27	0.30	1.00	0.22	0.49	1.74	1.07	0.38	1.32
T critical	2.78	2.78	4.30	4.30	2.78	2.78	2.78	2.78	2.78
p value	0.80	0.78	0.42	0.85	0.65	0.16	0.34	0.73	0.26
Significant?	No	No	No	No	No	No	No	No	No
Percent change (%)									

Table S-37. TN whole water irradiation two-tailed t-test results (α=0.05) between initial and final Day 3 light and dark endpoints. The f-tests were not able to be performed for this set due to the initial TOC concentration only having one replicate. The t-test assuming equal variances was used. Percent change is only shown for significant t-tests.

T tests between initial and final samples	Photochemistry Blue (P1) Light	Photochemistry Brown (P2) Light	Wisconsin Point (WP) Light	Photochemistry Blue (P1) Dark	Photochemistry Brown (P2) Dark	Wisconsin Point (WP) Dark
T stat	2.23	0.30	2.87	5.15	0.09	0.60
T critical	4.30	4.30	4.30	4.30	4.30	4.30
p value	0.16	0.79	0.10	0.04	0.94	0.61
Significant?	No	No	No	Yes	No	No
Percent change (%)				3.42		

Table S-38. e2/e3 whole water irradiation two-tailed t-test results between light and dark treatments. Percent change is only shown for significant t-tests.

T tests between light and dark treatments	Photochemistry Blue (P1) Day 1	Photochemistry Brown (P2) Day 1	Wisconsin Point (WP) Day 1	Photochemistry Blue (P1) Day 2	Photochemistry Brown (P2) Day 2	Wisconsin Point (WP) Day 2	Photochemistry Blue (P1) Day 3	Photochemistry Brown (P2) Day 3	Wisconsin Point (WP) Day 3
F stat	1.12	1.61	6.32	71.14	5.91	6.38	1.02	2.06	18.18
F critical	648	648	648	648	648	648	39	39	39
Variances	Equal	Equal	Equal	Equal	Equal	Equal	Equal	Equal	Equal
T stat	11.38	12.66	3.83	19.89	11.99	2.14	32.99	6.14	4.78

T critical	4.30	4.30	4.30	4.30	4.30	4.30	2.78	2.78	2.78
p value	0.008	0.006	0.06	0.003	0.007	0.17	5.03E-6	0.004	0.009
Significant?	Yes	Yes	No	Yes	Yes	No	Yes	Yes	Yes
Percent change (%)	19.57	13.70		23.23	18.40		22.36	27.59	7.21

Table S-39. e2/e3 whole water irradiation two-tailed t-test results (α=0.05) between initial and final Day 3 light and dark endpoints. Percent change is only shown for significant t-tests. P2 results are not shown because there was no initial sample taken due to volume constraints.

T tests between initial and final samples	Photochemistry Blue (P1) Light	Photochemistry Brown (P2) Light	Wisconsin Point (WP) Light	Photochemistry Blue (P1) Dark	Photochemistry Brown (P2) Dark	Wisconsin Point (WP) Dark
F stat	1.19		2.10	1.21		38.24
F critical	39		39	39		39
Variances	Equal		Equal	Equal		Equal
T stat	46.26		23.17	14.92		1.67
T critical	2.78		2.78	2.78		2.78
p value	1.31E-6		2.06E-5	1.18E-4		0.17
Significant?	Yes		Yes	Yes		No

Percent change (%)	36.82		9.93	11.82	

Table S-40. Whole water irradiation CDOM absorbance two-tailed t-test results between light and dark treaments. Percent change is only shown for significant t-tests.

T tests between light and dark treatments	Photochemistry Blue (P1) Day 1	Photochemistry Brown (P2) Day 1	Wisconsin Point (WP) Day 1	Photochemistry Blue (P1) Day 2	Photochemistry Brown (P2) Day 2	Wisconsin Point (WP) Day 2	Photochemistry Blue (P1) Day 3	Photochemistry Brown (P2) Day 3	Wisconsin Point (WP) Day 3
F stat	3.53	13.28	2.15	47.19	4.25	12.90	1.10	2.08	14.11
F critical	648	648	648	648	648	648	39	39	39
Variances	Equal	Equal	Equal	Equal	Equal	Equal	Equal	Equal	Equal
T stat	18.08	22.15	2.81	15.62	29.47	1.75	14.74	18.23	3.69
T critical	4.30	4.30	4.30	4.30	4.30	4.30	2.78	2.78	2.78
p value	0.003	0.002	0.11	0.004	0.001	0.22	1.23E-4	5.32E-5	0.02
Significant?	Yes	Yes	No	Yes	Yes	No	Yes	Yes	Yes
Percent change (%)	-12.68	-11.26		-13.46	-16.92		-13.96	-24.42	-11.83

Table S-41. CDOM absorbances for whole water irradiation two-tailed t-test results (α=0.05) between initial and final Day 3 light and dark endpoints. Percent change is only shown for significant t-tests. P2 results are not shown because there was no initial sample taken due to volume constraints.

T tests between initial and final samples	Photochemistry Blue (P1) Light	Photochemistry Brown (P2) Light	Wisconsin Point (WP) Light	Photochemistry Blue (P1) Dark	Photochemistry Brown (P2) Dark	Wisconsin Point (WP) Dark
F stat	10.31		1.42	9.36		9.95
F critical	39		39	39		39
Variances	Equal		Equal	Equal		Equal
T stat	24.31		7.78	5.09		0.57
T critical	2.78		2.78	2.78		2.78
p value	1.70E-5		0.001	0.007		0.60
Significant?	Yes		Yes	Yes		No
Percent change (%)	-16.87		-10.16	-3.38		

Table S-42. Whole water irradiation $SUVA_{254}$ for OM two-tailed t-test results between light and dark endpoints. Percent change is only shown for significant t-tests.

T tests between light and dark treatments	Photochemistry Blue (P1) Day 1	Photochemistry Brown (P2) Day 1	Wisconsin Point (WP) Day 1	Photochemistry Blue (P1) Day 2	Photochemistry Brown (P2) Day 2	Wisconsin Point (WP) Day 2	Photochemistry Blue (P1) Day 3	Photochemistry Brown (P2) Day 3	Wisconsin Point (WP) Day 3

F stat	14.6	1.88	6.15	1.23	2.89	2.84	2.06	1.46	6.49
F critical	648	648	648	648	648	648	39	39	39
Variances	Equal	Equal	Equal	Equal	Equal	Equal	Equal	Unequal	Equal
T stat	0.40	0.20	3.14	0.42	8.40	1.52	0.15	6.06	1.76
T critical	4.30	4.30	4.30	4.30	4.30	4.30	2.78	2.78	2.78
p value	0.73	0.86	0.09	0.72	0.01	0.27	0.89	0.004	0.15
Significant?	No	No	No	No	Yes	No	No	Yes	No
Percent change (%)					-9.69			-13.18	

Table S-43. Whole water irradiation $SUVA_{254}$ for OM two-tailed t-test results (α=0.05) between initial and final Day 3 light and dark endpoints. Percent change is only shown for significant t-tests. P2 results are not shown because there was no initial sample taken due to volume constraints.

T tests between initial and final samples	Photochemistry Blue (P1) Light	Photochemistry Brown (P2) Light	Wisconsin Point (WP) Light	Photochemistry Blue (P1) Dark	Photochemistry Brown (P2) Dark	Wisconsin Point (WP) Dark
F stat	288.08		4.38	592.47		28.44
F critical	39		39	39		39
Variances	Unequal		Equal	Unequal		Equal

T stat	1.44		4.40	0.83		0.02
T critical	4.30		2.78	4.30		2.78
p value	0.29		0.01	0.49		0.98
Significant?	No		Yes	No		No
Percent change (%)			-8.76			

Table S-44. Ammonium filtered and whole water irradiation two-tailed t-test results between light and dark endpoints. Percent change is only shown for significant t-tests.

T tests between light and dark treatments	Photochemistry Blue (P1) Day 3		Photochemistry Brown (P2) Day 3		Wisconsin Point (WP) Day 3	
	Filtered	Whole	Filtered	Whole	Filtered	Whole
F stat	1.13	1.17	1.47	1.92	1003.63	1.51
F critical	39	39	39	39	39	39
Variances	Equal	Equal	Equal	Equal	Unequal	Equal
T stat	6.18	1.08	1.76	5.33	0.58	0.75
T critical	2.78	2.78	2.78	2.78	4.30	4.30

p value	0.003	0.34	0.15	0.006	0.62	0.53
Significant?	Yes	No	No	Yes	No	No
Percent change	-41.82			25.98		

Table S-45. Filtered water irradiation ammonia two-tailed t-test results (α=0.05) between initial and final Day 3 light and dark endpoints. Percent change is only shown for significant t-tests. Whole water WP samples are not shown because an initial sample was not taken due to volume constraints.

T tests between initial and final samples	Photochemistry Blue (P1) Light		Photochemistry Brown (P2) Light		Wisconsin Point (WP) Light		Photochemistry Blue (P1) Dark		Photochemistry Brown (P2) Dark		Wisconsin Point (WP) Dark	
	Filtered	Whole	Filtered	Whole	Filtered	Whole	Filtered	Whole	Filtered	Whole	Filtered	Whole
T stat	0.22	2.24	1.83	1.67	0.17		4.04	3.26	2.65	2.24	3.90	
T critical	4.30	4.30	4.30	4.30	4.30		4.30	4.30	4.30	4.30	4.30	
p value	0.85	0.15	0.21	0.24	0.88		0.06	0.08	0.12	0.15	0.06	
Significant?	No	No	No	No	No		No	No	No	No	No	
Percent change												

Table S-46. TDP filtered and whole water irradiation two-tailed t-test results between light and dark treatments. Percent change is only shown for significant t-tests.

T tests between light and dark treatments	Photochemistry Blue (P1) Day 3		Photochemistry Brown (P2) Day 3		Wisconsin Point (WP) Day 3	
	Filtered	Whole	Filtered	Whole	Filtered	Whole
F stat	4.26	2.99	4.72	2.14	8.67	4.71
F critical	39	39	39	39	39	39
Variances	Equal	Equal	Equal	Equal	Equal	Equal
T stat	0.20	0.90	0.54	0.46	0.91	2.02
T critical	2.78	2.78	2.78	2.78	2.78	2.78
p value	0.85	0.42	0.61	0.67	0.41	0.11
Significant?	No	No	No	No	No	No
Percent change						

Table S-47. Filtered water irradiation TDP two-tailed t-test results (α=0.05) between initial and final Day 3 light and dark endpoints. Percent change is only shown for significant t-tests. Whole water WP samples are not shown because an initial sample was not taken due to volume constraints.

T tests between initial and final samples	Photochemistry Blue (P1) Light		Photochemistry Brown (P2) Light		Wisconsin Point (WP) Light		Photochemistry Blue (P1) Dark		Photochemistry Brown (P2) Dark		Wisconsin Point (WP) Dark	
	Filtered	Whole	Filtered	Whole	Filtered	Whole	Filtered	Whole	Filtered	Whole	Filtered	Whole
T stat	0.40	0.10	0.36	0.93	0.78		0.31	0.46	0.13	0.95	0.87	
T critical	4.30	4.30	4.30	4.30	4.30		4.30	4.30	4.30	4.30	4.30	
p value	0.73	0.93	0.75	0.45	0.52		0.79	0.69	0.91	0.44	0.48	
Significant?	No	No	No	No	No		No	No	No	No	No	
Percent change												

Table S-48. TP filtered and whole water irradiation two-tailed t-test results between light and dark treatments. Percent change is only shown for significant t-tests.

T tests between light and dark treatments	Photochemistry Blue (P1) Day 3	Photochemistry Brown (P2) Day 3	Wisconsin Point (WP) Day 3
F stat	13.00	1.51	1.05
F critical	39	39	39
Variances	Equal	Equal	Equal

T stat	1.17	0.21	0.73
T critical	2.78	2.78	2.78
p value	0.31	0.84	0.51
Significant?	No	No	No
Percent change			

Table S-49. Filtered water irradiation TP two-tailed t-test results (α=0.05) between initial and final Day 3 light and dark endpoints. Percent change is only shown for significant t-tests. P2 results are not shown because there was no initial sample taken due to volume constraints.

T tests between initial and final samples	Photochemistry Blue (P1) Light	Photochemistry Brown (P2) Light	Wisconsin Point (WP) Light	Photochemistry Blue (P1) Dark	Photochemistry Brown (P2) Dark	Wisconsin Point (WP) Dark
T stat	1.92		6.53		0.21	7.23
T critical	4.30		4.30		2.78	4.30
p value	0.19		0.02		0.84	0.02
Significant?	No		Yes		No	Yes
Percent change			-40.75			-43.93

Table S-50. SRP filtered and whole water irradiation two-tailed t-test results between light and dark treatments. Percent change is only shown for significant t-tests.

T tests between light and dark treatments	Photochemistry Blue (P1) Day 3		Photochemistry Brown (P2) Day 3		Wisconsin Point (WP) Day 3	
	Filtered	Whole	Filtered	Whole	Filtered	Whole
F stat	11.93	3.32	12.87	12.54	2.62	1.21
F critical	39	39	39	39	39	39
Variances	Equal	Equal	Equal	Equal	Equal	Equal
T stat	0.64	0.14	0.32	0.61	3.65	2.77
T critical	2.78	2.78	2.78	2.78	2.78	2.78
p value	0.56	0.90	0.76	0.57	0.02	0.05
Significant?	No	No	No	No	Yes	No
Percent change					-17.66	

Table S-51. Filtered water irradiation SRP two-tailed t-test results (α=0.05) between initial and final Day 3 light and dark endpoints. Percent change is only shown for significant t-tests. Whole water WP samples are not shown because an initial sample was not taken due to volume constraints.

T tests between initial and final samples	Photochemistry Blue (P1) Light		Photochemistry Brown (P2) Light		Wisconsin Point (WP) Light		Photochemistry Blue (P1) Dark		Photochemistry Brown (P2) Dark		Wisconsin Point (WP) Dark	
	Filtered	Whole	Filtered	Whole	Filtered	Whole	Filtered	Whole	Filtered	Whole	Filtered	Whole
T stat	0.60	3.05	0.05	4.13	1.57		0.93	1.59	0.77	0.85	0.94	
T critical	4.30	4.30	4.30	4.30	4.30		4.30	4.30	4.30	4.30	4.30	
p value	0.61	0.09	0.97	0.05	0.26		0.45	0.25	0.52	0.49	0.45	
Significant?	No	No	No	No	No		No	No	No	No	No	
Percent change												

Table S-52. 0.22 μm PES filter sorption test of Lake Superior water taken from the shore near Glensheen on 2/17/21. A t test (assuming equal variances as proved by an f test) between the two filtered samples revealed that there was no significant difference between the two means (p=0.676).

	TOC/DOC (mg/L)
Initial whole sample	1.550 ± 0.017
Filtered once	1.600 ± 0.029
Filtered twice	1.610 ± 0.025

Table S-53. Tukey HSD test values (Abs(Dif)-HSD). Positive values show pairs of means that are significant (values are italicized).

	DOC	TOC	TDN	TN	e2/e3	CDOM	$SUVA_{254}$	NH_3	TDP	TP	SRP
P1-P2	*1.8845*	*1.8801*	-0.11337	*0.03606*	*1.0249*	*5.0*	*2.3136*	*0.06553*	-0.00064	*0.00496*	-0.00043
P1-WP	*6.0378*	*5.7319*	-0.10892	*0.09224*	*2.4497*	*4361.6*	*4.3768*	*0.18930*	*0.00067*	*0.03355*	-0.00060
P2-WP	*3.8937*	*3.5363*	-0.15661	*0.03929*	*0.2886*	*2587.1*	-0.1062	-0.52368	-0.00306	*0.02484*	-0.00041
Filtered-Whole	-1.6777		-0.01327		*0.4301*	*114.5*	*0.5386*	*0.26335*	*0.00361*		*0.00054*
Light-Dark	-1.8281	-2.6393	-0.00161	-0.04033	-0.5459	-1683.9	-1.8036	-0.42955	-0.00255	-0.01649	-0.00028

Figure S-1. Filtered and whole water irradiations k_λ rate constants averages from 200 to 450 nm for Site P1 (as shown in Figures 3.12 and Figure 3.13 on the same graph for comparison). Error bars shown are calculated from the three k_λ values calculated from the three UV-Vis replicates.

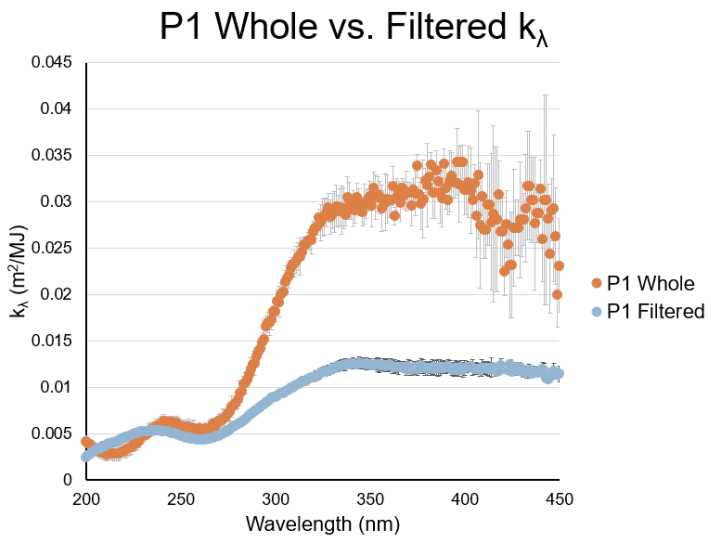
P1 Whole vs. Filtered kλ
0.045
0.04
0.035
0.03
0.025
0.02
0.015
0.01
0.005
0
kλ (m²/MJ)
200
250
300
350
400
450
Wavelength (nm)
P1 Whole
P1 Filtered